MR No. E5K30

NATIONAL ADVISORY COMMITTEE FOR AERONAUTICS

WARTIME REPORT

ORIGINALLY ISSUED

January 1946 as
Memorandum Report E5K30

AN INVESTIGATION OF COWL INLETS FOR THE B-29 POWER-PLANT INSTALLATION

By Louis L. Monroe and Martin J. Saari

Aircraft Engine Research Laboratory
Cleveland, Ohio

NACA

WASHINGTON

NACA MR No. E5K30

NATIONAL ADVISORY COMMITTEE FOR AERONAUTICS

MEMORANDUM REPORT

for the

Air Technical Service Command, Army Air Forces

AN INVESTIGATION OF COWL INLETS FOR THE B-29 POWER-PLANT INSTALLATION

By Louis L. Monroe and Martin J. Saari

SUMMARY

An investigation of five cowl-inlet configurations for the B-29 airplane was made in the NACA Cleveland altitude wind tunnel to obtain design information for improving the cowl performance. Tests were made to determine the effect of propeller spinners and increased inlet diameters on the cooling-air pressures at the cowl inlet and at the face of the engine and on the drag and the critical speed of the cowl.

The cooling-air pressures at the cowl inlet and at the face of the engine were appreciably greater for a 43-inch-diameter inlet than for a 38½- by 35-inch oval inlet. The addition of a 27-inch-diameter spinner to the 43-inch-diameter inlet further increased the pressures at the face of the engine, whereas the addition of a 32-inch-diameter spinner to the same inlet did not appreciably affect the pressures. The critical speed of the 38½- by 35-inch oval inlet was slightly greater than that of the 43-inch-diameter inlet. The addition of the 32-inch-diameter spinner to the 43-inch-diameter inlet increased the critical Mach number to nearly that of the oval inlet. The cooling drag of the installation with the 43-inch-diameter inlet was considerably less than with the 38½- by 35-inch oval inlet.

INTRODUCTION

Flight tests of the B-29 airplane by the Boeing Aircraft Company have shown that the cooling-air pressure recoveries at the face of the engine were low and that pressure losses of as much as 0.30 of the free-stream impact pressure occurred ahead of the engine. An investigation was therefore conducted in the NACA Cleveland altitude wind

tunnel to determine the origin of these losses and to investigate the characteristics of several alternate cowl-inlet designs. The tests were part of an extensive investigation requested by the Air Technical Service Command, Army Air Forces, to improve the cooling and reduce the cooling drag of the B-29 power-plant installation.

Each of the inlet configurations was tested over a range of inlet velocity ratios, angles of attack, and propeller thrust coefficients. An analysis is presented of the effect of varying those operating conditions on critical speed of the cowl, total pressures at the cowl inlet, pressures at the face of the engine, and drag of the installation. Comparisons are made of the different inlet configurations to show the effect of changes in cowl geometry on cowl performance.

SYMBOLS

D	propeller diameter, feet
H	local total pressure, pounds per square foot
$(H-p_o)/q_o$	total-pressure coefficient
$(H_1-H_2)/q_o$	diffuser pressure-loss coefficient
M_o	Free-stream Mach number
p	local static pressure, pounds per square foot
p_o	free-stream static pressure, pounds per square foot
$(p-p_o)/q_o$	static-pressure coefficient
Δp	average pressure drop across engine, pounds per square foot
$\Delta p/q_o$	cooling-air pressure-drop coefficient
q_c	free-stream impact pressure $(H-p_o)$, pounds per square foot
q_o	free-stream dynamic pressure $\left(\frac{1}{2}\rho V_o^2\right)$, pounds per square foot
T	propulsive thrust, pounds
T_c	propeller thrust coefficient $(T/\rho V_o^2 D^2)$

V_o free-stream velocity, feet per second

V_1 velocity at cowl inlet, feet per second

V_1/V_o inlet velocity ratio

ρ mass density of air (free stream), slugs per cubic foot

DESCRIPTION OF APPARATUS

The tests were made on a right inboard nacelle (fig. 1) of a B-29 airplane, which was powered by an 18-cylinder, double-row radial with a normal cruising rating of 1350 brake horsepower at an engine speed of 2100 rpm and a normal rating of 2000 brake horsepower at 2400 rpm. The engine was equipped with a single-stage engine-driven supercharger, two turbosuperchargers, and a four-bladed propellor. The propeller was 16 feet and 7 inches in diameter and rotated at 0.35 engine speed.

Cowl Inlets

Five cowl-inlet configurations were investigated:

(1) Original production cowl with an oval inlet 38½ by 35 inches (fig. 2(a))

(2) 39½-inch-diameter cowl inlet

(3) 43-inch-diameter cowl inlet (fig. 2(b))

(4) 43-inch-diameter cowl inlet with 27-inch-diameter propeller spinner

(5) 43-inch-diameter cowl inlet with 32-inch-diameter propeller spinner (fig. 2(c))

A comparison of these inlets is shown in figures 3 to 5. The oval inlet and the 39½-inch-diameter inlet were tested with the production cowl afterbody, whereas the 43-inch-diameter inlet was tested with an enlarged cowl afterbody. The cowl-inlet modifications were made forward of the bulkhead at station -40, which was the same for all configurations. (See figs. 3 and 4.) The modifications to the cowl inlet were made without changing the lower lip of the nacelle duct inlet. (See figs. 3 and 5.)

The coordinates of the upper and lower lips of the three cowls and of the two spinners are given in tables I and II. A fixed afterbody was used with the larger spinner. A description of the cowl outlets and flaps is given in reference 1.

Instrumentation

The static-pressure distributions over the upper cowl lips and the lower duct lips were determined by static-pressure orifices installed flush with the lip surfaces, as shown in figure 6. Total pressures at the cowl inlets were measured by eight rakes of shielded total-pressure tubes, which were turned to approximately aline them with the propellor slipstream. (See figs. 6 and 7.) Total pressures at the face of the engine were measured by nine rakes of shielded total-pressure tubes located between adjacent front-row cylinders. (See figs. 8 and 9.) The pressure in front of each of the 18 cylinder heads was measured by a shielded total-pressure tube Hhl located as shown in figures 8 and 9.

The mass rate of cooling-air flow used to determine the cowl-inlet velocity ratio was obtained from measurements of total pressures, static pressures, and temperatures at the cowl outlet. (See fig. 6.) Thrust and drag measurements were recorded by the wind-tunnel balance equipment.

TESTS AND METHODS

Tests were made of each cowl-inlet configuration for a range of inlet-velocity ratios, angles of attack, and propellor thrust coefficients with the propellor operating and for a range of inlet velocity ratios and angles of attack with the propellor removed. The inlet velocity ratio was varied by adjusting the cowl-flap deflection. Tests of the different configurations were made at the same engine and tunnel operating conditions to permit direct comparisons. Each configuration was tested at a pressure altitude of 15,000 feet, indicated airspeeds of 190 miles per hour at angles of attack of -2° and 1° and 150 miles per hour at an angle of attack of 3°. The angle of attack is defined as the inclination of the thrust axis to the wind-tunnel axis.

The two top cowl flaps were fixed at a $2\frac{1}{2}$-inch gap throughout the investigation. For the tests made with the propellor removed, the intercooler flap deflection was maintained at 8° and the oil-cooler flap deflection at 4° for all configurations. For the comparative tests of the different inlets made with the propellor operating, the intercooler and oil-cooler flaps were maintained at approximately the same deflections.

RESULTS AND DISCUSSION

The performance characteristics of a satisfactory cowl include: (1) high critical speeds; (2) high pressure recoveries at the cowl inlet; (3) high pressure recoveries at the face of the engine; and (4) low drag over the range of operating conditions. The cowls tested are evaluated on the basis of these performance characteristics in the following sections.

Critical Speed

The surface static pressures of the upper cowl lips and the lower duct lips are presented as static-pressure coefficients $(p-p_0)/q_0$. The critical speeds of the cowl inlets are discussed as functions of inlet velocity ratio, angle of attack, propeller thrust coefficient, and geometry of the cowl inlet.

Effect of inlet velocity ratio. - The variation of inlet velocity ratio with cowl-flap trailing-edge gap for the different cowl inlets is given in figure 10. With the exception of the 32-inch-diameter spinner installation, the range of inlet velocity ratios over which each of the inlets was tested was small.

The effects of inlet velocity ratio on the pressure distributions over the upper cowl lip and lower duct lip are given in figure 11 for the five cowl-inlet configurations. As the value of V_1/V_0 was increased, the stagnation point moved outward on the upper cowl lips of all configurations, which resulted in lower negative pressure peaks and therefore higher critical speeds.

Changing the inlet velocity ratio has the effect of changing the angle of attack of the lip. At low values of V_1/V_0, the greater portion of the air approaching the cowl flows around it and only a relatively small quantity enters the cowl. The streamlines therefore diverge sharply ahead of the inlet and in effect increase the angle of attack of the cowl-lip sections (sketch (a)), which results in an increase in the negative pressures on the outer surface of the lip. (See reference 2.) Increasing the value of V_1/V_0 decreases the effective angle of attack of the cowl lip and therefore decreases the negative pressure peaks. (See sketch (b).)

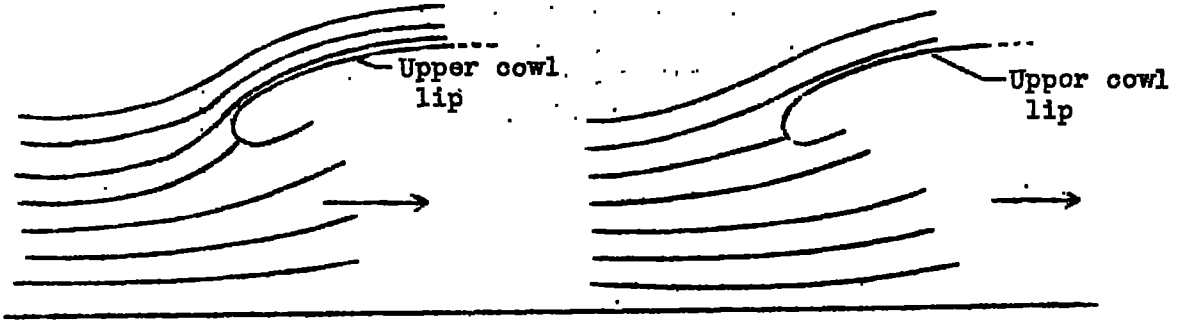

Sketch (a) Sketch (b)

The pressures on the lower lip were not so greatly affected by changes in the cowl-inlet velocity ratio as were the pressures on the upper lip. The pressures on the lower duct lip are principally dependent on the inlet velocity ratio of the nacelle duct inlet. The variation of static pressures on the lower duct lip with oil-cooler and intercooler flap deflections, which control the inlet velocity ratio of the nacelle duct inlet, is shown in figure 12.

Effect of angle of attack. - The effect of angle of attack on the pressure distribution over the upper cowl lip and the lower duct lip of the inlets is presented in figure 13. Increasing the angle of attack of the nacelle increased the negative pressure peaks on the upper cowl lips and decreased the pressure peaks on the lower duct lips. The increase in the negative pressure peaks with increasing angle of attack is attributed to the shifting of the stagnation point on the upper lip to the inner surface of the lip, which results in high local velocities over the leading-edge radius and therefore high negative pressures. Inasmuch as the lower duct lip acts as an inverted airfoil, the effects of changes in angle of attack on the pressure peaks of the lower duct lip were opposite to those that occurred on the upper cowl lip. (See fig. 13.)

Effect of propeller operation. - The pressure coefficients of the upper cowl lip and the lower duct lip were not greatly influenced by changes in propeller thrust. (See figs. 14 and 15.) The data show that the negative pressure coefficients were slightly reduced on both the upper cowl and lower duct lips with an increase in the value of T_c. Greater reductions in the maximum negative pressure coefficients were obtained on the lower duct lip than on the upper cowl lip for the same increase in the value of T_c owing to the increased charge-air flow through the nacelle duct at the higher power, which resulted in a higher inlet velocity ratio of the nacelle duct inlet.

Effect of changes in cowl-inlet geometry. - A comparison was made of the effect on cowl-lip pressure distribution of the changes in the cowl-inlet geometry resulting from increasing the inlet area and from installing the propeller spinners. (See figs. 16 to 19.)

As the size of the cowl inlet was increased from a $38\frac{1}{2}$- by 35-inch oval to a 43-inch diameter, the negative pressure peaks on the upper cowl lip increased 0.30 q_o at an angle of attack of -2° and 0.60 q_o at an angle of attack of 3° for the same cooling-air flow. (See fig. 16.) The greater negative pressures and the lower critical speed experienced with the larger inlet are the result of the combined influence of the lower value of V_1/V_o and the decreased camber of the upper lip of the larger inlet. (See sketch (c).)

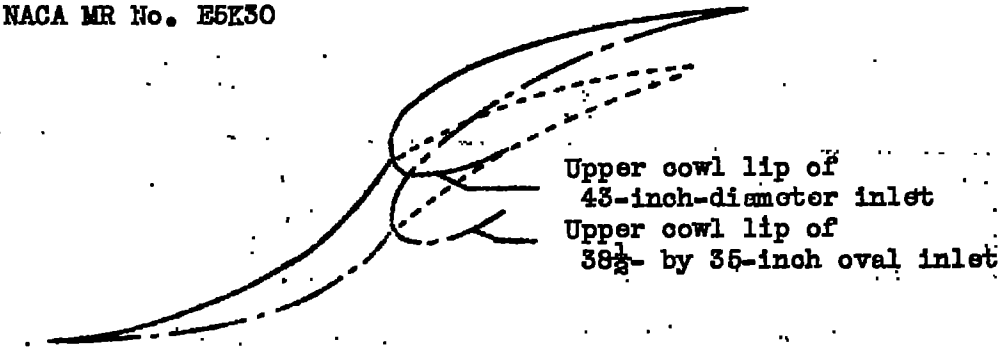

Sketch (c)

Inasmuch as the contours of the upper cowl lips of the oval and the 39⅓-inch-diameter inlets were approximately the same (fig. 4), the pressure distributions over the upper cowl lips were similar. The peak negative pressures on the lower duct lips of the inlets were greater than on the upper lips at an angle of attack of -2° (figs. 16 to 19) and, consequently, the critical speeds of the cowls at an angle of attack of -2° were determined by the lower duct lips.

The negative pressure peaks on the upper cowl lip of the 43-inch-diameter inlet were reduced 0.20 q_o at an angle of attack of -2° by the addition of the 27-inch-diameter spinner and 0.30 q_o by the addition of the 32-inch-diameter spinner. (See fig. 17.) At an angle of attack of 3 , the negative pressure peaks were reduced 0.20 q_o by the 27-inch-diameter spinner and 0.55 q_o by the 32-inch-diameter spinner. These comparisons were made at the same air flows through the inlet. The addition of the spinners increased the cowl-inlet velocity ratio and permitted a more gradual deflection of the streamlines around the cowl, thereby reducing the effective angle of attack of the cowl lips. (See sketches (d) and (e).)

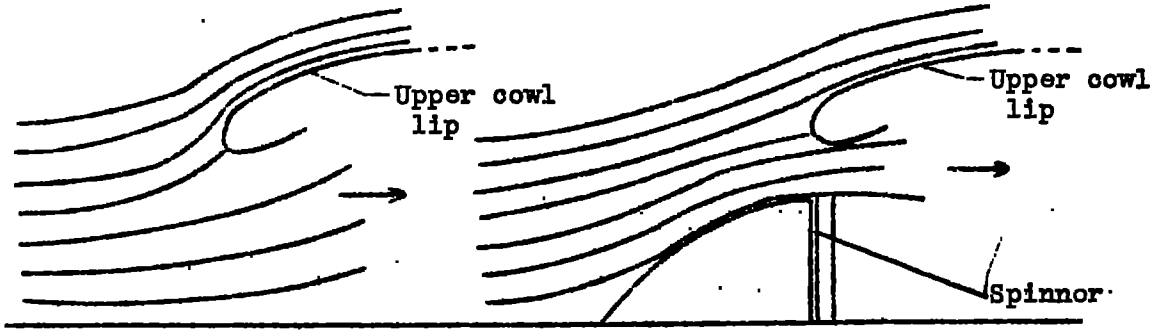

Sketch (d) Sketch (e)

The lower duct-lip pressures (figs. 18 and 19) were arrproximately the same for all configurations tested, with the peak negative pressures for the large inlet slightly higher than for the other inlets.

A summary of the data showing the effects of inlet velocity ratio, angle of attack, and changes in the geometry of the cowl inlet on the peak negative pressures on the upper cowl lips is presented in figure 20 for the different configurations.

Based on the peak negative pressures given in figures 16 and 18, the critical Mach numbers (fig. 21) of the different cowls were determined by the method given in reference 3. Inasmuch as the data have not been corrected for the effects of tunnel-wall restriction, the critical Mach numbers presented serve only as a basis for comparison. The true critical Mach numbers obtained in flight would be somewhat greater than those obtained in the wind tunnel.

A comparison of the critical speeds of the different cowl inlets (fig. 21) shows that the critical speed of the $38\frac{1}{2}$- by 35-inch oval inlet was slightly greater than that of the 43-inch-diameter inlet. The addition of the 32-inch-diameter spinner to the 43-inch-diameter inlet increased the critical Mach number to nearly that of the oval inlet. For all the inlets investigated the critical Mach number of the lower duct lips was from 0.05 to 0.09 less than for the upper cowl lips.

Total Pressures at Cowl Inlet

The total pressures at the cowl inlet are less than the total pressure of the free stream by an amount equal to the losses ahead of the inlet. These losses result from the drag of the propeller blade shanks and the hub or spinner. The effects of the increased inlet diameters and the propeller spinners on the cowl-inlet pressures are presented in this section as functions of inlet velocity ratio, angle of attack, and propeller operating conditions. The distributions of total pressures at the cowl inlet are presented as contour maps in figures 22 to 25 and the average weighted total pressures at the upper and lower halves of the different inlets are given in figure 26.

Effect of inlet velocity ratio. - The total-pressure contours for the oval and the 43-inch-diameter inlets were not appreciably affected by changes in the inlet velocity ratio. (See figs. 22 and 23.) For the spinner configurations, however, the total-pressure distribution around the inlet annulus was not so uniform at low values as at high values of V_1/V_0. (See figs. 24 and 25.) The pressures at the upper half of the inlets of the spinner configurations decreased with a decrease in inlet velocity ratio, whereas the pres-

sures in the lower half of the inlets were unchanged. The decrease in the total pressures (about 0.12 q_c) at the upper half of the cowl inlet caused by the addition of the 32-inch-diameter spinner was more pronounced than that caused by the 27-inch-diameter spinner (only 0.03 q_c) at angles of attack of -2° and 3°.

The low recoveries in the upper portion of the inlet at low inlet velocity ratios are attributed to separation of the cooling-air flow from the upper surface of the spinner. A detailed discussion of the boundary-layer separation phenomena is given in references 2 and 4.

For the configurations without spinners, the cowl-inlet pressures measured with the propeller removed increased slightly with increased inlet velocity ratio. (See figs. 26(a) to 26(c).) With the propeller operating, changes in the inlet velocity ratio had little effect on the inlet total pressures.

Effect of angle of attack. - The total-pressure contours for the oval and 43-inch-diameter inlets were almost symmetrical about the thrust axis at an angle of attack of -2° for all test conditions. (See figs. 22 and 23.) For the configurations without spinners, an increase in angle of attack from -2° to 3° decreased the average pressures at the upper halves of the inlets by 0.10 q_c and increased the pressures in the lower halves by about 0.10 q_c. (See figs. 26(a) to 26(c).) For the configurations with spinners (figs. 26(d) and 26(e)) the effect of increasing the angle of attack on inlet pressures was more pronounced and losses of as much as 0.20 q_c occurred in the upper half of the cowl inlet.

Effect of propeller operation. - The total pressures at the inlet of each configuration were considerably higher and more uniform with the propeller removed than with the propeller operating. (See figs. 22 to 25.) The reduction in pressure resulting from the installation of the propeller was about 0.07 q_c for the 43-inch-diameter inlet and about 0.14 q_c for the smaller oval inlet. (See fig. 26.) Changes in the propeller thrust coefficient T_c (fig. 27) had no appreciable effect on the cowl-inlet pressures.

Effect of changes in cowl-inlet geometry. - The averages of the weighted total pressures at the cowl inlets of several configurations are compared at the same cooling-air flow in figure 28. With the propeller removed (fig. 28(a)), the average pressures at the oval inlet were slightly higher than the pressures at the 43-inch-diameter inlet. The most significant changes resulting from the addition of the 32-inch-diameter spinner to the 43-inch-diameter inlet were the decrease of the total pressures in the upper half of the inlet at an

angle of attack of 3° and the increase of the total pressures in the lower half of the inlet at an angle of attack of -2°.

With the propeller operating (fig. 28(b)), increasing the inlet area increased the average of the weighted total pressures over the entire inlet by about 0.07 q_c at all angles of attack. Proportionately less of the larger inlet is blocked by the propeller, which accounts for the higher pressures obtained at the 43-inch-diameter inlet. The average pressures at the 43-inch-diameter inlet were further increased by about 0.07 q_c at an angle of attack of -2° by the addition of the propeller spinners. At an angle of attack of 3°, the spinners improved the average inlet pressure by only 0.03 q_c.

Total Pressures at Face of Engine

The total pressures at the face of the engine are less than the pressures at the inlet owing to the diffuser losses. The diffuser losses, which vary with operating conditions and diffuser design, are shown in figures 29 and 30 for several inlet configurations. The values presented in these figures have been calculated from the average of the weighted total pressures measured over the entire face of the engine. Increasing the mass flow of cooling air corresponding to higher engine pressure drops $\Delta p/q_c$ increased the diffuser losses. The diffuser losses for the spinner configurations were considerably higher and increased more rapidly with an increase in the value of $\Delta p/q_c$ than the losses for the other configurations.

The contour maps showing the total-pressure distributions at the face of the engine are presented in figures 31 to 33 for several configurations. The average weighted total pressures at the upper and lower halves of the face of the engine, as measured by the intercylinder total-pressure rakes (figs. 8 and 9), and the average total pressures of the upper and lower nine cylinder heads with the different configurations, as measured by total-pressure tube Hh1, are given in figure 34.

Effect of inlet velocity ratio. - The pressure contours at the face of the engine for several inlet configurations were about the same for all inlet velocity ratios. (See figs. 31 to 33.)

Increasing the inlet velocity ratio had little effect on cylinder-head pressures for the different configurations. The pressures of the upper nine cylinder heads definitely increased for the configuration with the 32-inch-diameter spinner. (See fig. 34(e).) For all configurations, however, the average pressures over the face of the engine, which included both cylinder-head and barrel pressures, decreased with an increase in the value of V_1/V_0.

Effect of angle of attack. - The nonuniform pressures observed at the cowl inlets also occurred at the face of the engine. (See figs. 31 to 33.) The pressures at the face of the upper half of the engine (fig. 34) were much lower than the pressures at the lower half of the engine. As the angle of attack was increased from -2° to 3°, the difference between the pressures at the upper and lower halves of the engine increased; at an angle of attack of 3° the average pressures in the upper half of the engine were about 0.10 to 0.15 q_c less than at the lower half of the engine. (See figs. 34(a) to 34 (c).) The largest pressure differences between the upper and lower halves of the engine were measured for the configurations with spinners (fig. 34(e)).

Effect of changes in cowl-inlet geometry. - The average of the 18 cylinder-head pressures measured with the 43-inch-diameter inlet was about 0.10 q_c greater than that measured with the smaller oval inlet. (See figs. 35 and 36.) The addition of the 27-inch-diameter spinner to the large inlet increased the average cylinder-head pressure about 0.03 q_c, whereas the addition of the 32-inch-diameter spinner had no appreciable effect on the average cylinder-head pressures. The average pressures over the face of the engine, which included the pressures of both the cylinder heads and barrels, were also greater for the large circular inlet than for the small oval inlet.

The pressure gradients from the tunnel free stream to the face of the engine are compared at the same cooling-air flow in figure 37 at angles of attack of -2° and 3° for the different inlet configurations.

Installation Drag

The comparative drag of the 43-inch-diameter inlet and the 38½- by 35-inch oval inlet was determined by testing each of the inlets with a production afterbody. The tests were conducted at a pressure altitude of 15,000 feet and an indicated airspeed of 190 miles per hour. The drag of the 43-inch-diameter inlet with and without the 32-inch-diameter spinner is compared with the drag of the oval inlet in figure 38 over a range of cooling-air pressure drops $\Delta p/q_c$ for normal cruising and normal rated powers.

The average cooling drag of the installation with the 43-inch-diameter inlet was about 60 horsepower less at normal cruising power and 51 horsepower less at normal rated power than for the installation with the 38½- by 35-inch oval inlet. For high-speed flight of the airplane at an altitude of 15,000 feet and an indicated airspeed of 250 miles per hour, the lower cooling drag of the 43-inch-diameter inlet is equivalent to an increase of about 108 thrust horsepower. (See fig. 38(b).) This reduction in cooling drag results from lower pressure losses in the inlet and diffuser of the 43-inch-diameter inlet cowl.

The addition of the 32-inch-diameter spinner to the 43-inch-diameter inlet decreased the drag of the installation by about 7 horsepower at an indicated airspeed of 190 miles per hour and by about 15 horsepower at the high-speed condition of 250 miles per hour indicated airspeed.

SUMMARY OF RESULTS

The following results were obtained from an investigation in the altitude wind tunnel of cowl inlets for the B-29 power-plant installation:

1. The critical speeds of the upper cowl lips and lower duct lips of the five inlet configurations investigated increased with increases in the cowl-inlet velocity ratio. The maximum negative pressures at the lower duct lips were more affected by variation in the inlet velocity ratio of the nacelle duct than by variation in the inlet velocity ratio of the cowl inlet.

2. The critical Mach number of the upper lip of the 38½- by 35-inch oval inlet was somewhat greater than for the 43-inch-diameter inlet. The addition of the 32-inch-diameter spinner to the 43-inch-diameter inlet increased the critical Mach number to nearly that of the oval inlet. For all inlets tested the critical Mach number of the lower duct lips was from 0.050 to 0.092 less than for the upper cowl lips.

3. Increasing the cowl-inlet area from the 38½- by 35-inch oval inlet to the 43-inch-diameter inlet increased the average cowl-inlet pressures by about 0.07 of the free-stream impact pressure q_0 at all angles of attack, caused by the more effective blade sections behind which the larger inlet was located. The average cowl-inlet pressures were further increased by about 0.07 q_0 at an angle of attack of -2° by the addition of the 27-inch- and 32-inch-diameter propeller spinners to the 43-inch-diameter cowl inlet.

4. Changes in the propeller thrust coefficient had no appreciable effect on the cowl-inlet pressures.

5. With the propeller operating, changes in the inlet velocity ratio had little effect on the cowl-inlet pressures of the configurations without spinners. The average pressures at the upper half of the inlet with the 32-inch-diameter spinner, however, decreased 0.14 q_0 with a decrease in the value of inlet velocity ratio over the operating range investigated. This effect is attributed to separation of the air flow from the upper surface of the spinner.

6. Increasing the angle of attack from -2° to 3° reduced the total pressures in the upper half of the different inlets by about 0.10 to 0.20 q_0; the greatest reductions occurred with the spinner installations.

7. The cowl-diffuser losses for the 32-inch-diameter spinner installation were considerably higher and increased more rapidly with cooling-air flow than the losses for the installations without spinners.

8. The average of the 18 cylinder-head pressures obtained with the 43-inch-diameter inlet was about 0.10 q_0 higher than those obtained with the oval inlet at all angles of attack. The addition of the 27-inch-diameter spinner to the larger inlet further increased the average cylinder-head pressure by about 0.03 q_0, whereas the 32-inch-diameter spinner had no appreciable effect on the average pressure.

9. Changes in inlet velocity ratio, angle of attack, and propeller operation had the same general effect on the average pressures over the face of the engine as on the pressures at the cowl inlet.

10. At a pressure altitude of 15,000 feet and an indicated airspeed of 190 miles per hour, the average cooling drag of the installation with the 43-inch-diameter inlet was about 60 horsepower less at normal cruising power than with the 38- by 35-inch oval inlet. For the high-speed condition (indicated airspeed, 250 mph) the lower cooling drag of the 43-inch-diameter cowl inlet is equivalent to an increase of 108 thrust horsepower.

Aircraft Engine Research Laboratory,
National Advisory Committee for Aeronautics,
Cleveland, Ohio

REFERENCES

1. Wyatt, DeMarquis D., and Conrad, E. William: An Investigation of Cowl-Flap and Cowl-Outlet Designs for the B-29 Power-Plant Installation. NACA MR No. E5K30a, 1946.

2. Katzoff, Samuel: High-Altitude Cooling. V-Cowling and Ducting. NACA ARR No. L4I11d, 1944.

3. von Kármán, Th.: Compressibility Effects in Aerodynamics. Jour. Aero. Sci., vol. 8, no. 9, July 1941, pp. 337-356.

4. Czarnecki, K. R., and Nelson, W. J.: Wind-Tunnel Investigation of Rear Underslung Fuselage Ducts. NACA ARR No. 3I21, 1943.

TABLE I - COORDINATES OF UPPER COWL-LIP AND LOWER DUCT-LIP SECTIONS

X (in.)	Y, in.							
	Upper lip						Lower Lip	
	38½- by 35-inch oval cowl inlet		39½-inch diameter cowl inlet		43-inch diameter cowl inlet		All cowl inlets	
	Outer surface	Inner surface	Outer surface	Inner surface	Outer surface	Inner surface	Outer surface	Inner surface
0	0	0	0	0	0	0		
.25	1.44	-.87	1.18	-.68	1.18	-.56		
.50	2.12	-1.18	1.81	-.81	1.56	-.68		
.75	2.50	-1.28	2.25	-.81	1.94	-.75		
.87							0	0
1.00	2.75	-1.37	2.62	-.81	2.18	-.72	-.75	.37
1.25	3.12	-1.44	2.93	-.81	2.37	-.68	-1.25	.56
1.50	3.37	-1.46	3.18	-.81	2.63	-.65	-1.69	.62
1.75	3.62	-1.46	3.44	-.81	2.81	-.62	-2.00	.68
2.00	3.87	-1.43	3.62	-.81	3.00	-.59	-2.25	.68
2.25	4.06	-1.41	3.87	-.81	3.12	-.56	-2.50	.68
2.50	4.25	-1.37	4.06	-.81	3.25	-.53	-2.68	.65
2.75	4.41	-1.31	4.25	-.81	3.44	-.50	-2.87	.62
3.00	4.62	-1.25	4.44		3.56	-.47	-3.06	.59
3.25	4.78	-1.12	4.56		3.68	-.41	-3.25	.59
3.50	5.00	-.94	4.75		3.81	-.37	-3.37	.56
3.75	5.06	-.78	4.94		3.94	-.31	-3.56	.50
4.00	5.25	-.62	5.06		4.06	-.25	-3.75	.44
5.00	5.75	.44	5.62		4.50	0	-4.25	.12
6.00	6.25	2.25	6.06		4.94	.25	-4.63	-.12
7.00	7.71	3.50	6.50		5.31	.56	-4.94	-.50
8.00	7.06	4.12	6.94		5.62		-5.25	-.94
9.00	7.50	4.28	7.31		6.00		-5.50	-1.37
10.00	7.81	4.31	7.68		6.25		-5.87	-1.87
11.00	8.12	4.50	8.00		6.56		-6.12	-2.37
12.00	8.50	4.53	8.31		6.87		-6.31	-2.81
13.00	8.75	4.56	8.62		7.12		-6.62	-3.31
14.00	9.00	4.62	8.94		7.37		-6.87	-3.75
16.00	9.50						-7.31	-4.75
18.00	9.87						-7.75	-5.50
20.00	10.18						-8.25	-6.18
22.00	10.44						-8.62	-6.87
24.00	10.62						-9.00	-7.37

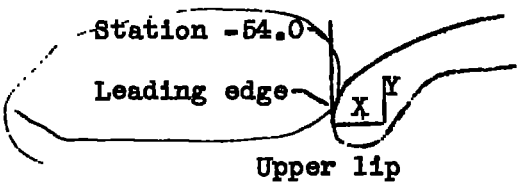

Upper lip

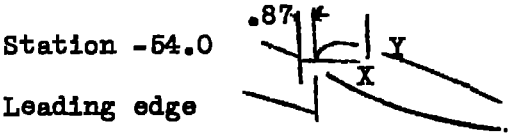

Lower lip

National Advisory Committee for Aeronautics

Reg. 18

TABLE II - COORDINATES OF 27-INCH- AND 32-INCH-DIAMETER PROPELLER SPINNERS

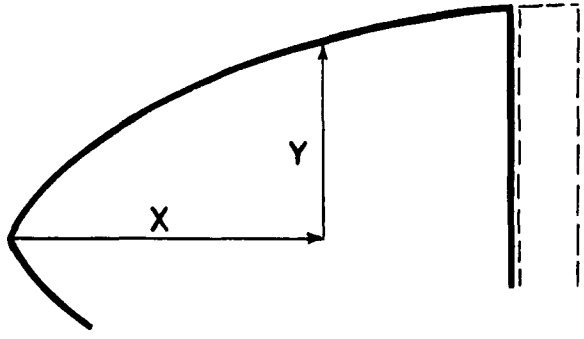

X	0	1	2	4	6	8	10	12	14	16	18	20	22	24	26	28	30
Y	0.	1.95	3.	4.57	5.88	7.03	8.04	8.92	9.69	10.38	11.01	11.58	12.10	12.57	12.98	13.32	13.50

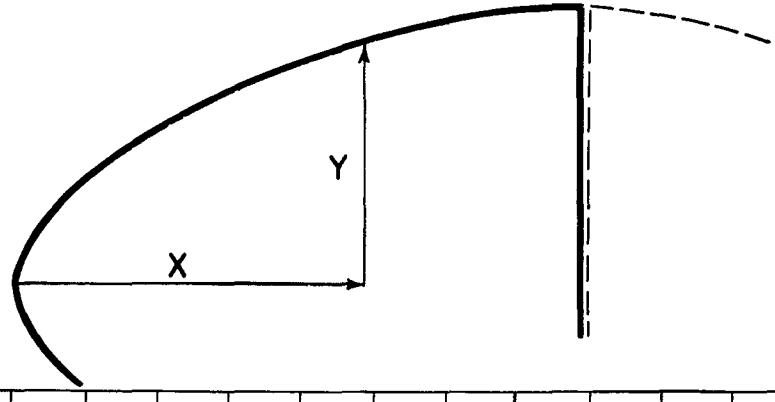

NATIONAL ADVISORY
COMMITTEE FOR AERONAUTICS

X	0	.5	1.0	2.0	4.0	6.0	8.0	10.0	12.0	14.0	16.0	18.0	20.0	22.0	24.0	26.0	28.0	30.0	32.0	34.0	34.9
Y	0	1.25	2.12	3.23	5.12	6.62	8.06	9.18	10.18	11.25	12.00	12.68	13.31	13.87	14.43	14.93	15.31	15.68	15.93	16.00	16.00

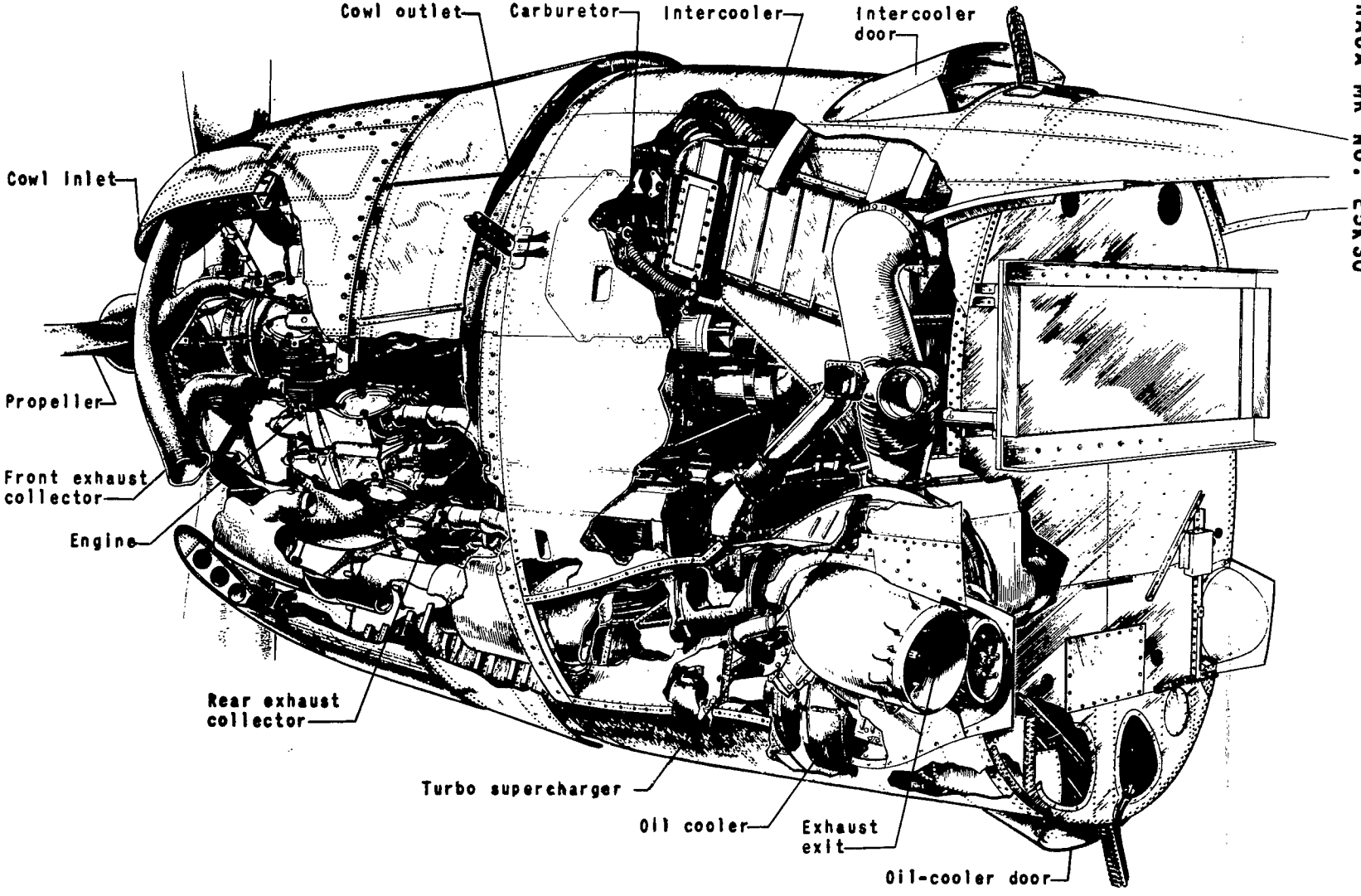

NATIONAL ADVISORY COMMITTEE FOR AERONAUTICS

Figure 1. - Right inboard nacelle with production cowl inlet.

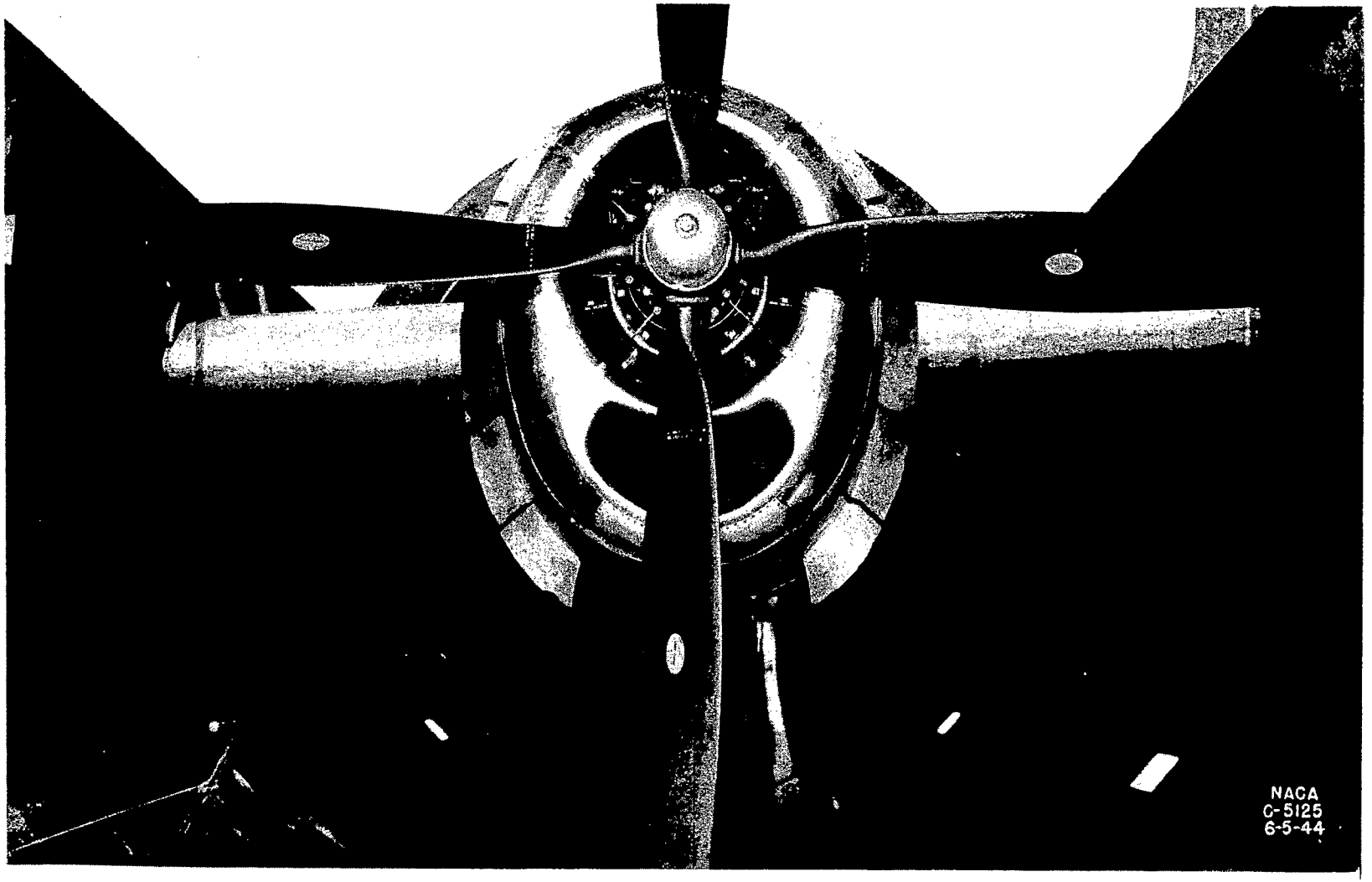

(a) $38\frac{1}{2}$- by 35-inch oval (original) cowl inlet.

Figure 2. - Front view of power-plant installation in altitude wind tunnel with various cowl-inlet configurations.

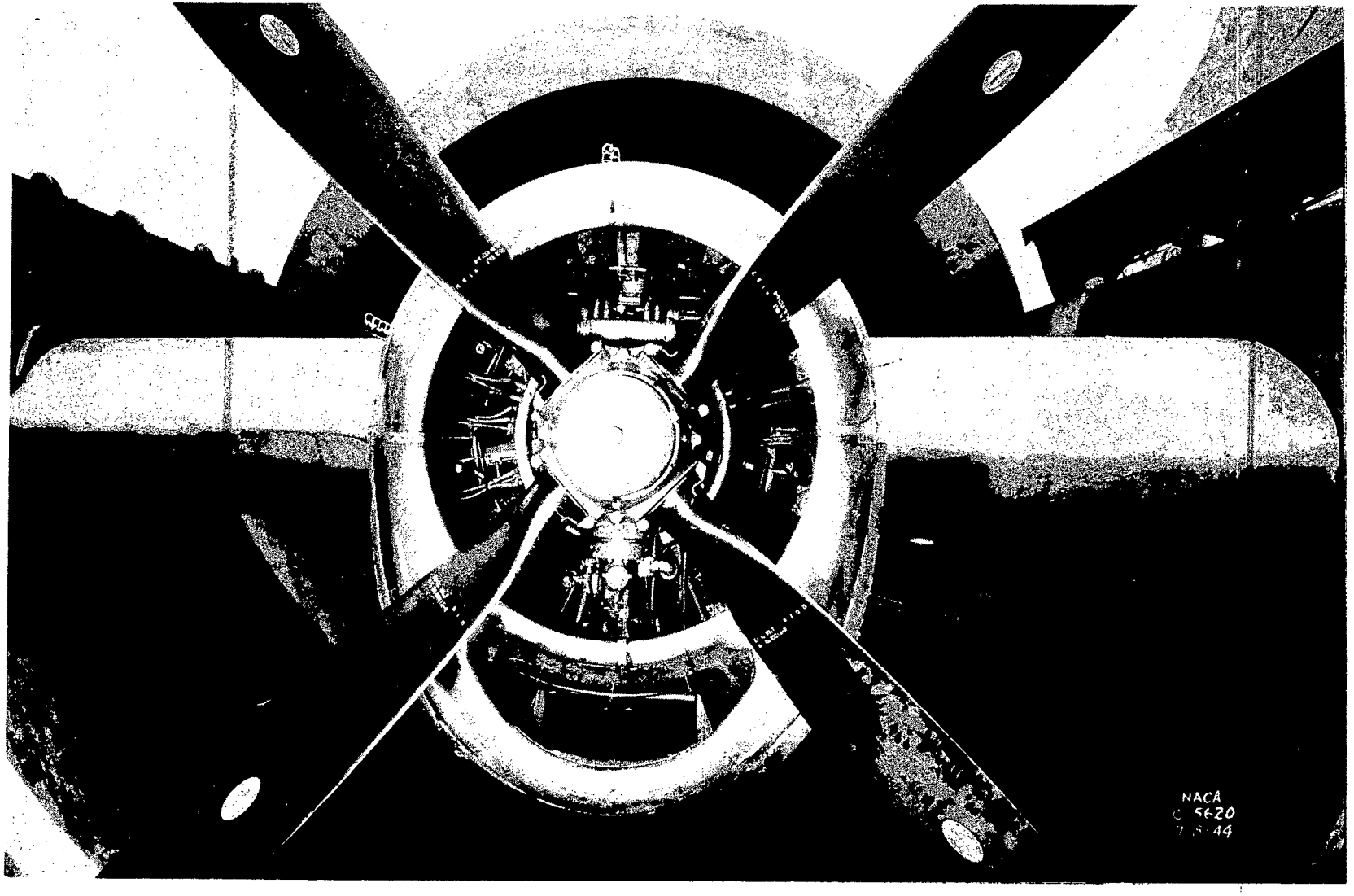

(b) 43-inch-diameter cowl inlet without spinner.

Figure 2. - Continued. Front view of power-plant installation in altitude wind tunnel with various cowl-inlet configurations.

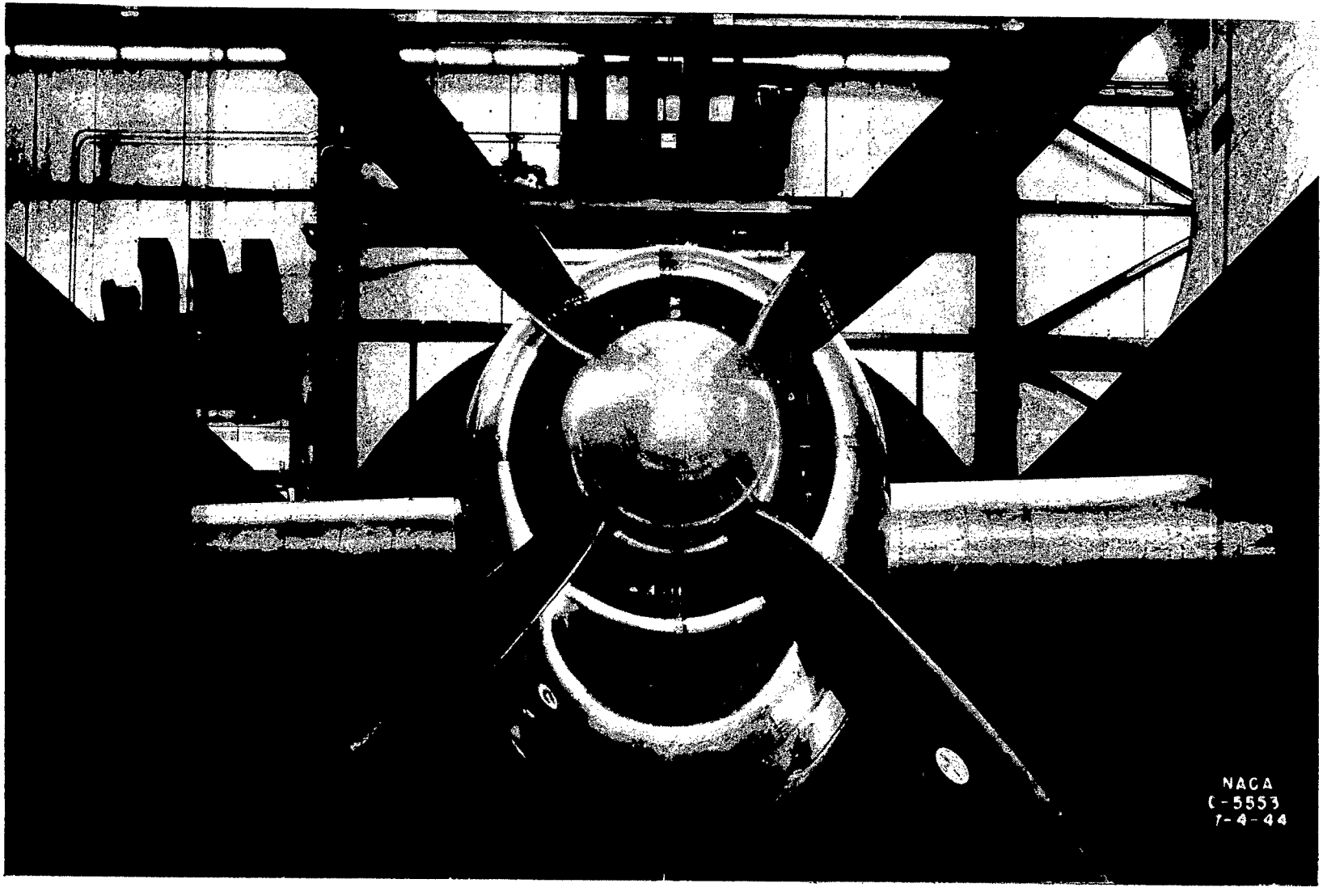

(c) 43-inch-diameter cowl inlet with 32-inch-diameter spinner.

Figure 2. - Concluded. Front view of power-plant installation in altitude wind tunnel with various cowl-inlet configurations.

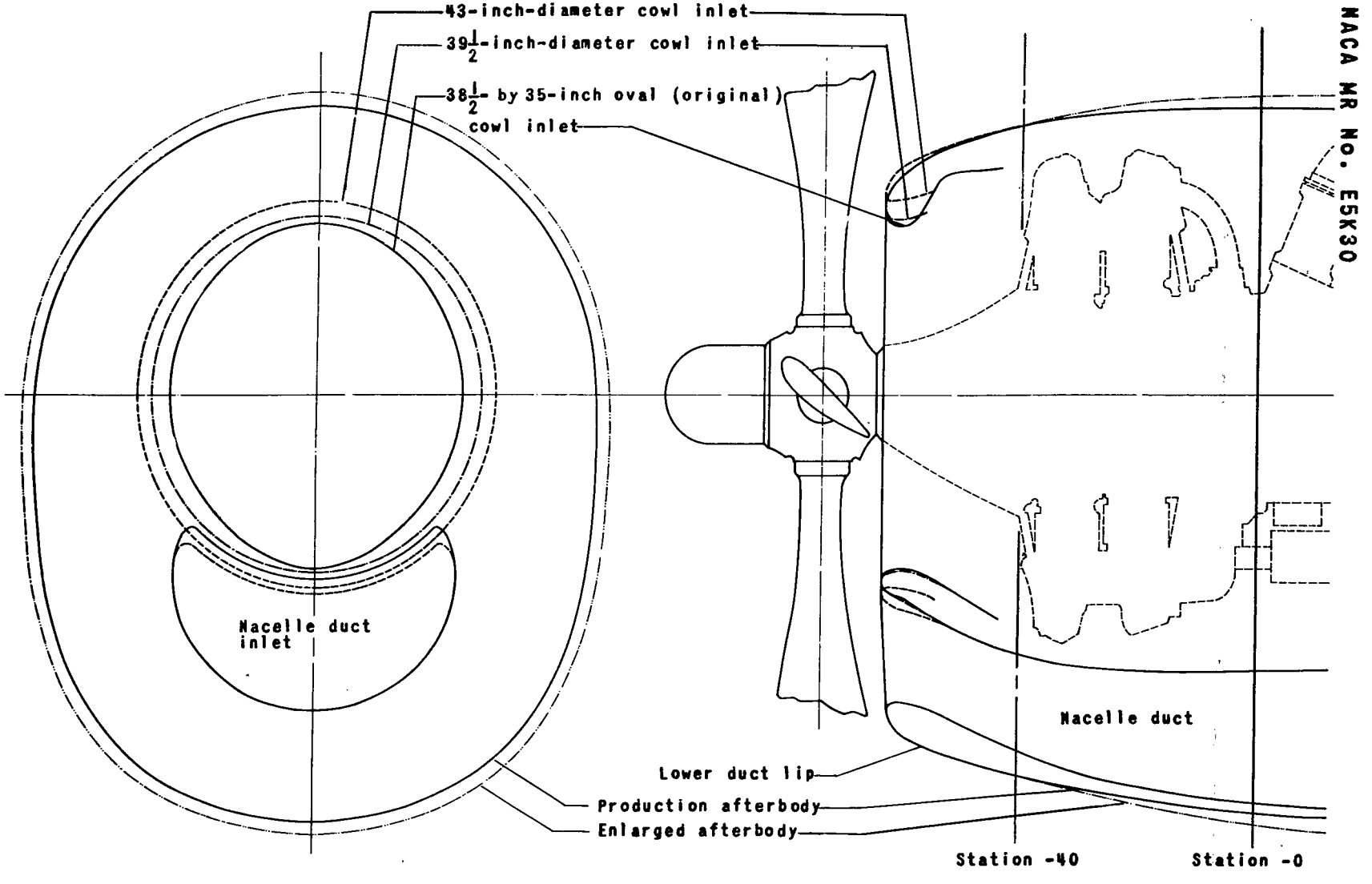

Figure 3. - Composite drawing showing cowl inlets.

NATIONAL ADVISORY
COMMITTEE FOR AERONAUTICS

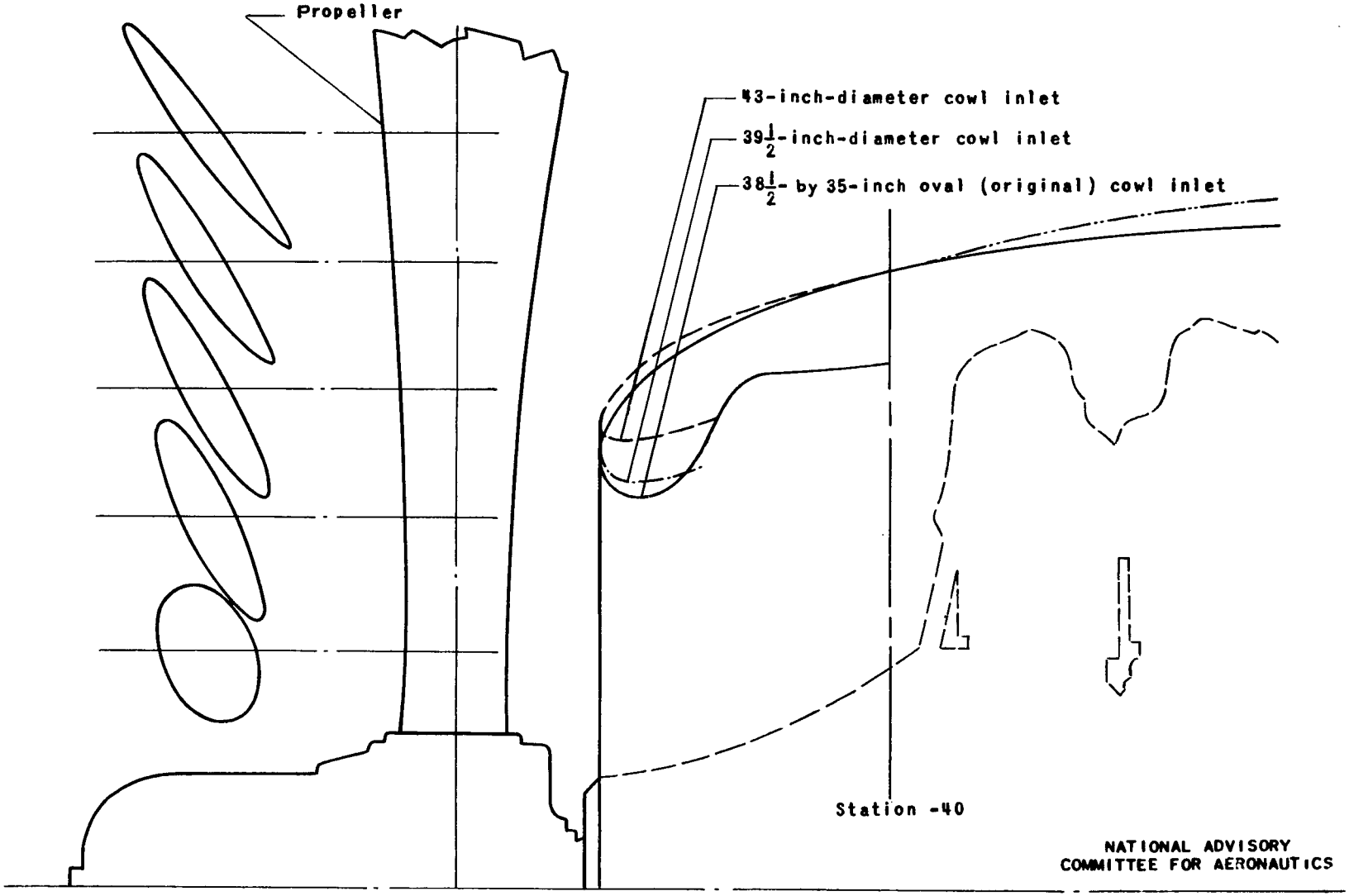

Figure 4. - Composite drawing of upper-lip sections of cowl inlets showing propeller blade sections.

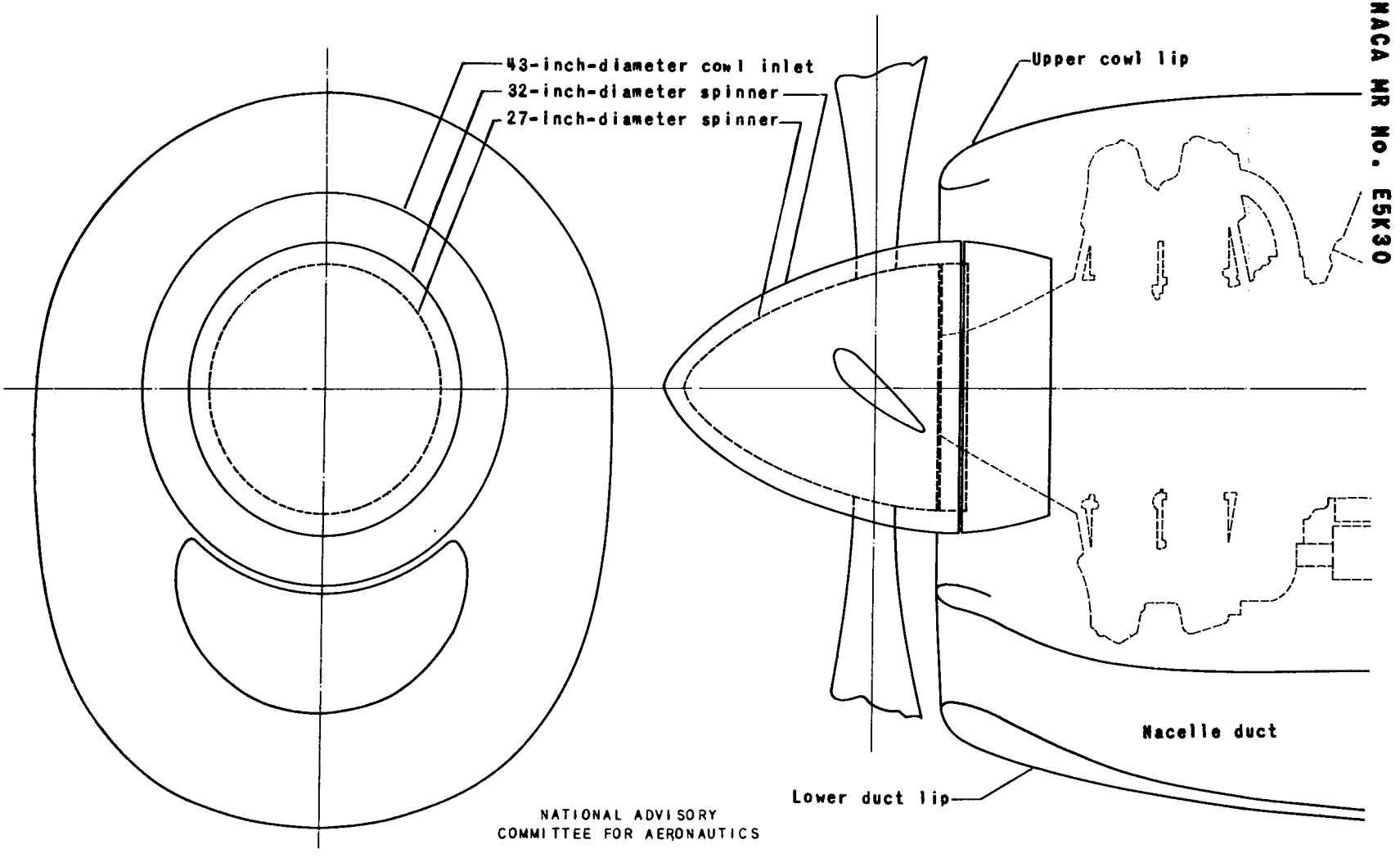

Figure 5. - Composite drawing showing 27-inch-and 32-inch-diameter propeller spinners installed on a 43-inch-diameter cowl inlet.

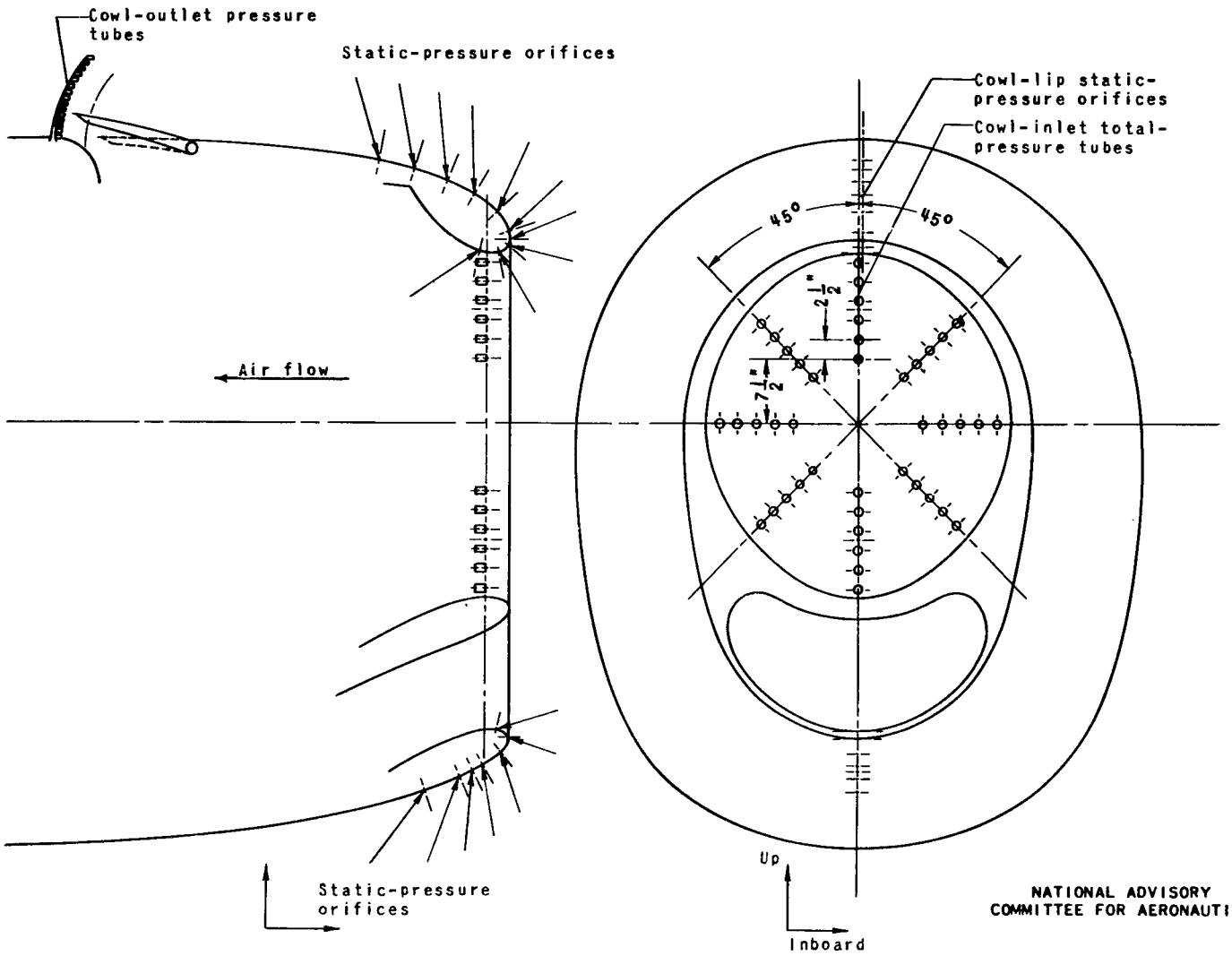

Figure 6. - Location of cowl-inlet and outlet total-pressure tubes and cowl-lip-surface static-pressure orifices on $38\frac{1}{2}$- by 35-inch oval (original) cowl inlet.

Figure 7. - Installation of cowl-inlet total-pressure tubes.

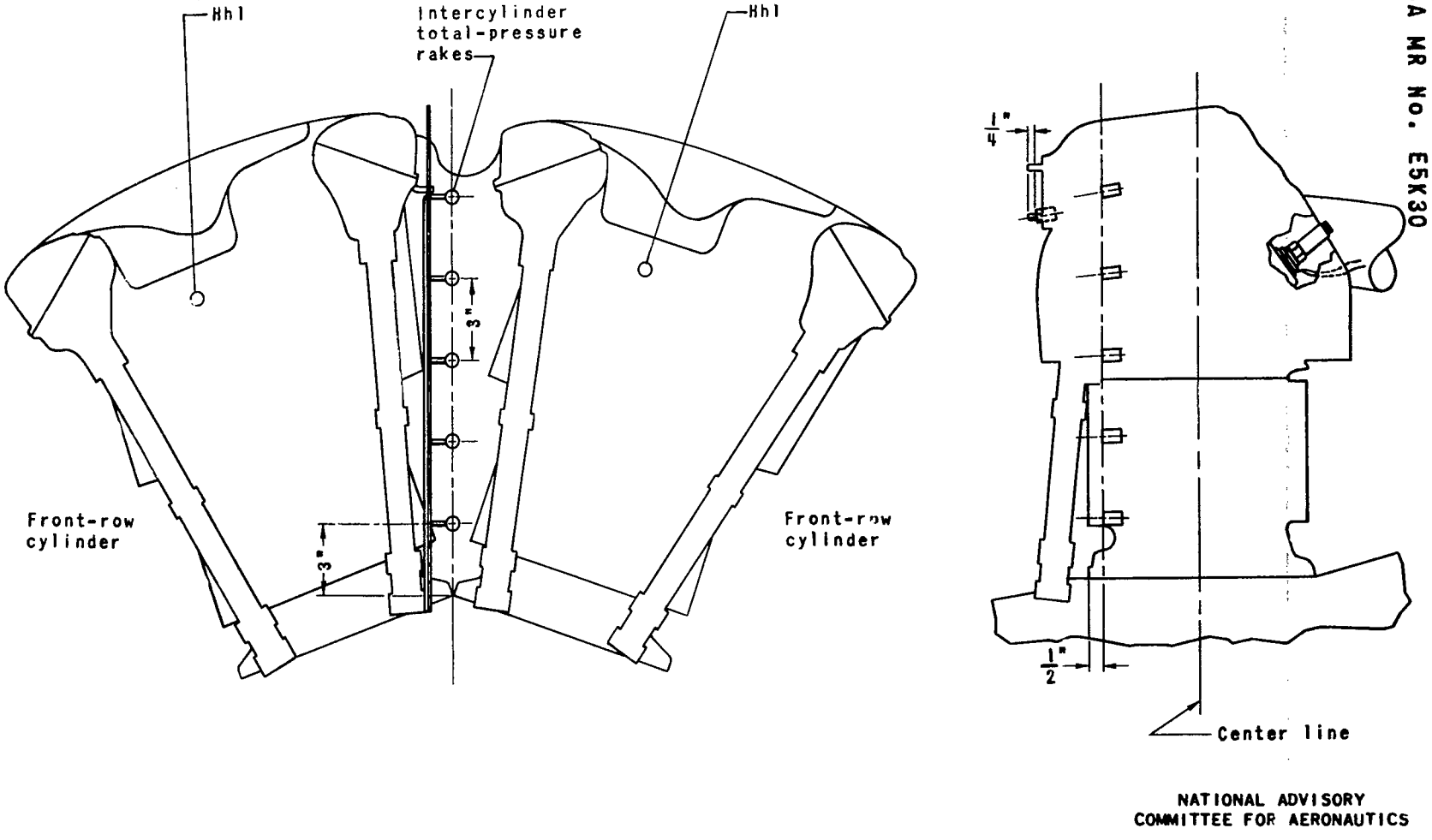

Figure 8. - Location of intercylinder total-pressure tube rakes and center front cylinder-head total-pressure tube Hhl.

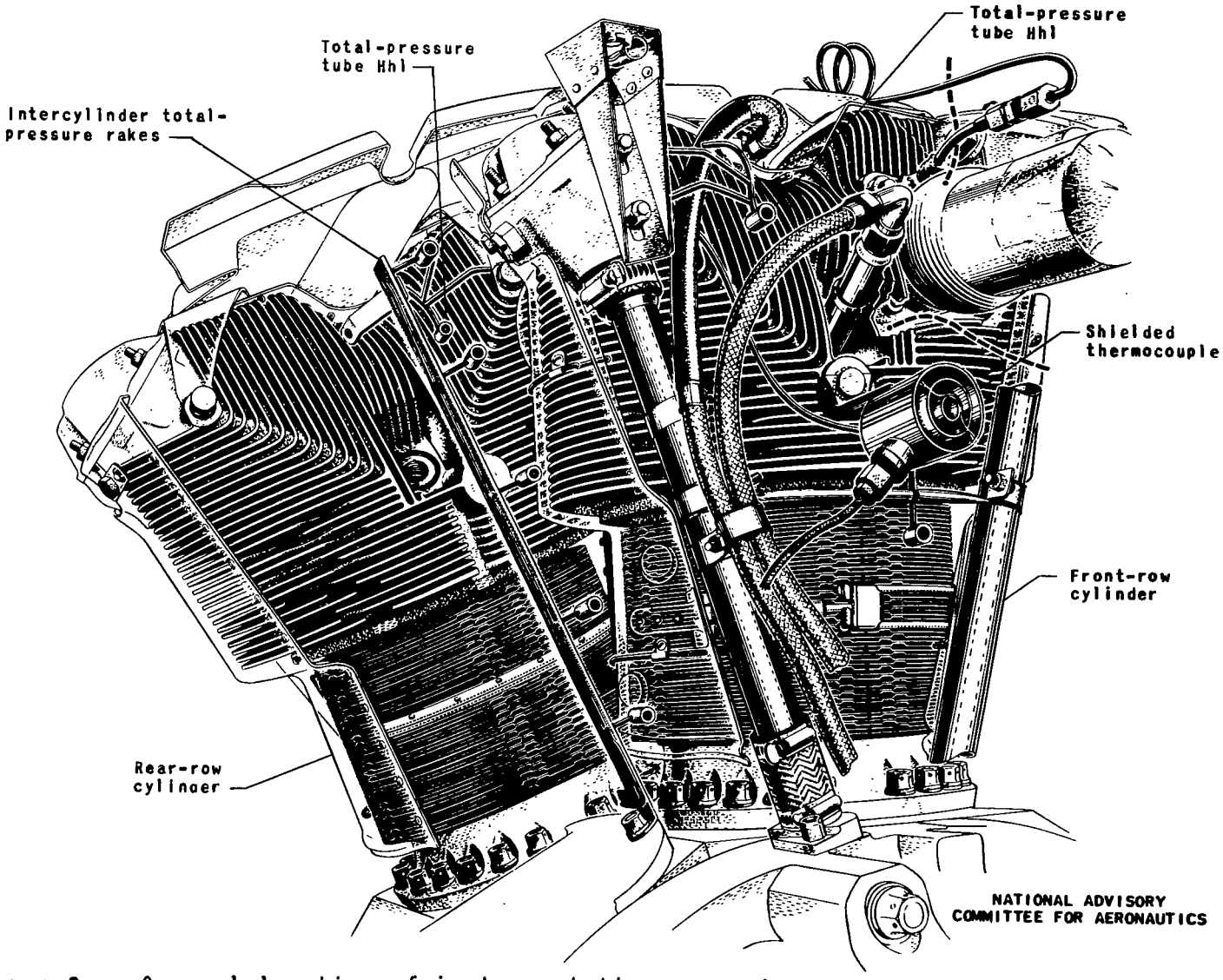

Figure 9. - General location of instrumentation on engine cylinders.

NACA MR No. E5K30

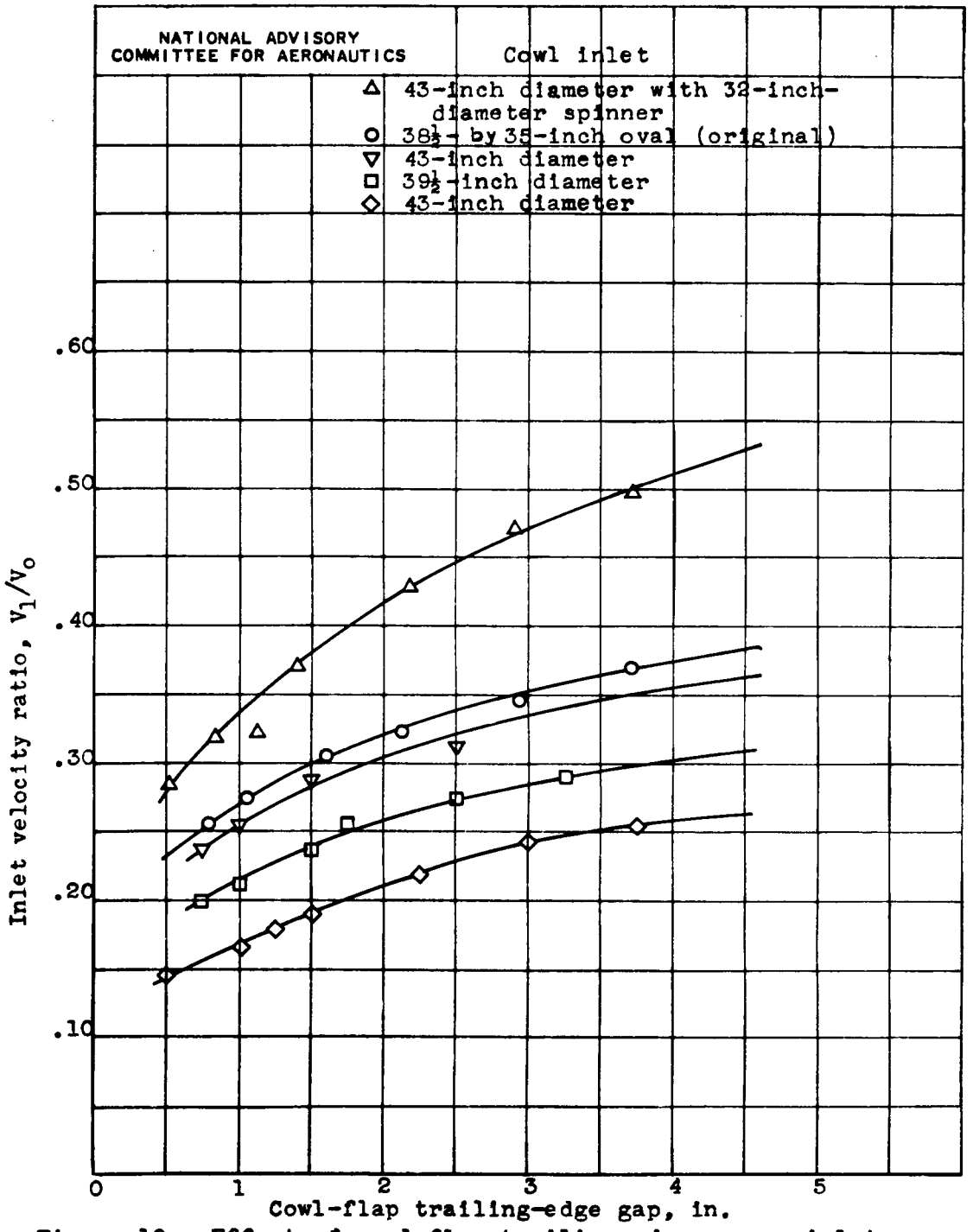

Figure 10.- Effect of cowl-flap trailing-edge gap on inlet velocity ratio. Pressure altitude, 15,000 feet; indicated airspeed, 190 miles per hour; angle of attack, -2°; thrust coefficient, 0.038.

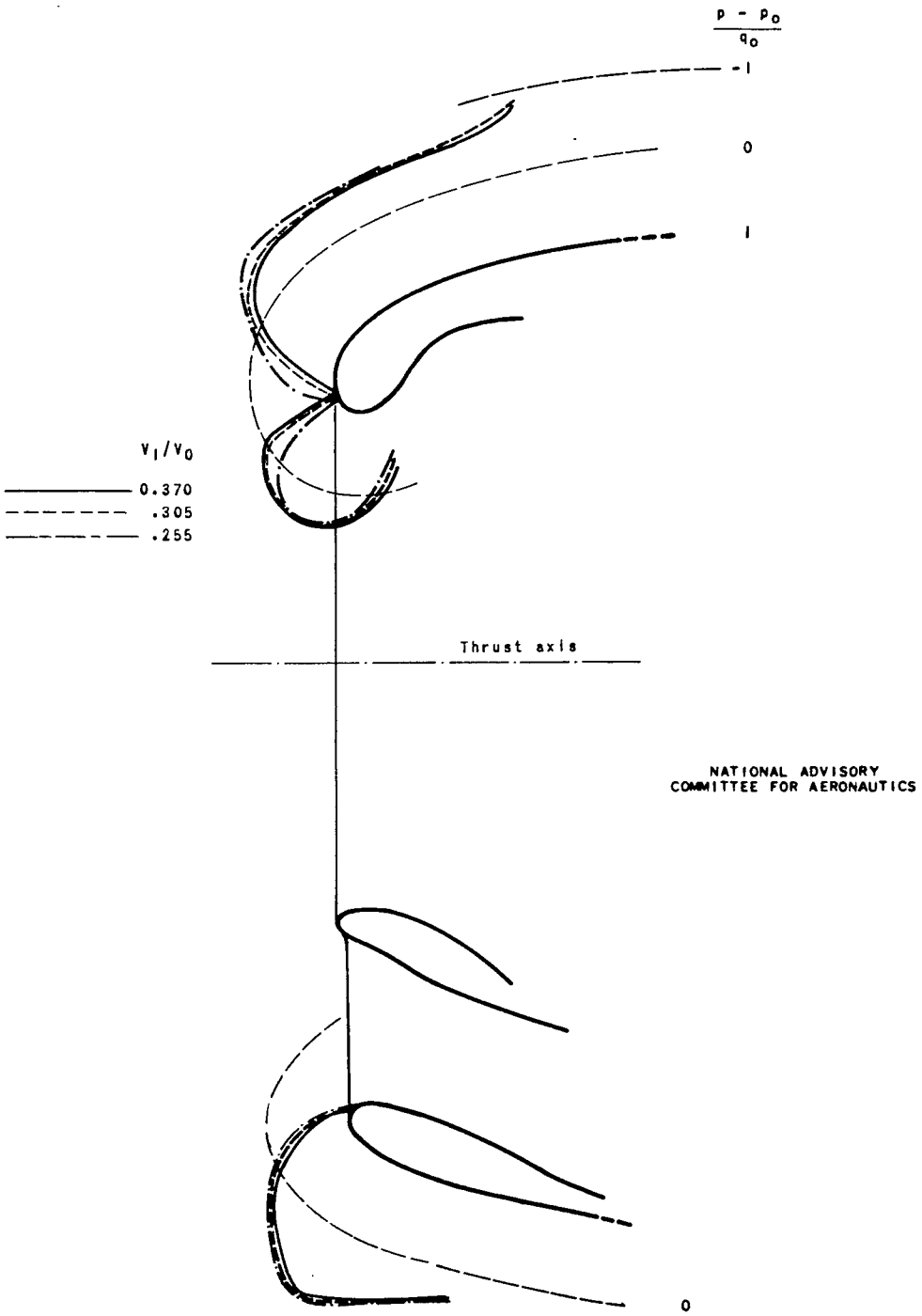

(a) $38\frac{1}{2}$ by 35-inch oval (original) cowl inlet.

Figure 11. - Effect of inlet velocity ratio on pressure distribution over the upper cowl lip and lower duct lip. Propeller operating; thrust coefficient, 0.038; angle of attack, -2°.

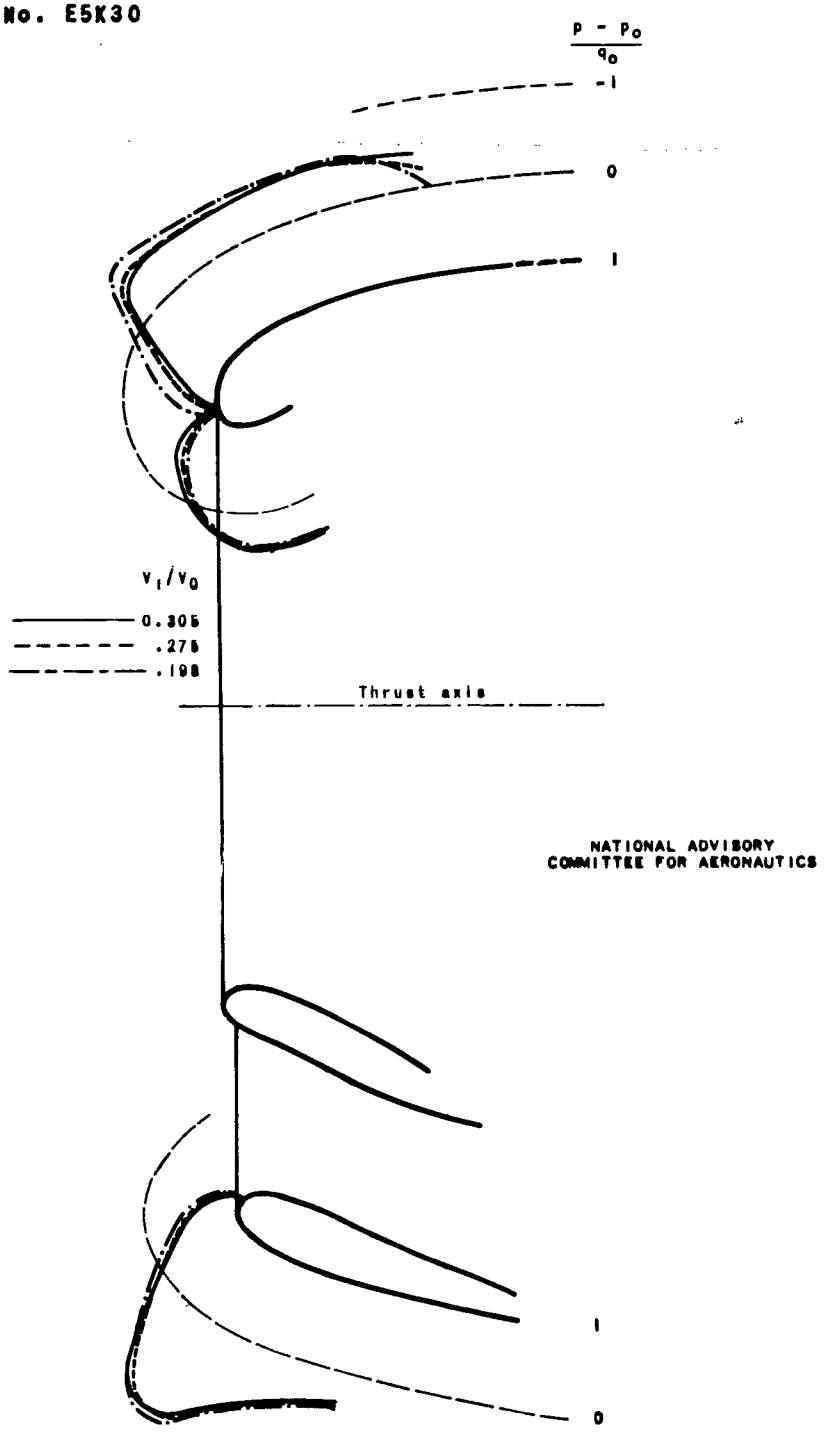

(b) $39\frac{1}{2}$-inch-diameter cowl inlet.

Figure 11. - Continued. Effect of inlet velocity ratio on pressure distribution over the upper cowl lip and lower duct lip. Propeller operating; thrust coefficient, 0.038; angle of attack, -2°.

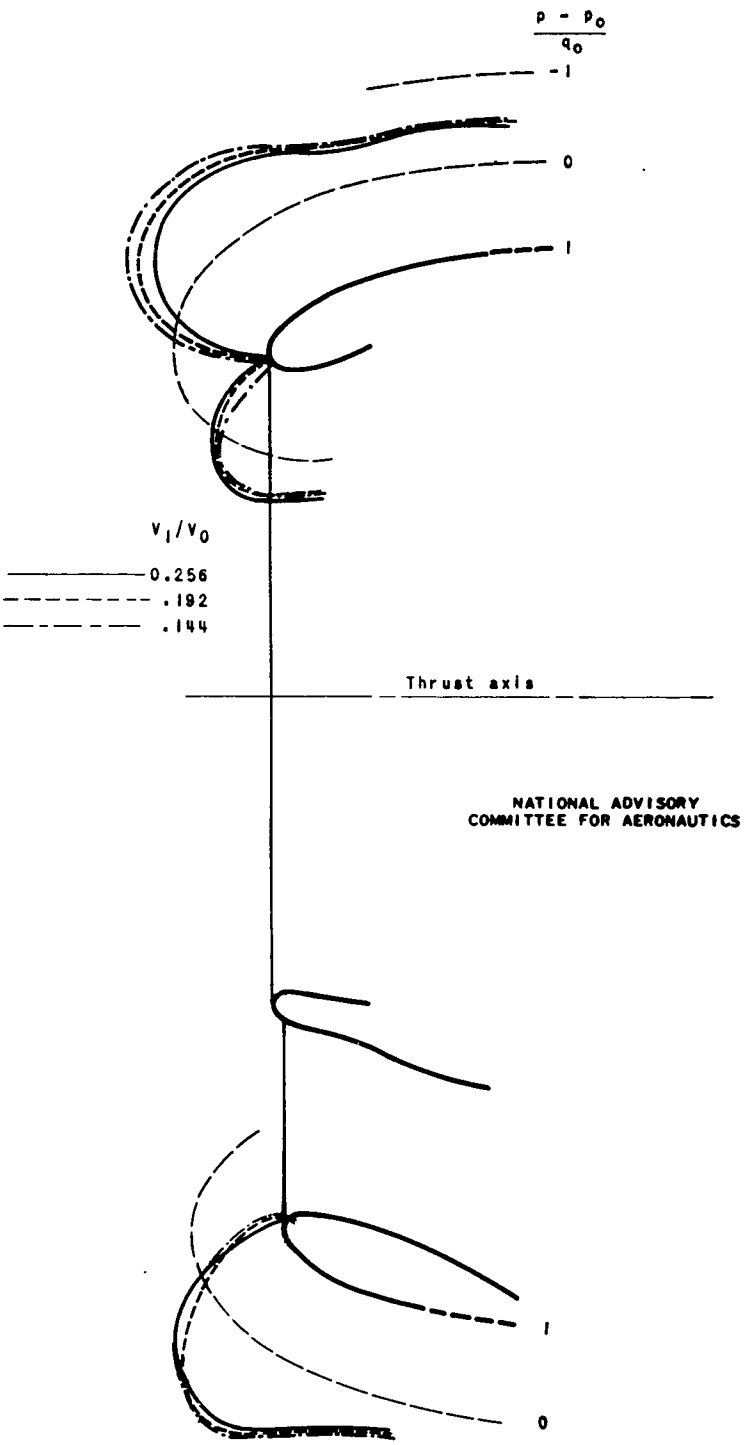

(c) 43-inch-diameter cowl inlet.

Figure 11. - Continued. Effect of inlet velocity ratio on pressure distribution over the upper cowl lip and lower duct lip. Propeller operating; thrust coefficient, 0.038; angle of attack, -2°.

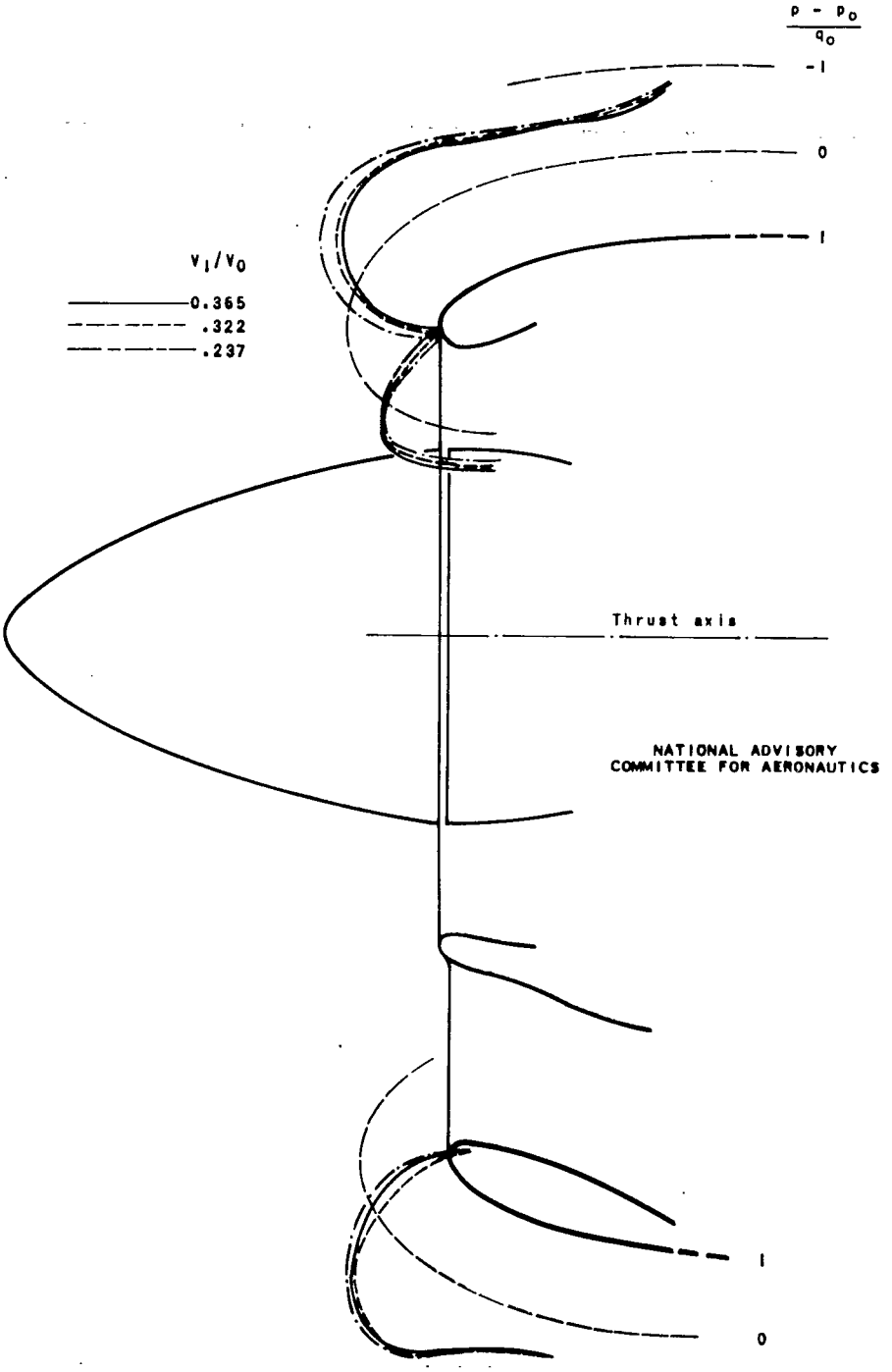

(d) 43-inch-diameter cowl inlet with 27-inch-diameter spinner.

Figure 11. - Continued. Effect of inlet velocity ratio on pressure distribution over the upper cowl lip and lower duct lip. Propeller operating; thrust coefficient, 0.038; angle of attack, -2°.

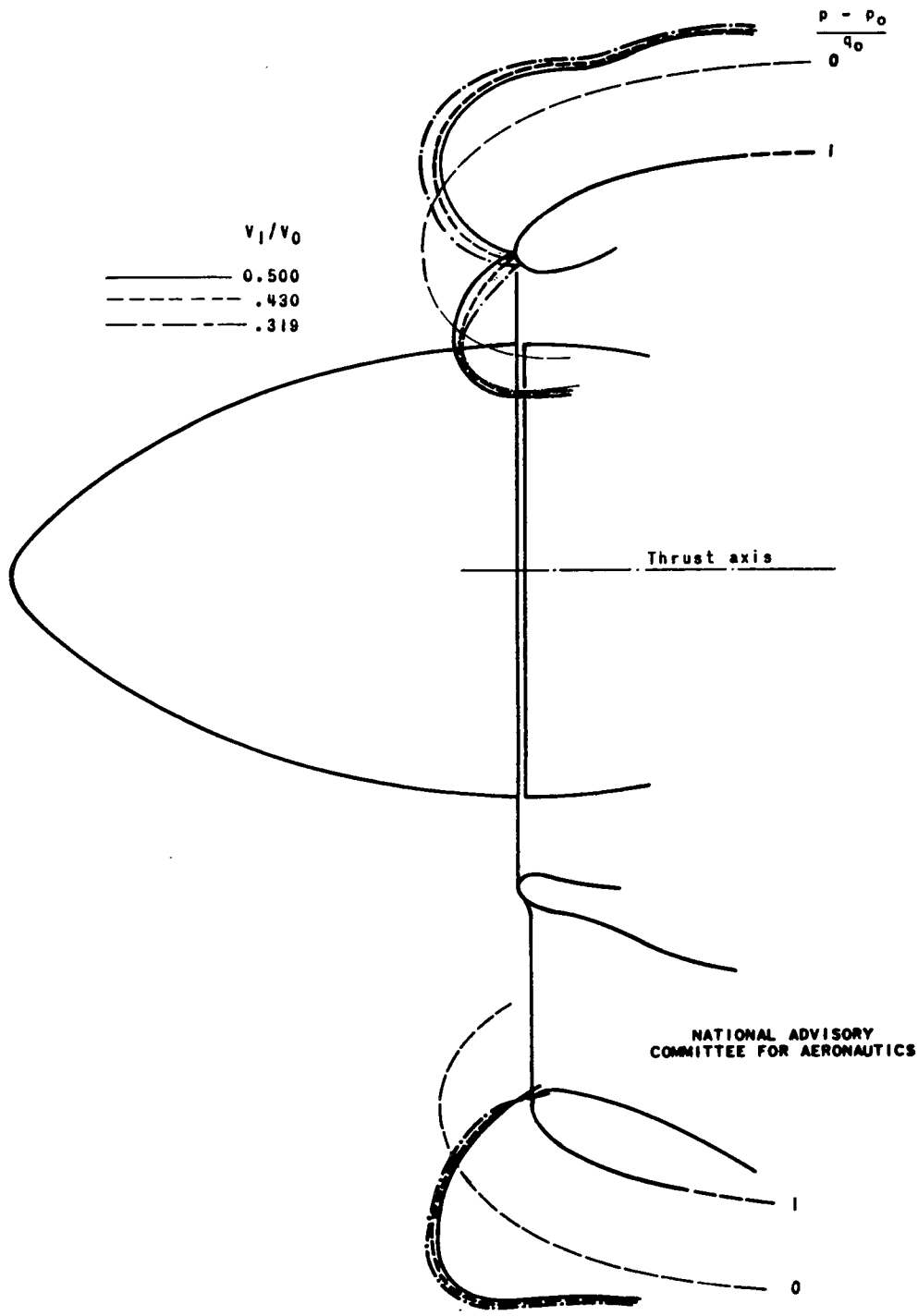

(e) 43-inch-diameter cowl inlet with 32-inch-diameter spinner.

Figure 11. - Concluded. Effect of inlet velocity ratio on pressure distribution over the upper cowl lip and lower duct lip. Propeller operating; thrust coefficient, 0.038; angle of attack, -2°.

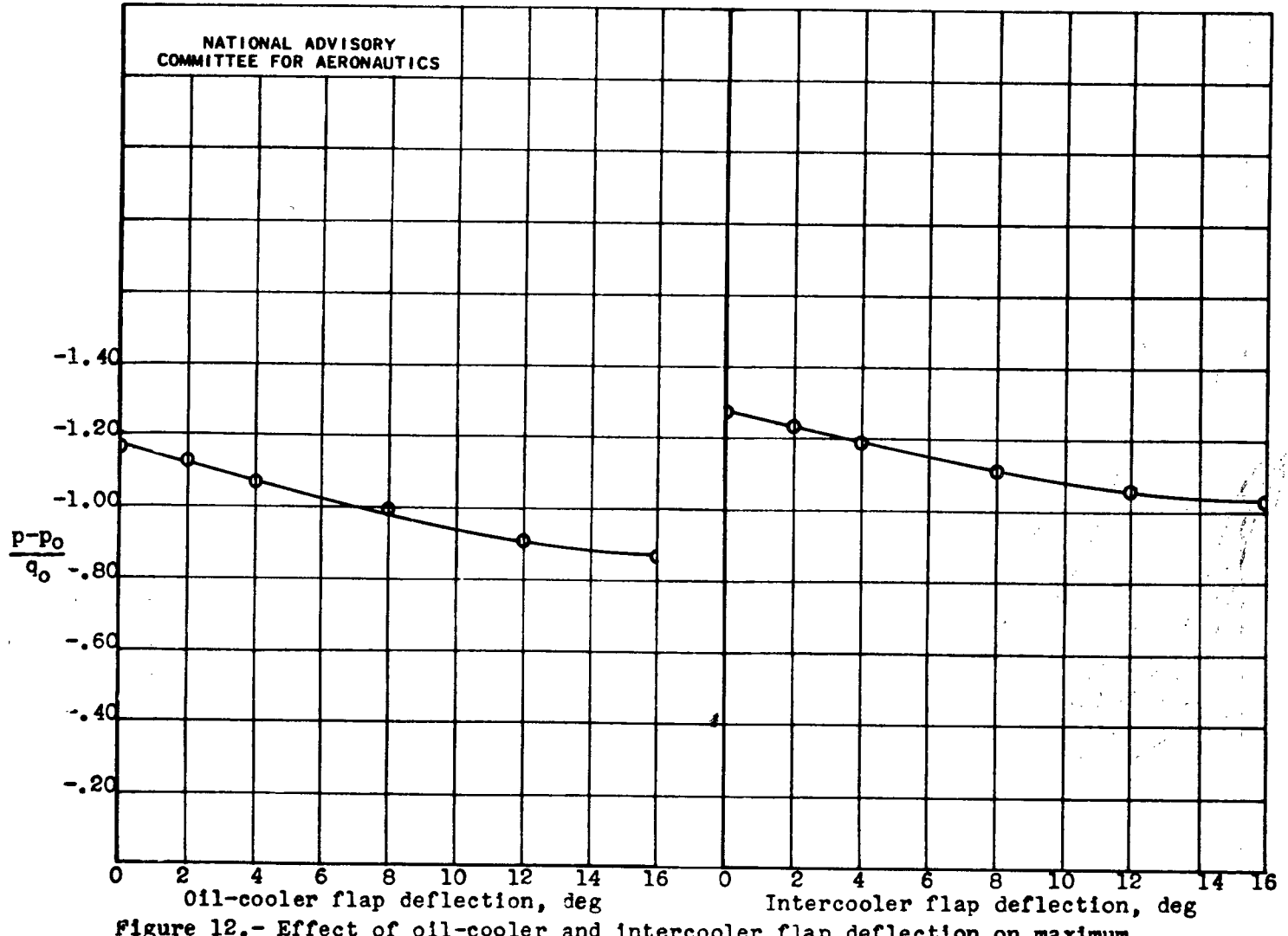

Figure 12.- Effect of oil-cooler and intercooler flap deflection on maximum negative pressure coefficients of lower duct lip. Propeller removed; 43-inch-diameter cowl inlet.

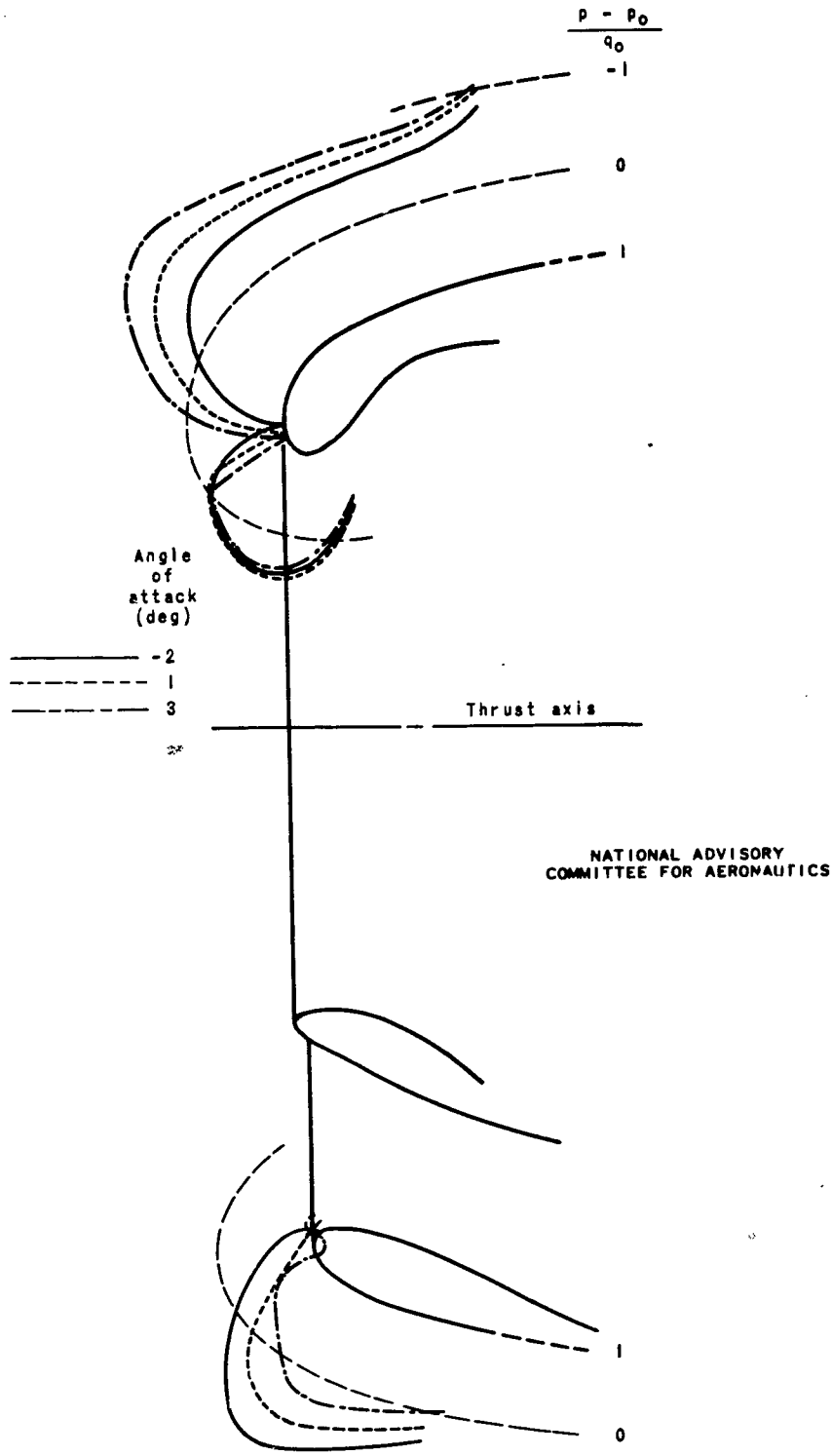

(a) $38\frac{1}{2}$- by 35-inch oval (original) cowl inlet; inlet velocity ratio, 0.324.

Figure 13. - Effect of angle of attack on pressure distribution over the upper cowl lip and lower duct lip. Propeller operating; thrust coefficient, 0.038.

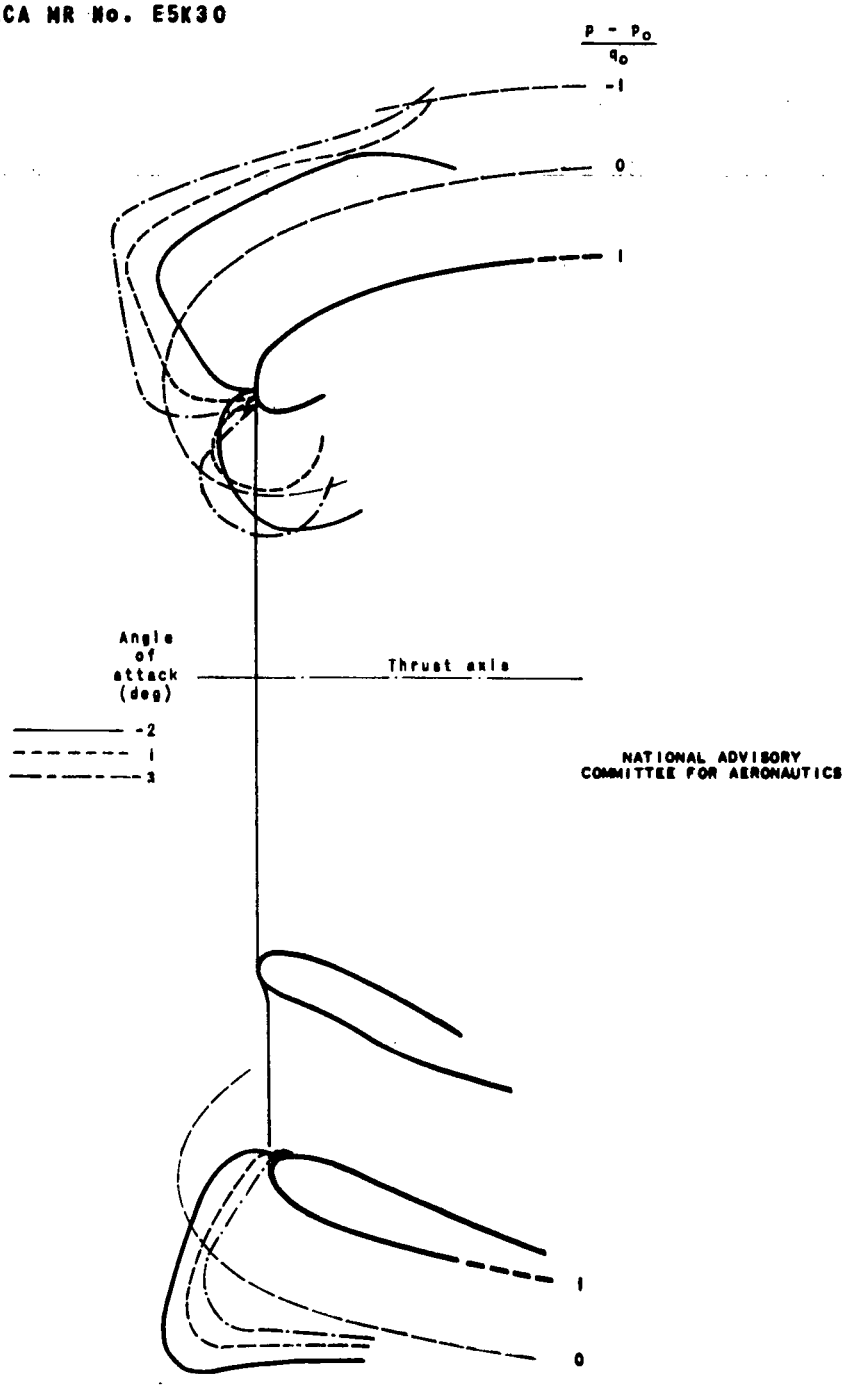

(b) $39\frac{1}{2}$-inch-diameter cowl inlet; inlet velocity ratio, 0.240.

Figure 13. - Continued. Effect of angle of attack on pressure distribution over the upper cowl lip and lower duct lip. Propeller operating; thrust coefficient, 0.038

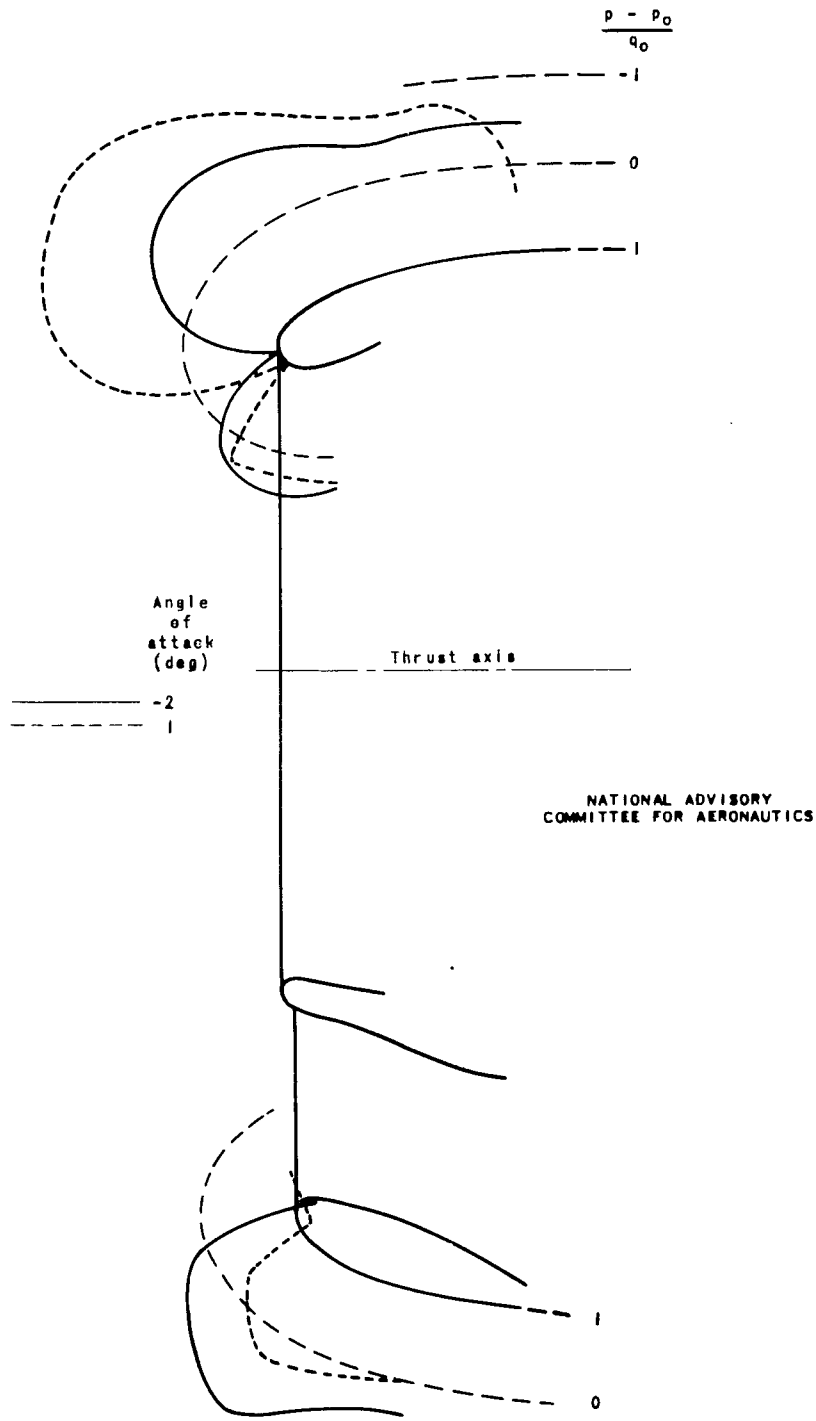

(c) 43-inch-diameter cowl inlet; inlet velocity ratio, 0.192.

Figure 13. - Continued. Effect of angle of attack on pressure distribution over the upper cowl lip and lower duct lip. Propeller operating; thrust coefficient, 0.038.

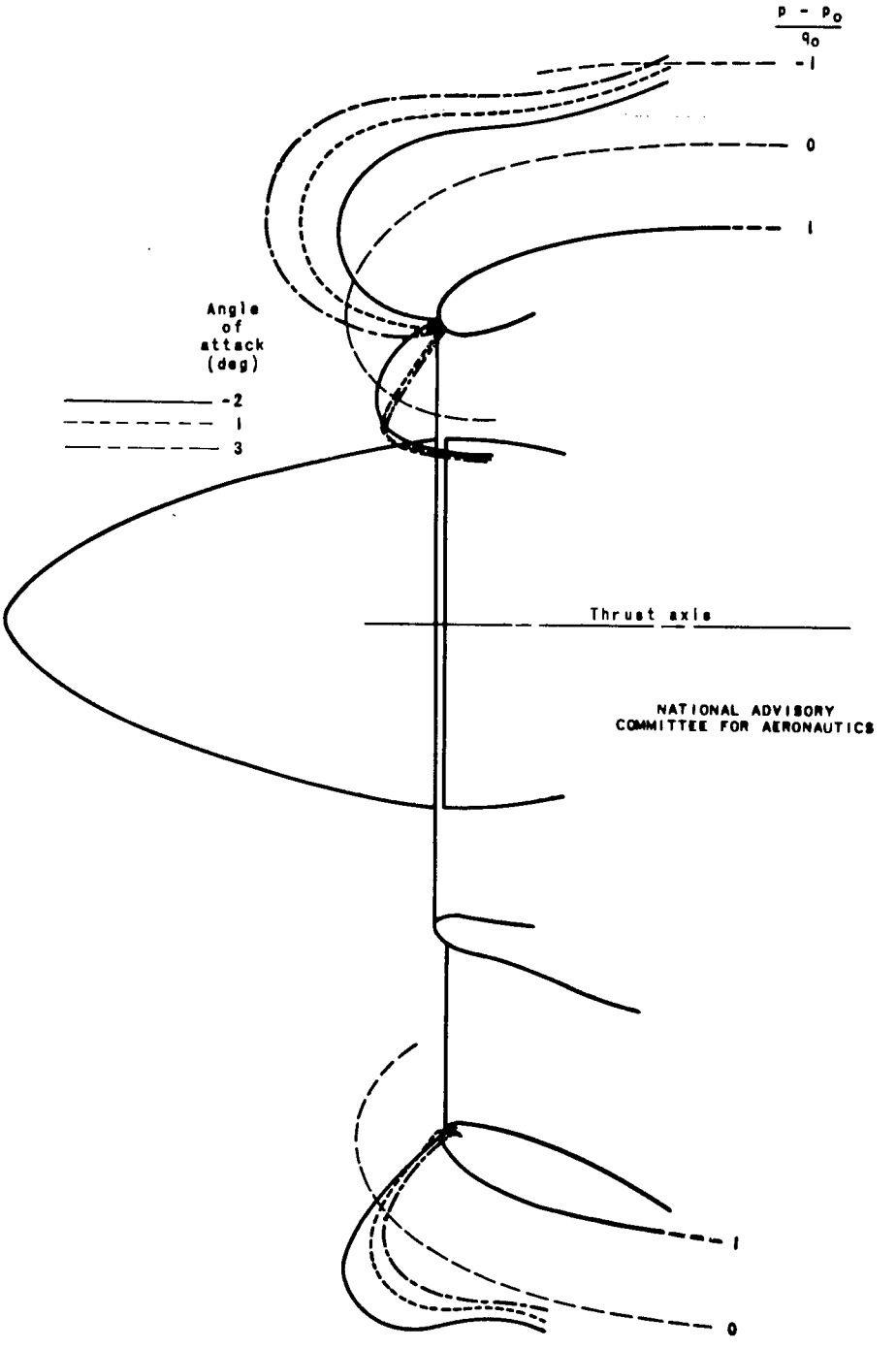

(d) 43-inch-diameter cowl inlet with 27-inch-diameter spinner; inlet velocity ratio, 0.322.

Figure 13. - Continued. Effect of angle of attack on pressure distribution over the upper cowl lip and lower duct lip. Propeller operating; thrust coefficient, 0.038.

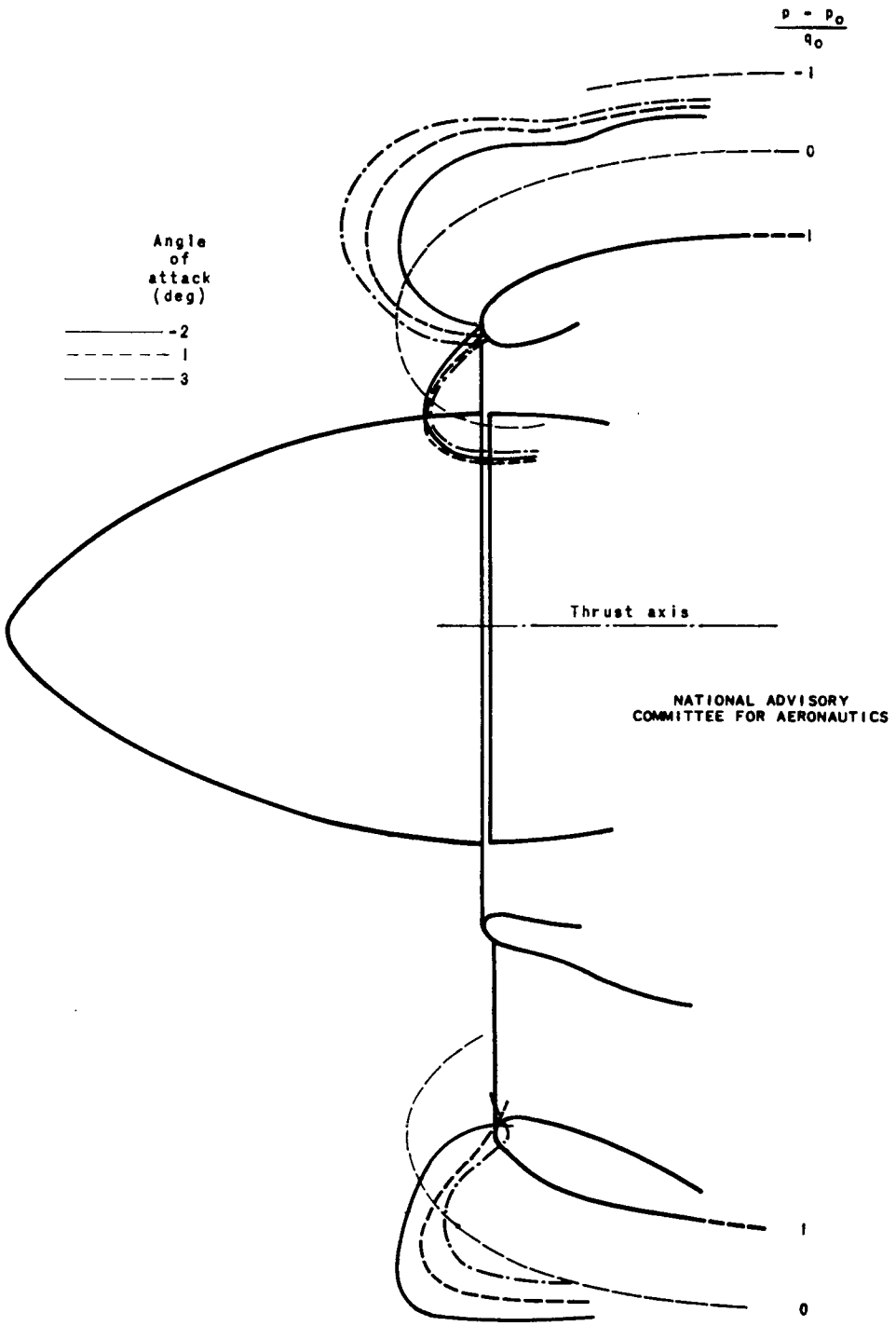

(e) 43-inch-diameter cowl inlet with 32-inch-diameter spinner; inlet velocity ratio, 0.381.

Figure 13. - Concluded. Effect of angle of attack on pressure distribution over the upper cowl lip and lower duct lip. Propeller operating; thrust coefficient, 0.038

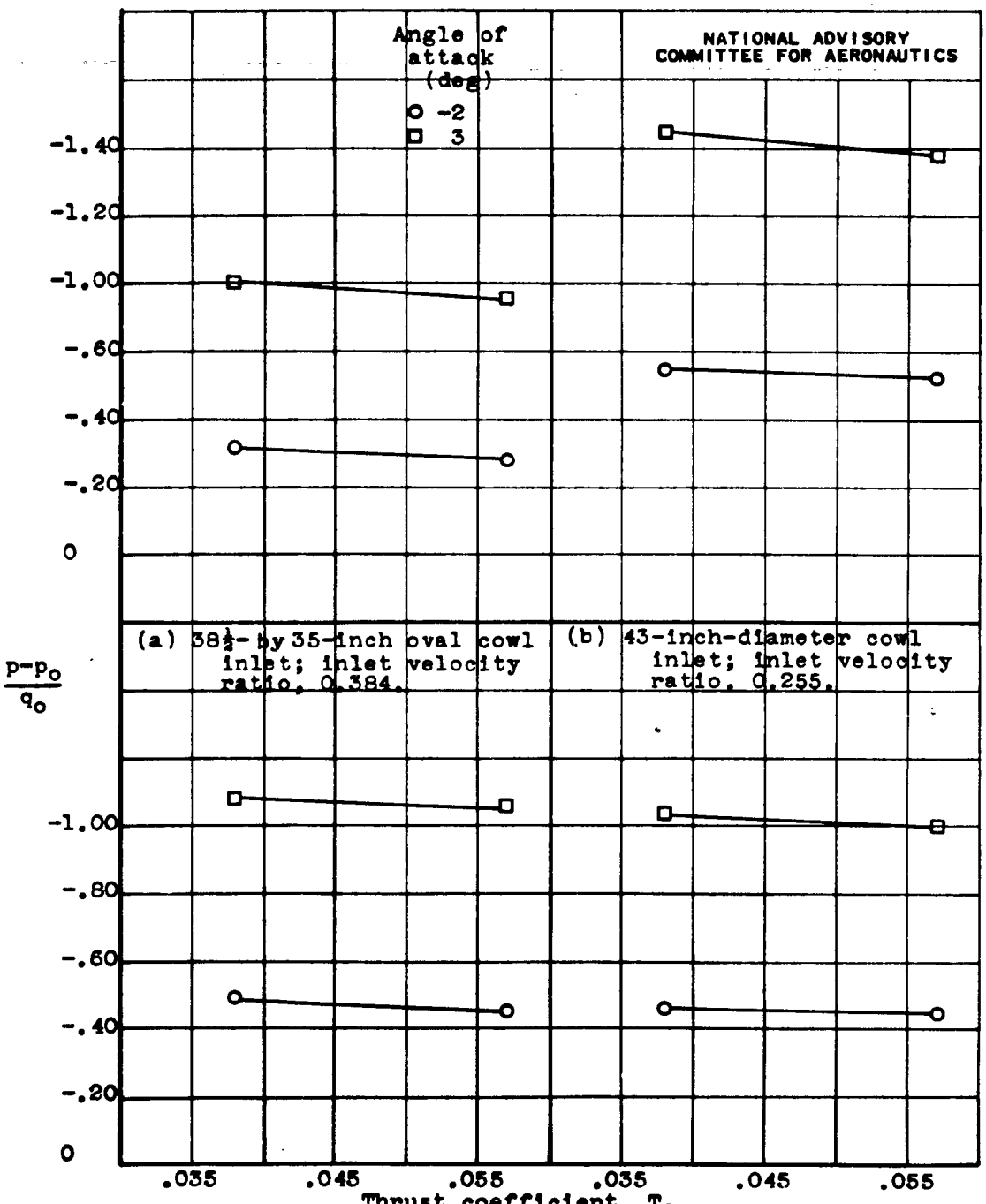

Figure 14.- Effect of thrust coefficient on maximum negative pressure coefficients of upper cowl lip.

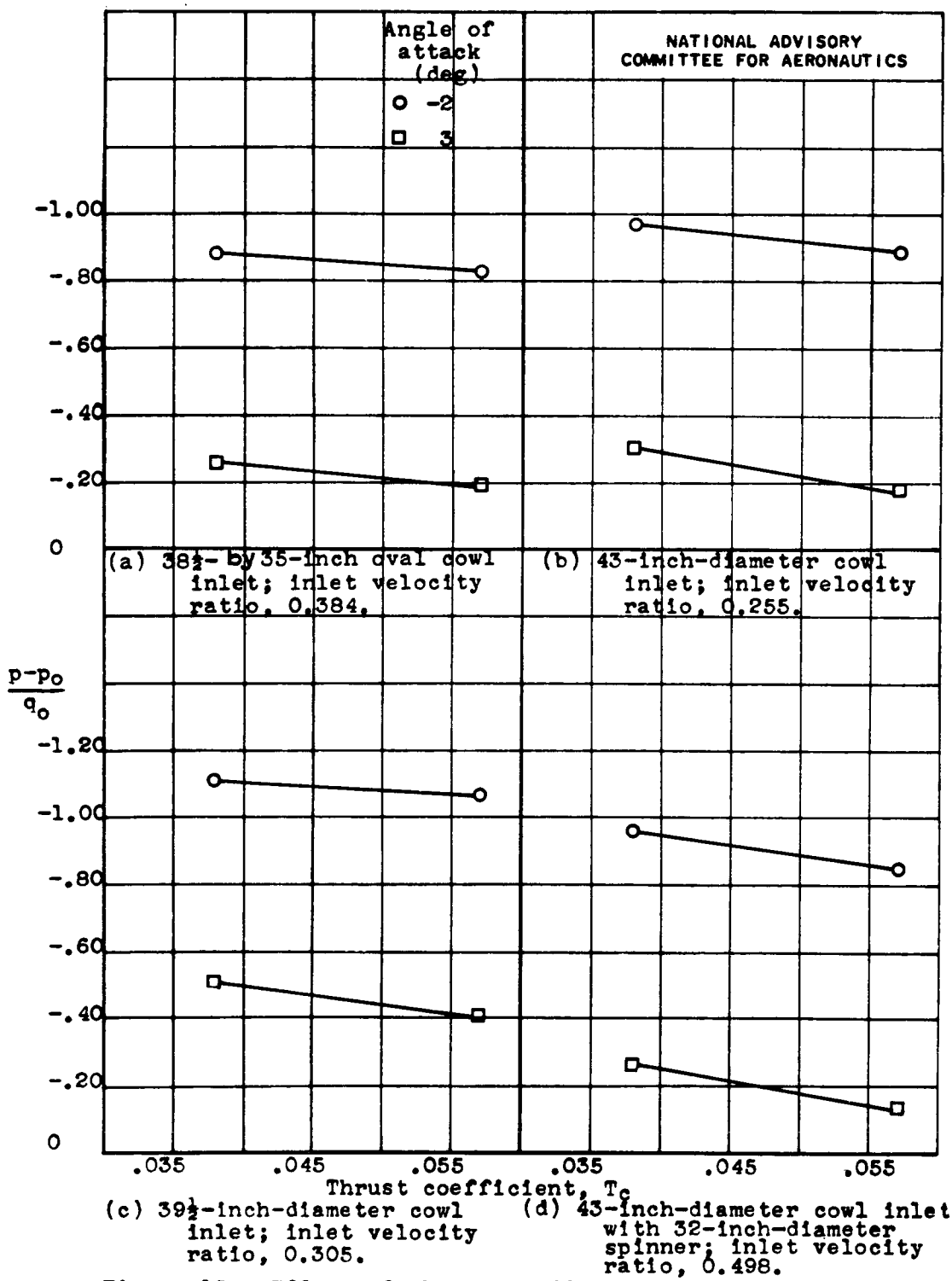

Figure 15.- Effect of thrust coefficient on maximum negative pressure coefficients of lower duct lip.

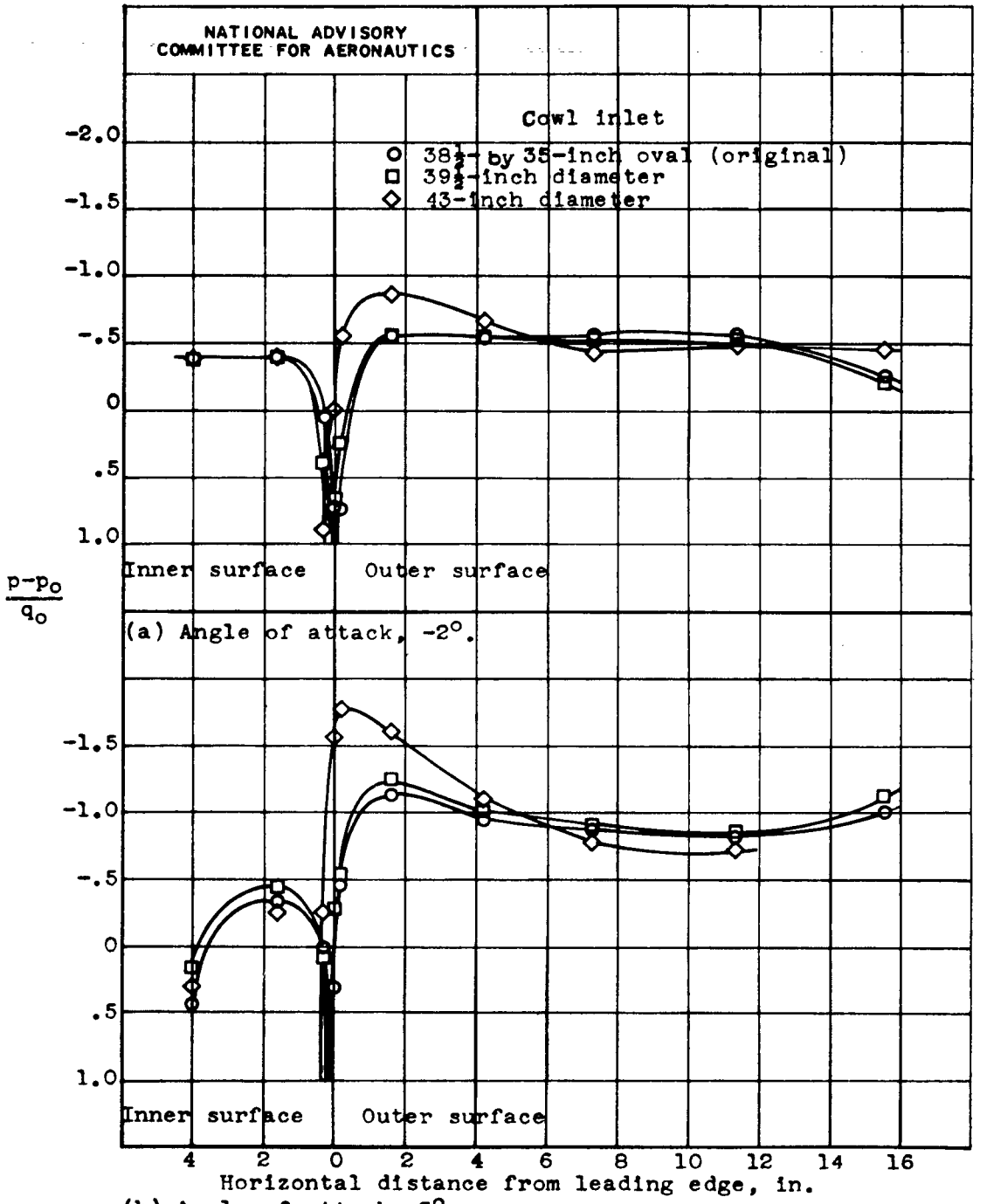

$\frac{p-p_o}{q_o}$

(b) Angle of attack, 3°.

Figure 16.- Comparison of pressure distribution on upper cowl lip for various cowl-inlet configurations; cooling-air pressure-drop coefficient, 0.58; thrust coefficient 0.038.

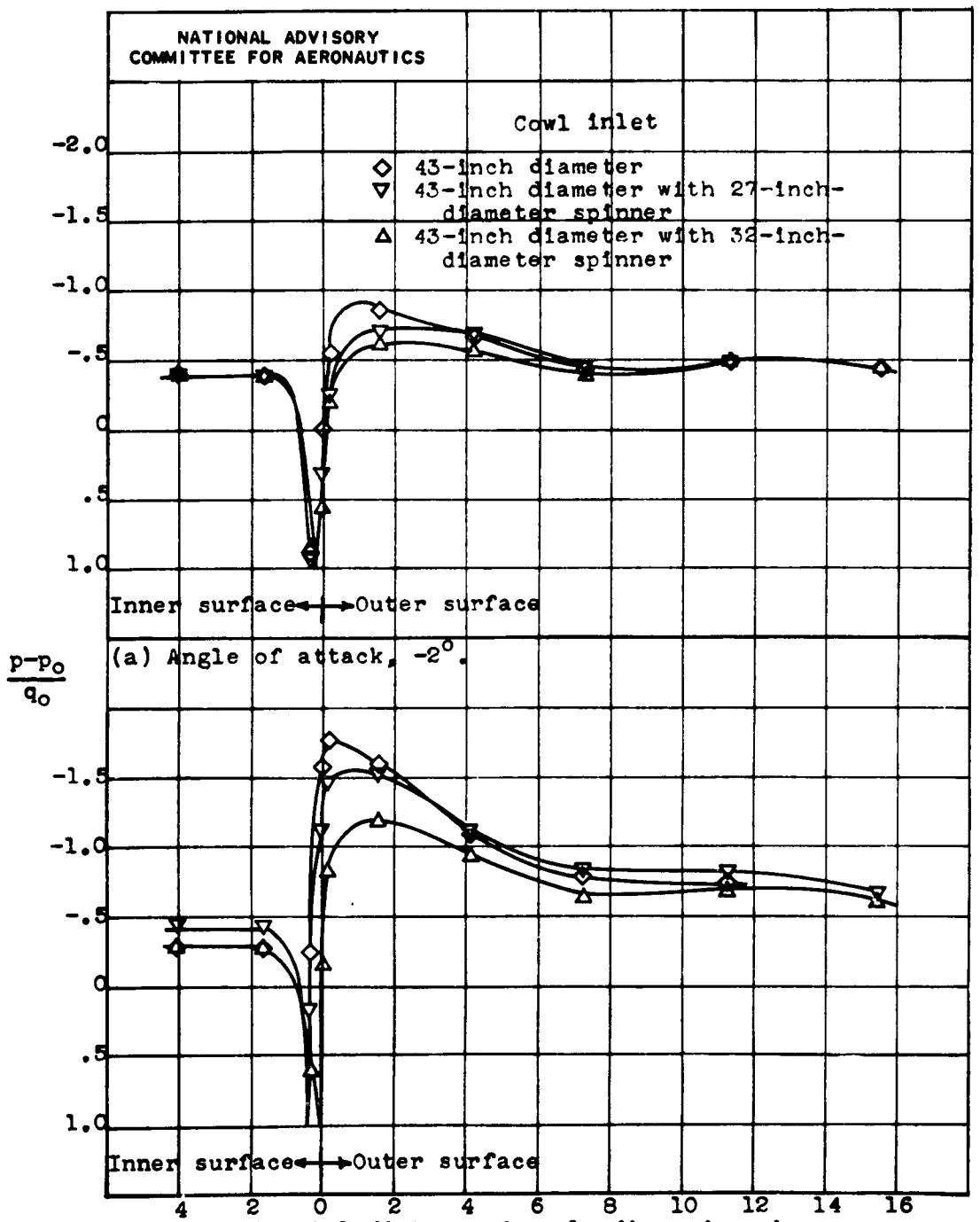

(b) Angle of attack, 3°.

Figure 17.- Comparison of pressure distribution on upper cowl lip for various cowl-inlet configurations; cooling-air pressure-drop coefficient, 0.65; thrust coefficient, 0.038.

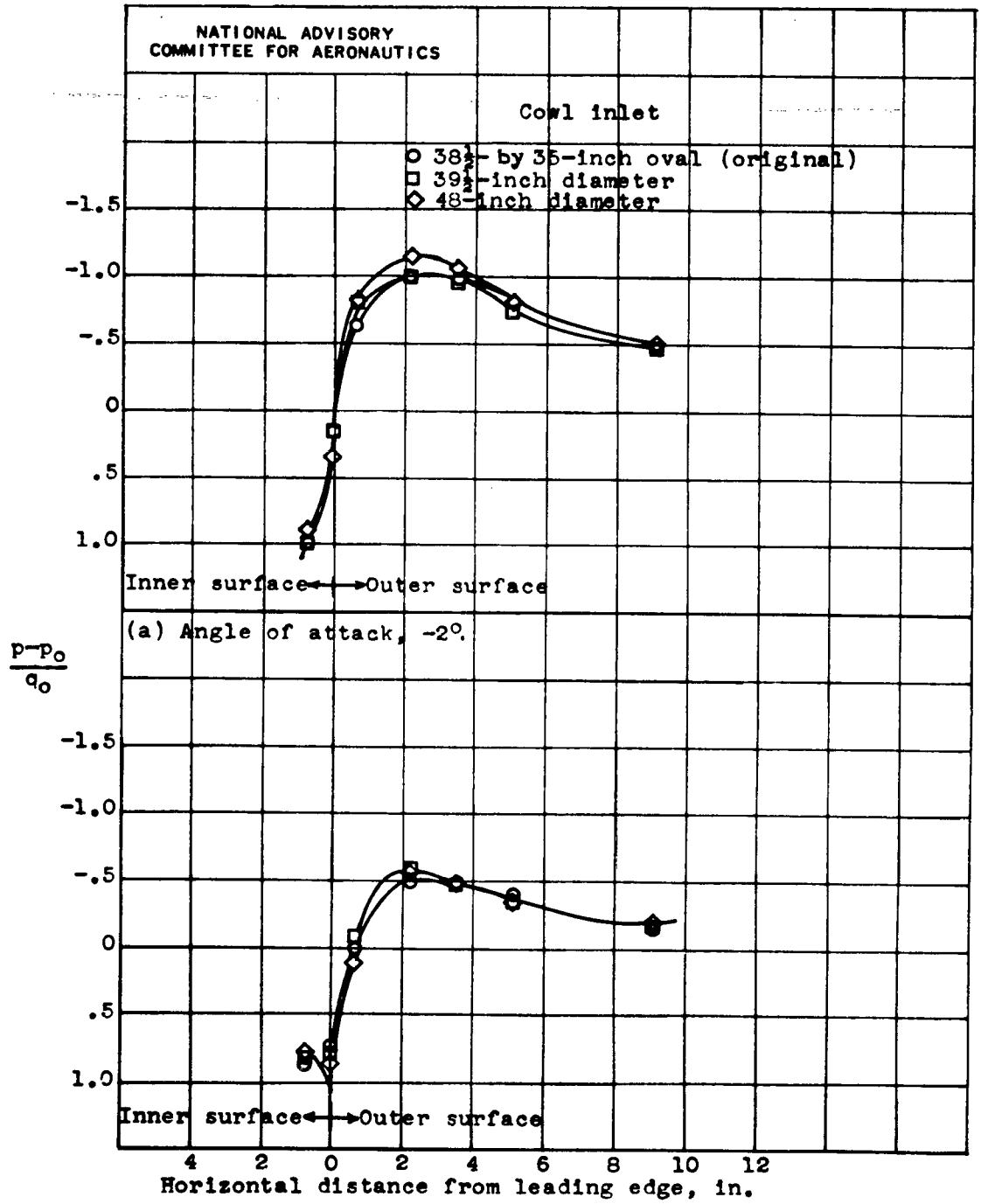

(b) Angle of attack, 3°.

Figure 18.- Comparison of pressure distribution on lower duct lip for various cowl-inlet configurations; cooling-air pressure-drop coefficient, 0.58; thrust coefficient, 0.038.

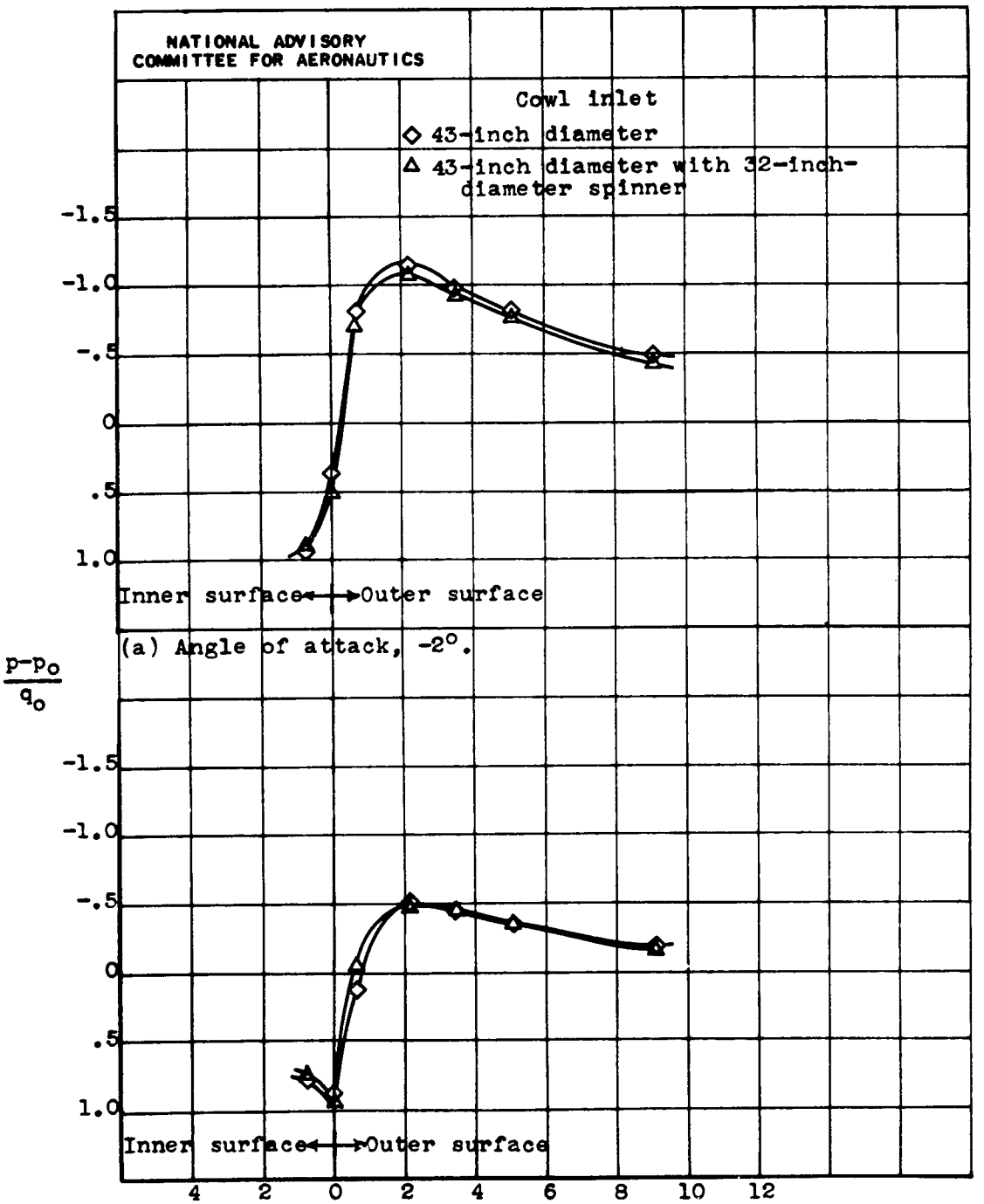

(b) Angle of attack, 3°.

Figure 19.- Comparison of pressure distribution on lower duct lip for various cowl-inlet configurations; cooling-air pressure-drop coefficient, 0.65; thrust coefficient, 0.038.

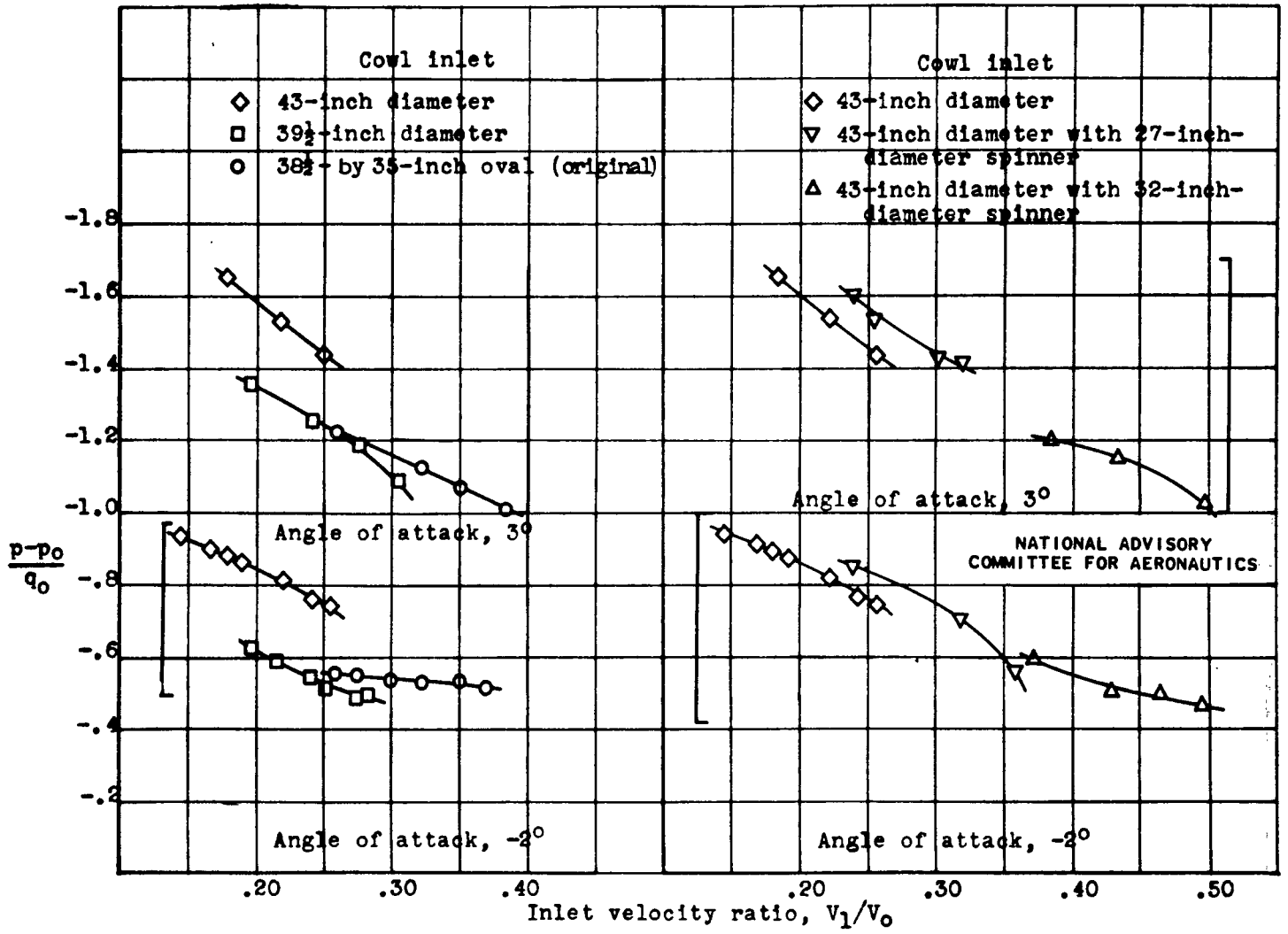

Figure 20.- Comparison of maximum negative pressure coefficients of upper cowl lip for various cowl-inlet configurations. Thrust coefficient, 0.038.

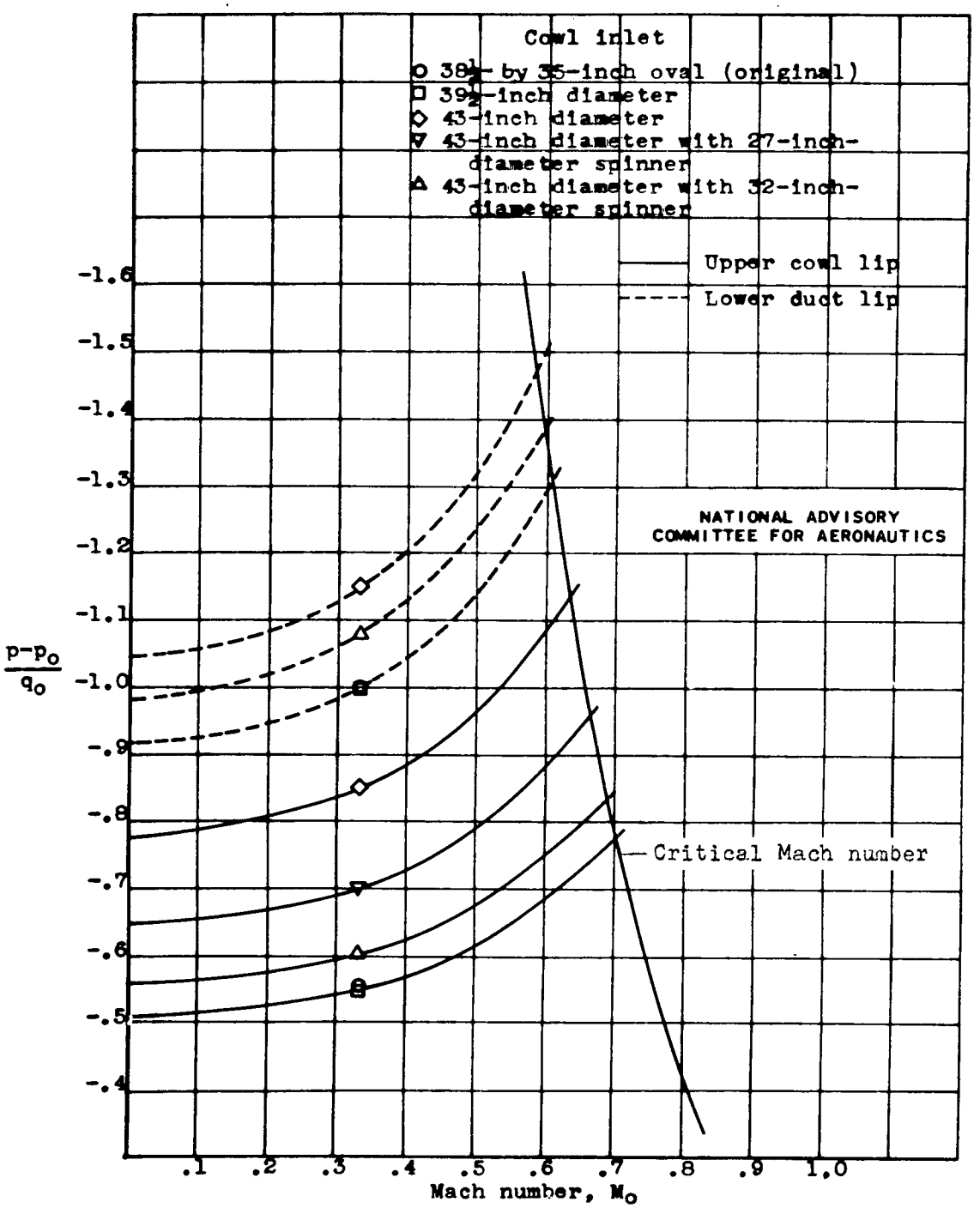

Figure 21.- Comparative critical speeds of the five cowl-inlet configurations. Propeller operating; thrust coefficient, 0.038; angle of attack, -2°; cooling-air pressure-drop coefficient, 0.58.

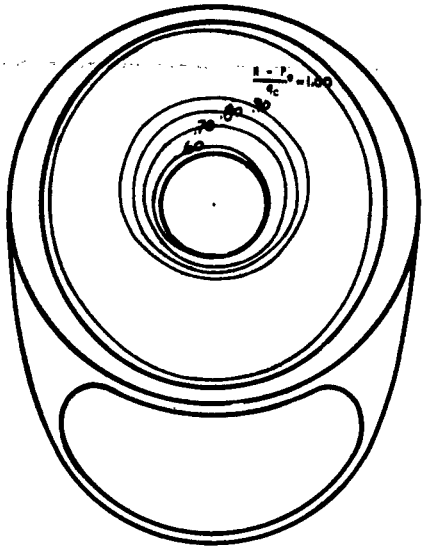

Angle of attack, -2°; inlet velocity ratio, 0.383.

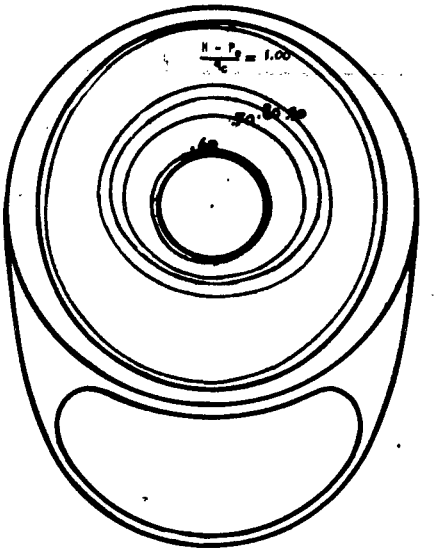

Angle of attack, -2°; inlet velocity ratio, 0.300.

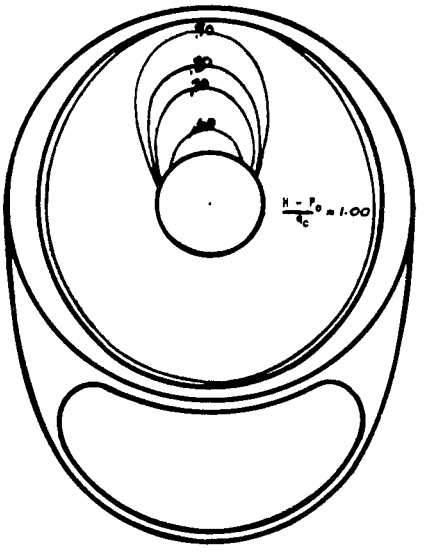

Angle of attack, 3°; inlet velocity ratio, 0.383.

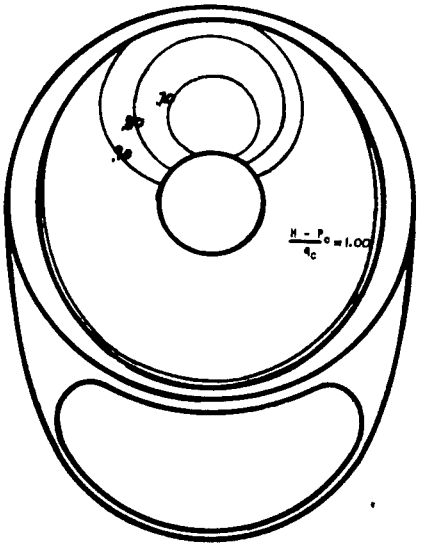

Angle of attack, 3°; inlet velocity ratio, 0.300.

NATIONAL ADVISORY
COMMITTEE FOR AERONAUTICS

(a) Propeller removed.

Figure 22. - Total-pressure distribution at $38\frac{1}{2}$- by 35-inch oval cowl inlet.

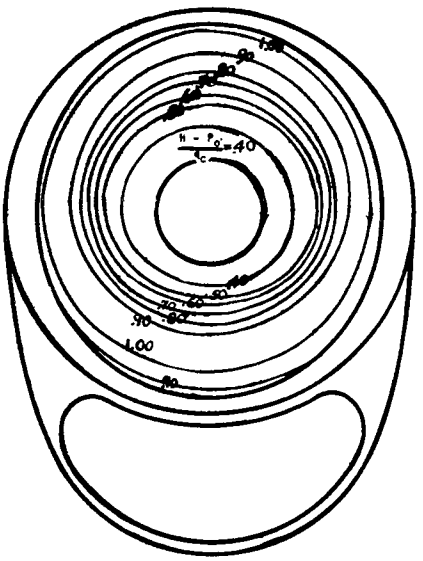

Angle of attack, -2°; inlet velocity ratio, 0.383.

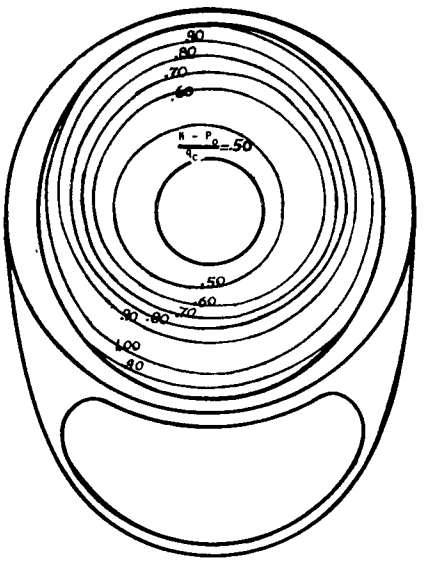

Angle of attack, -2°; inlet velocity ratio, 0.255.

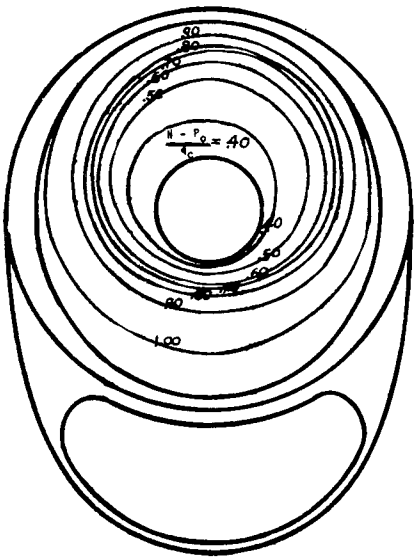

Angle of attack, 3°; inlet velocity ratio, 0.385.

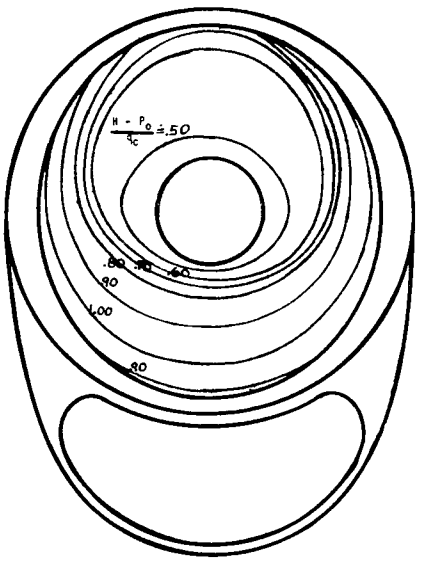

Angle of attack, 3°; inlet velocity ratio, 0.255.

NATIONAL ADVISORY
COMMITTEE FOR AERONAUTICS

(b) Propeller operating; thrust coefficient, 0.038.

Figure 22. - Concluded. Total-pressure distribution at $38\frac{1}{2}$ by 35-inch oval cowl inlet.

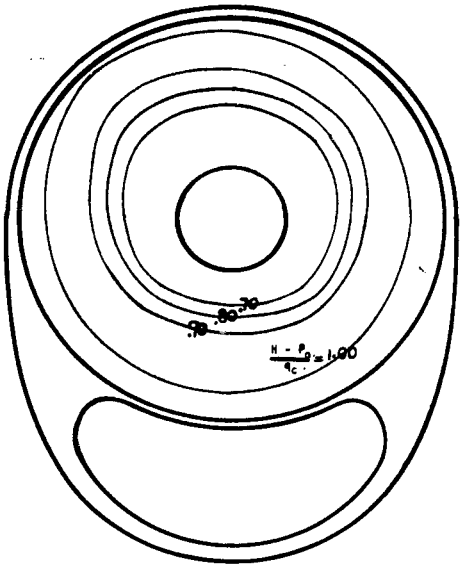

Angle of attack, -2°; inlet velocity ratio, 0.255.

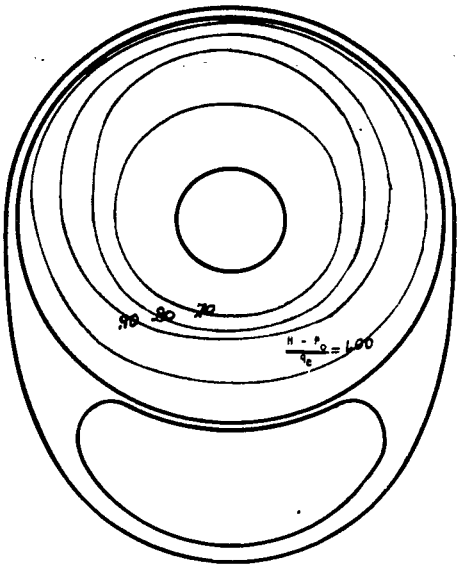

Angle of attack, -2°; inlet velocity ratio, 0.180.

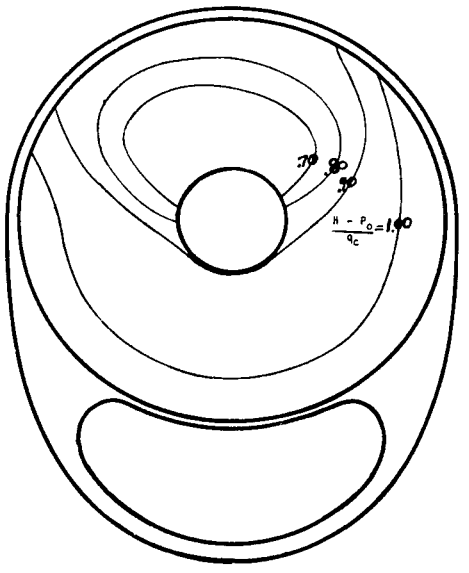

Angle of attack, 3°; inlet velocity ratio, 0.255.

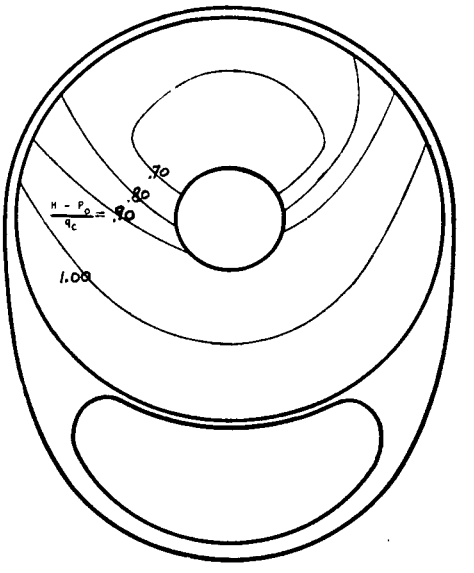

Angle of attack, 3°; inlet velocity ratio, 0.180.

(a) Propeller removed.

Figure 23. - Total-pressure distribution at the 43-inch-diameter cowl inlet.

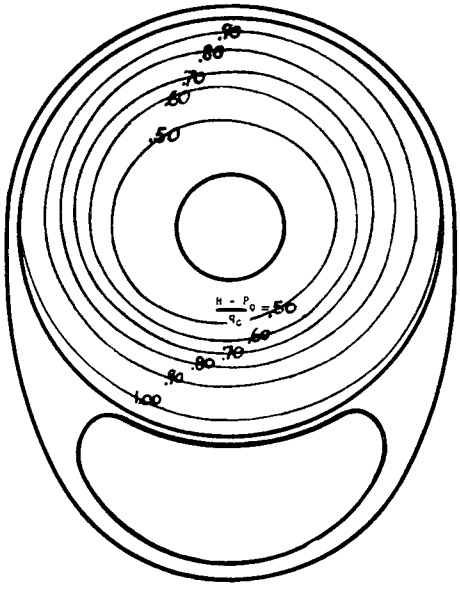

Angle of attack, -2°; inlet velocity ratio, 0.255.

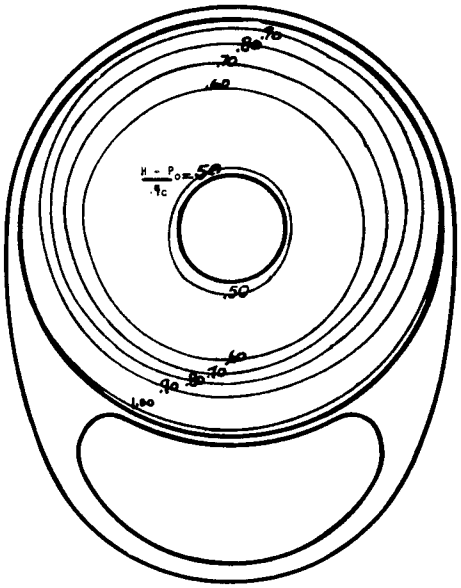

Angle of attack, -2°; inlet velocity ratio, 0.190.

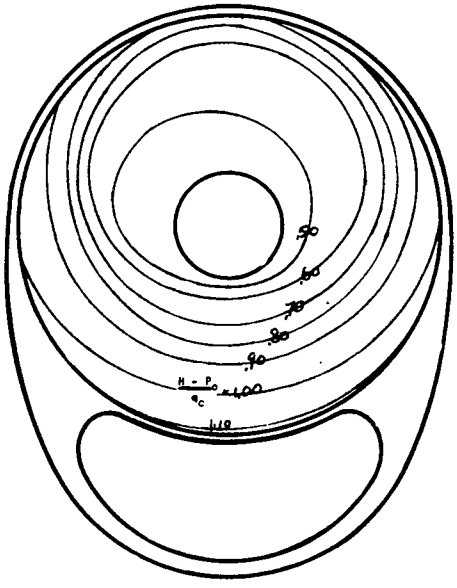

Angle of attack, 3°; inlet velocity ratio, 0.255.

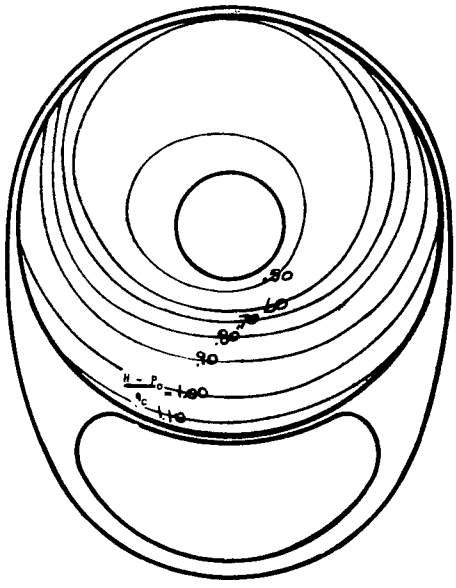

Angle of attack, 3°; inlet velocity ratio, 0.190.

NATIONAL ADVISORY
COMMITTEE FOR AERONAUTICS

(b) Propeller operating; thrust coefficient, 0.038.

Figure 23. - Concluded. Total-pressure distribution at the 43-inch-diameter cowl inlet.

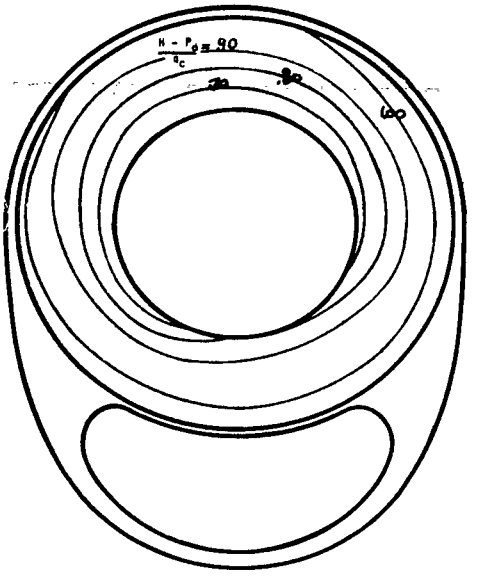

Angle of attack, -2°; inlet velocity ratio, 0.355.

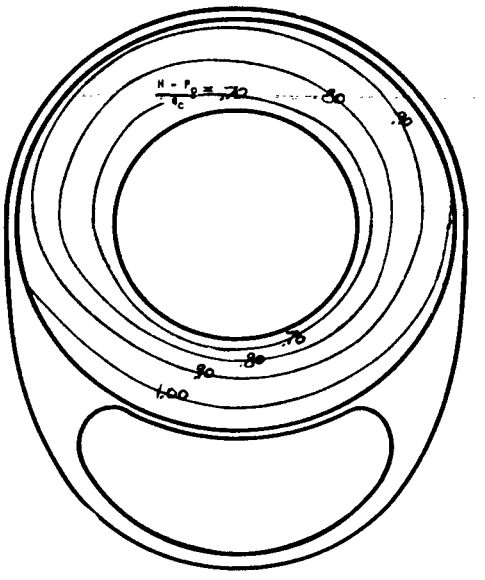

Angle of attack, -2°; inlet velocity ratio, 0.235.

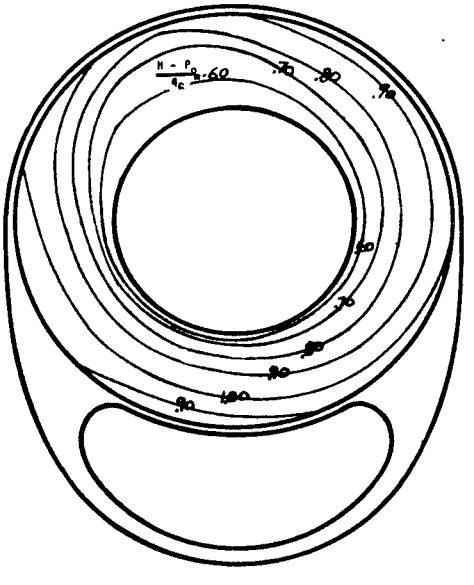

Angle of attack, 3°; inlet velocity ratio. 0.355.

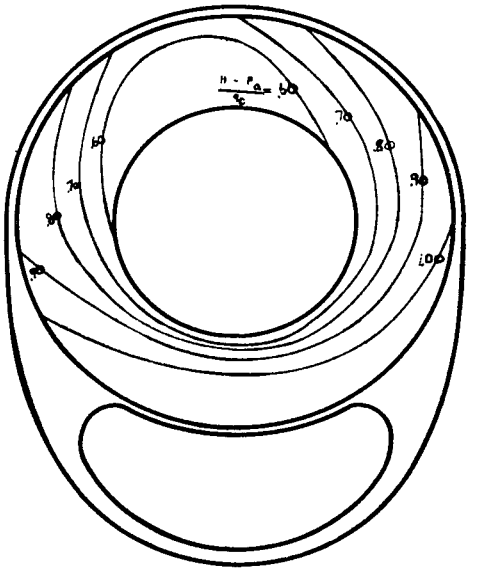

Angle of attack, 3°; inlet velocity ratio, 0.235.

NATIONAL ADVISORY
COMMITTEE FOR AERONAUTICS

Figure 24. - Total-pressure distribution at 43-inch-diameter cowl inlet with 27-inch-diameter spinner. Propeller operating; thrust coefficient, 0.038.

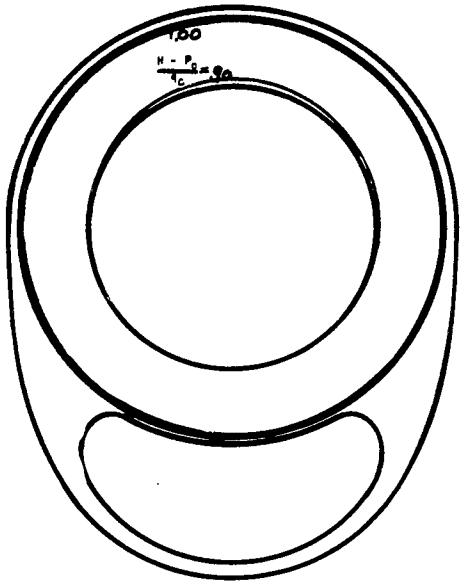

Angle of attack, -2°; inlet velocity ratio, 0.500

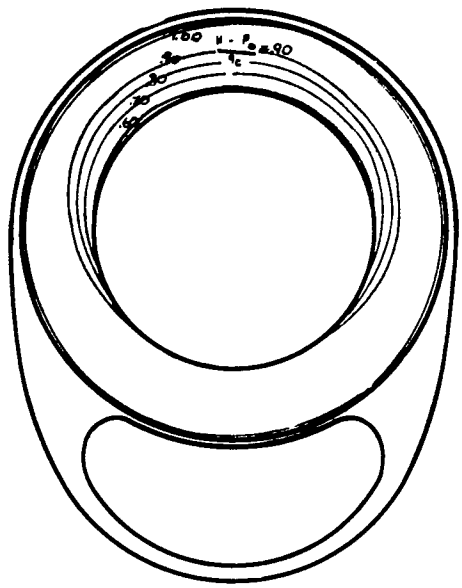

Angle of attack, -2°; inlet velocity ratio, 0.350.

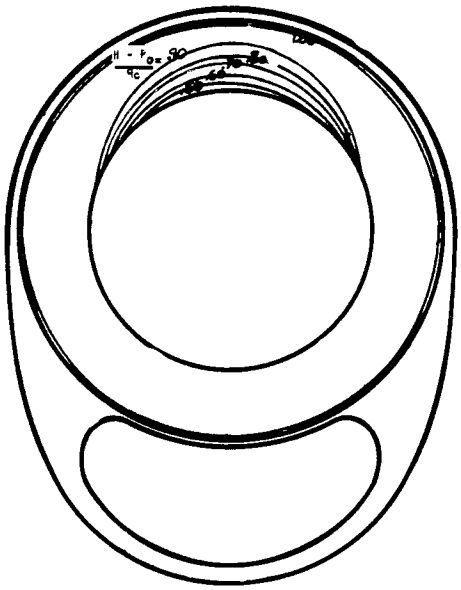

Angle of attack, 3°; inlet velocity ratio, 0.500.

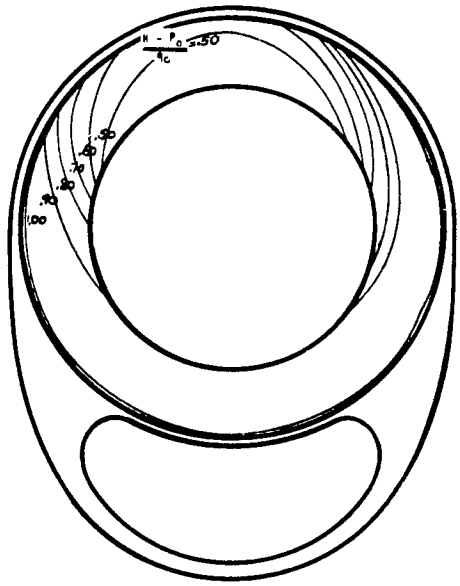

Angle of attack, 3°; inlet velocity ratio, 0.350.

NATIONAL ADVISORY
COMMITTEE FOR AERONAUTICS

(a) Propeller removed.

Figure 25. - Total-pressure distribution at 43-inch-diameter cowl inlet with 32-inch-diameter spinner.

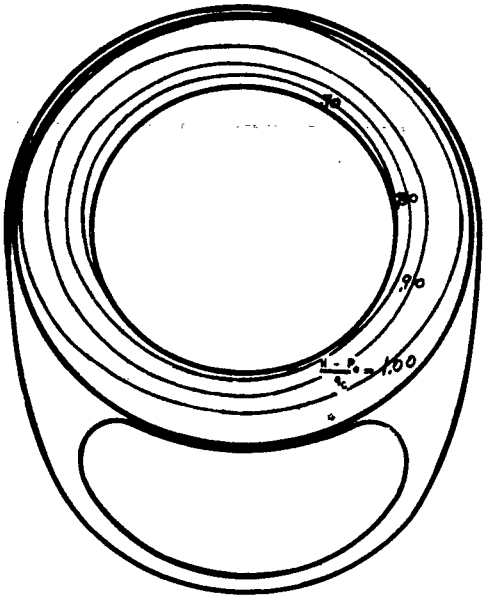

Angle of attack, -2°; inlet velocity ratio, 0.500.

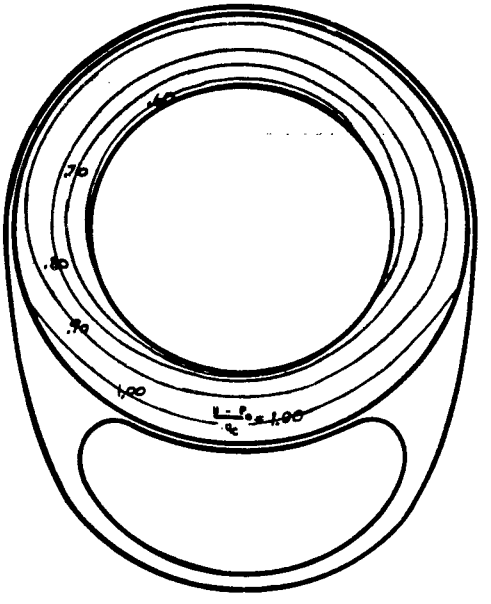

Angle of attack, -2°; inlet velocity ratio, 0.350.

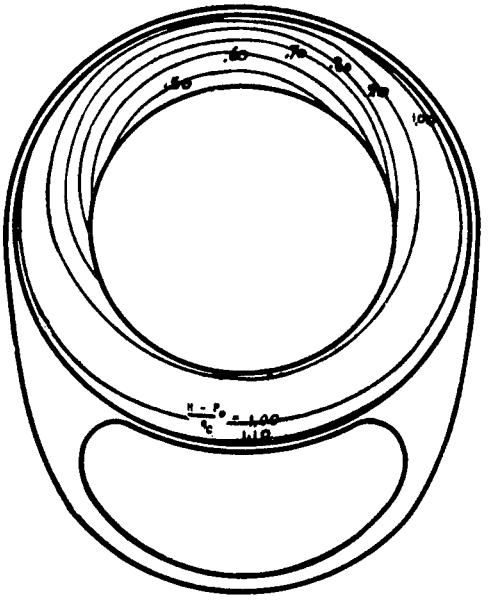

Angle of attack, 3°; inlet velocity ratio, 0.500.

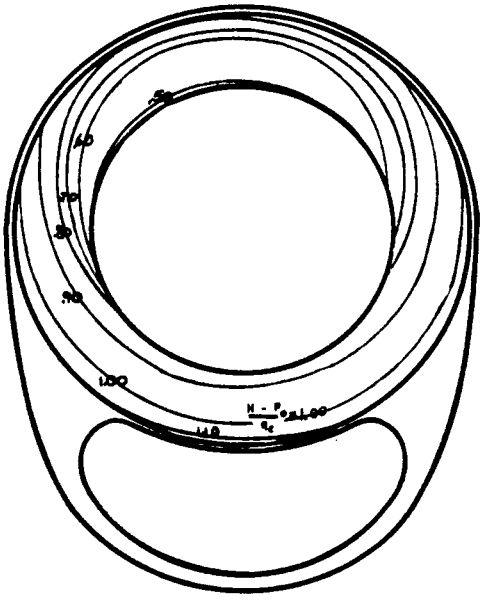

Angle of attack, 3°; inlet velocity ratio, 0.350.

NATIONAL ADVISORY
COMMITTEE FOR AERONAUTICS

(b) Propeller operating; thrust coefficient, 0.038.

Figure 25. - Concluded. Total-pressure distribution at 43-inch-diameter cowl inlet with 32-inch-diameter spinner.

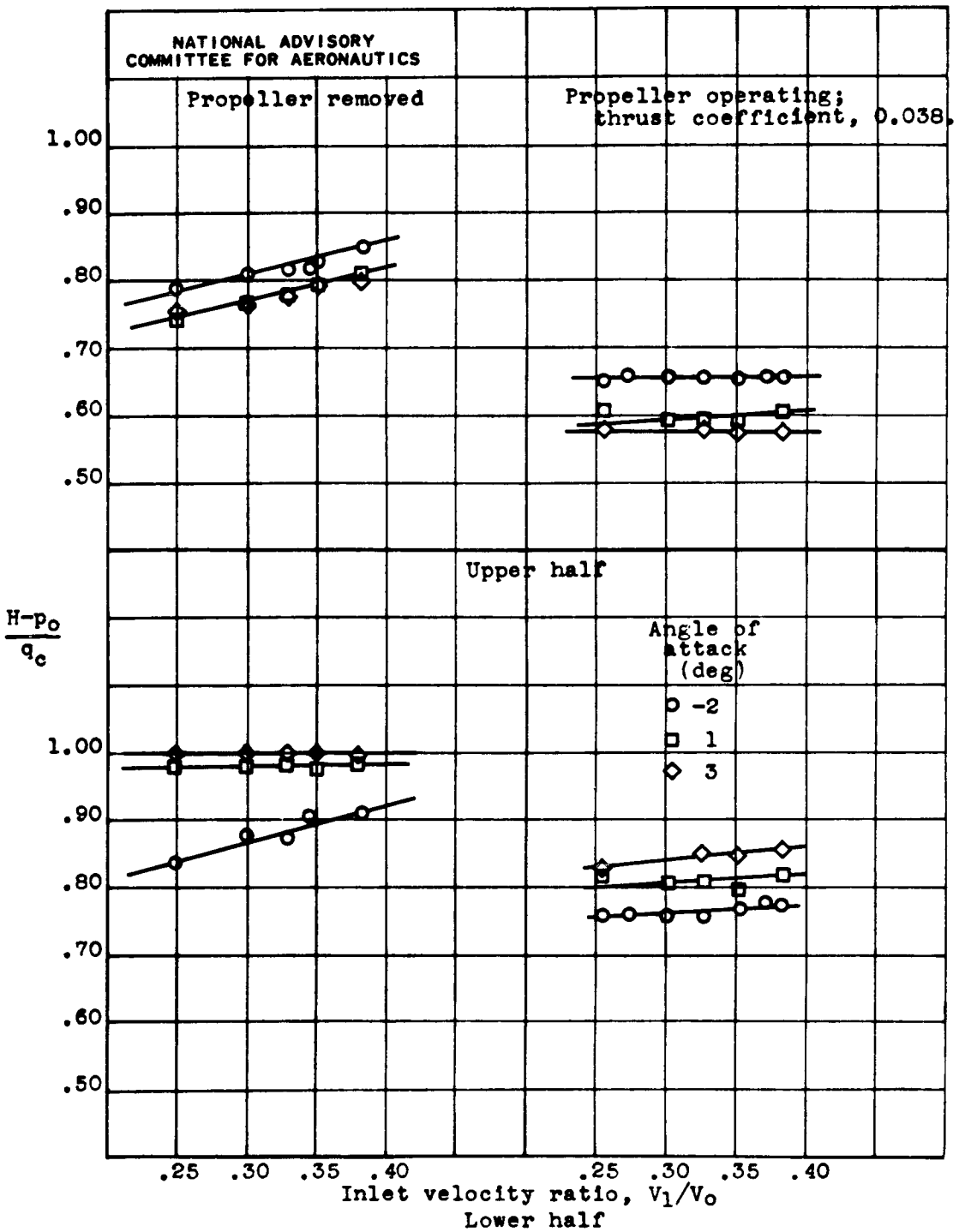

(a) 38½- by 35-inch cowl inlet.

Figure 26.- Effect of inlet velocity ratio on average weighted total pressures at upper and lower halves of cowl inlets.

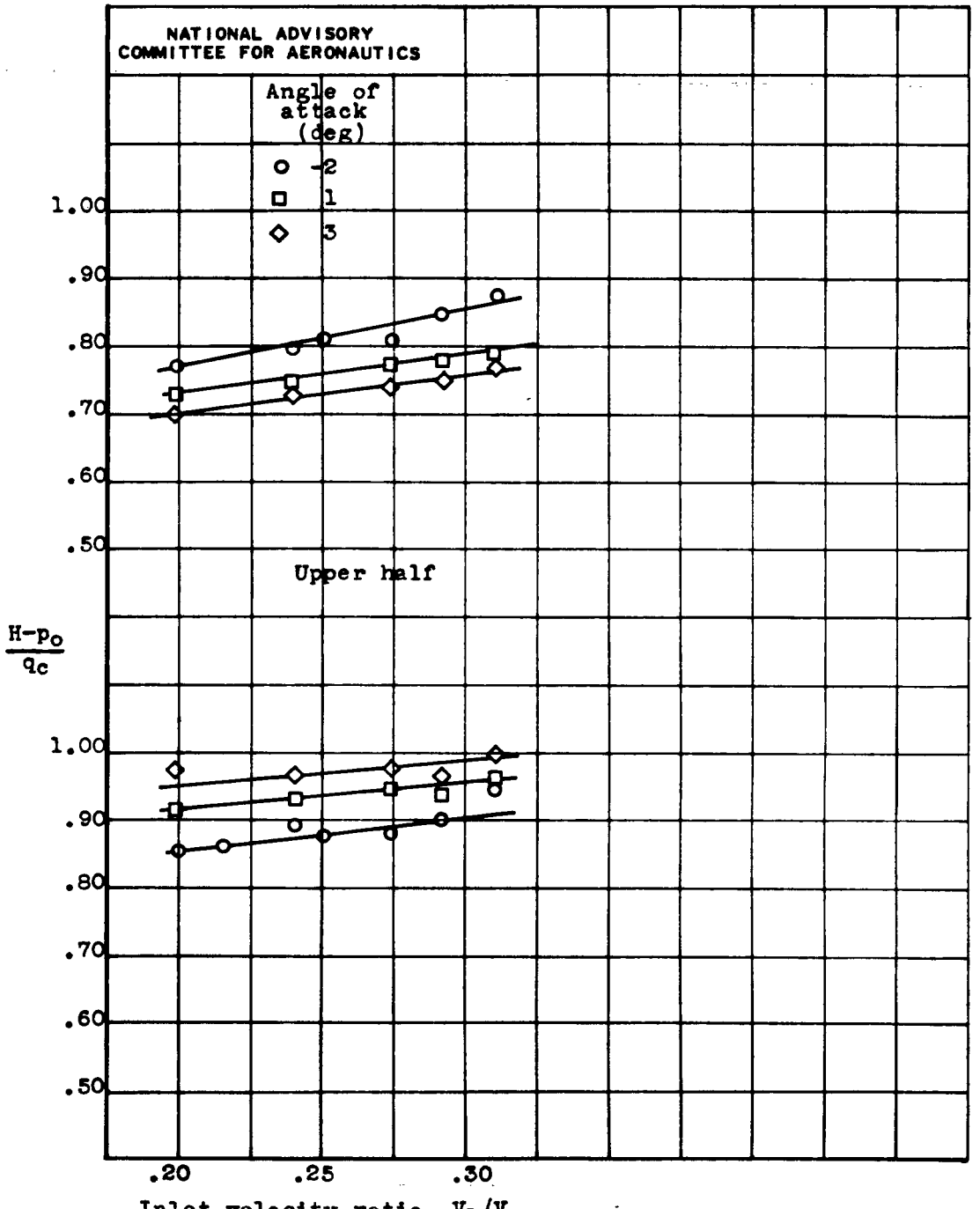

(b) 39½-inch-diameter cowl inlet; propeller removed.

Figure 26. - Continued. Effect of inlet velocity ratio on average weighted total pressures at upper and lower halves of cowl inlets.

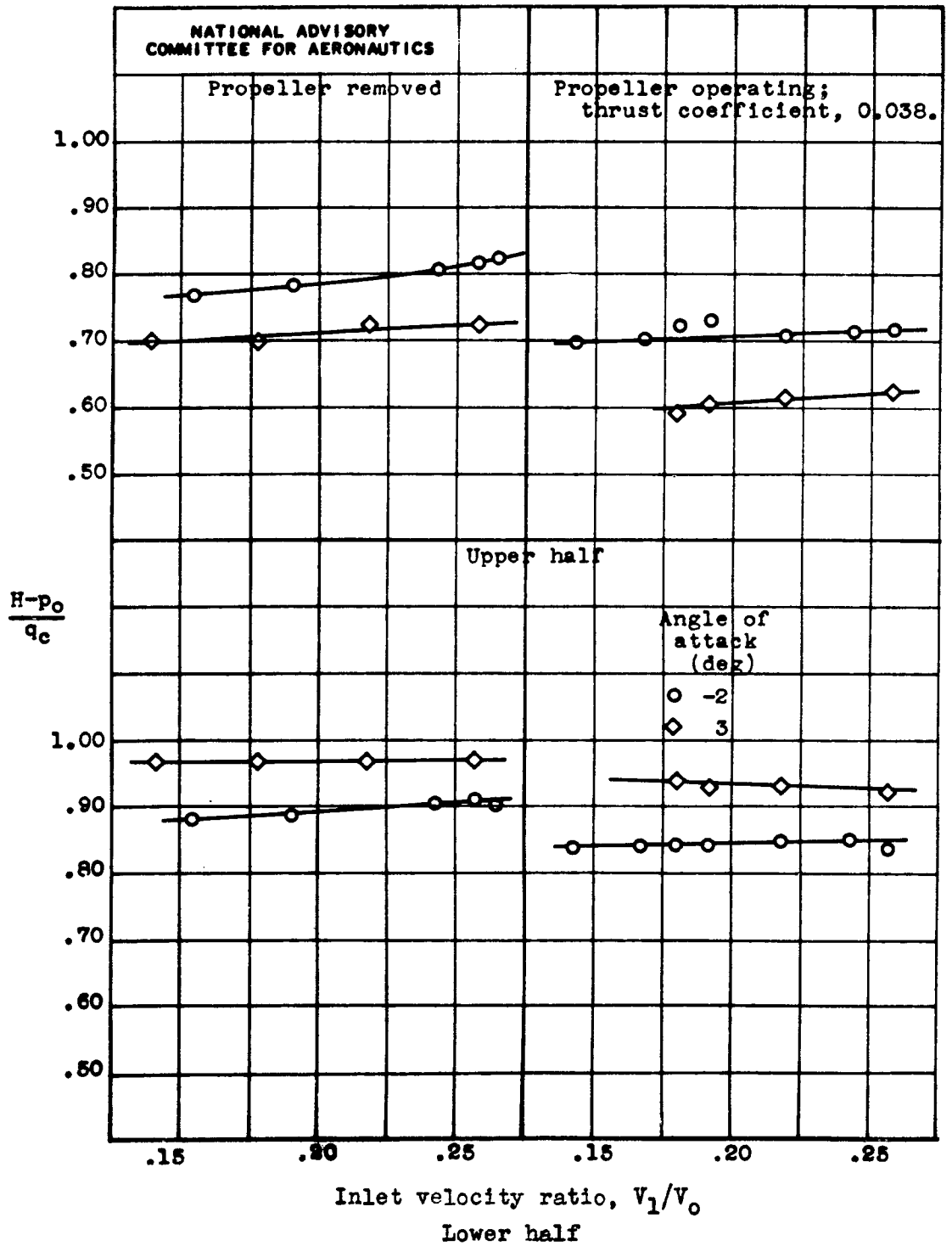

(c) 43-inch-diameter cowl inlet.

Figure 26. - Continued. Effect of inlet velocity ratio on average weighted total pressures at upper and lower halves of cowl inlets.

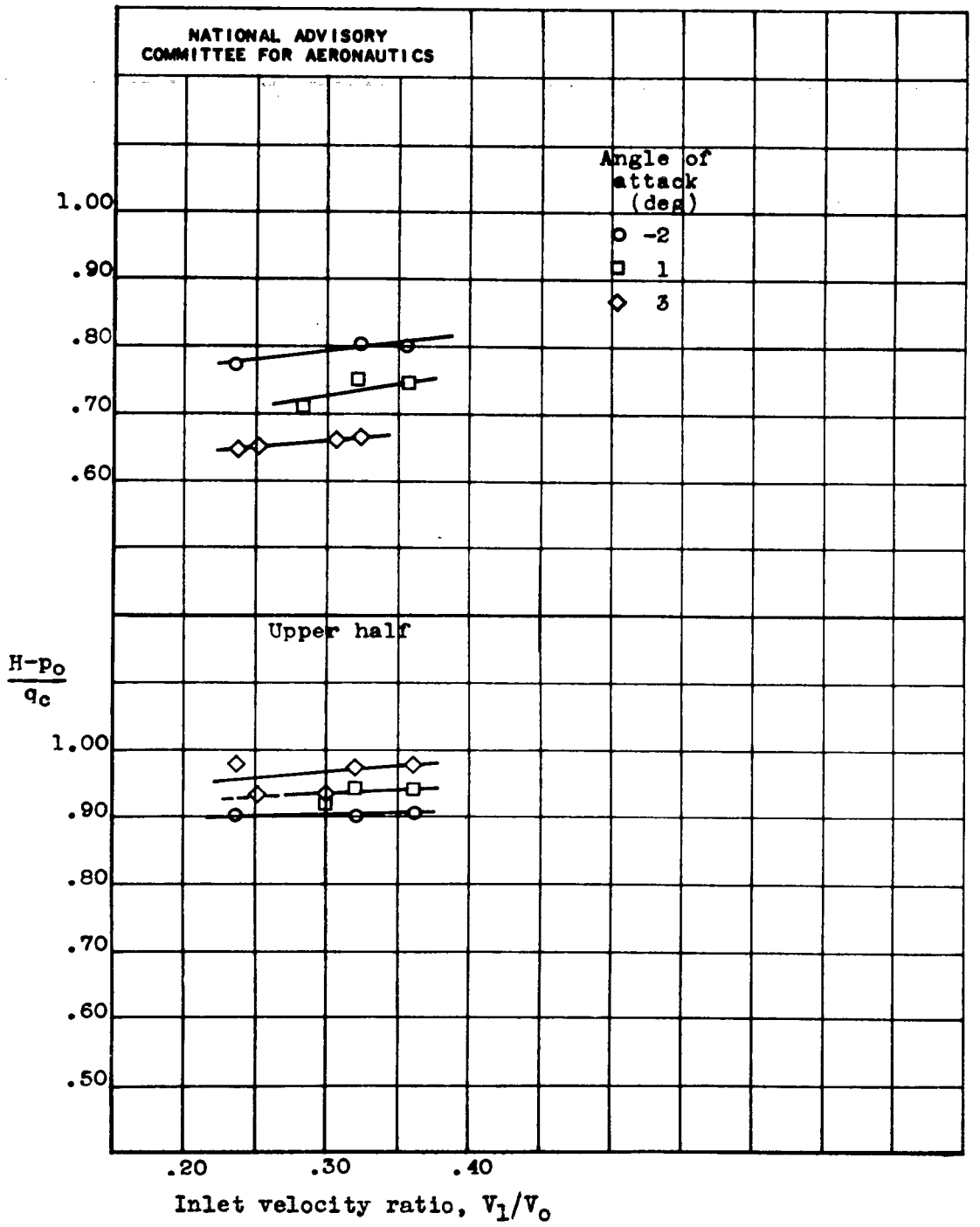

Lower half

(d) 43-inch-diameter cowl inlet with 27-inch-diameter spinner; propeller operating; thrust coefficient, 0.038.

Figure 26. - Continued. Effect of inlet velocity ratio on average weighted total pressures at upper and lower halves of cowl inlets.

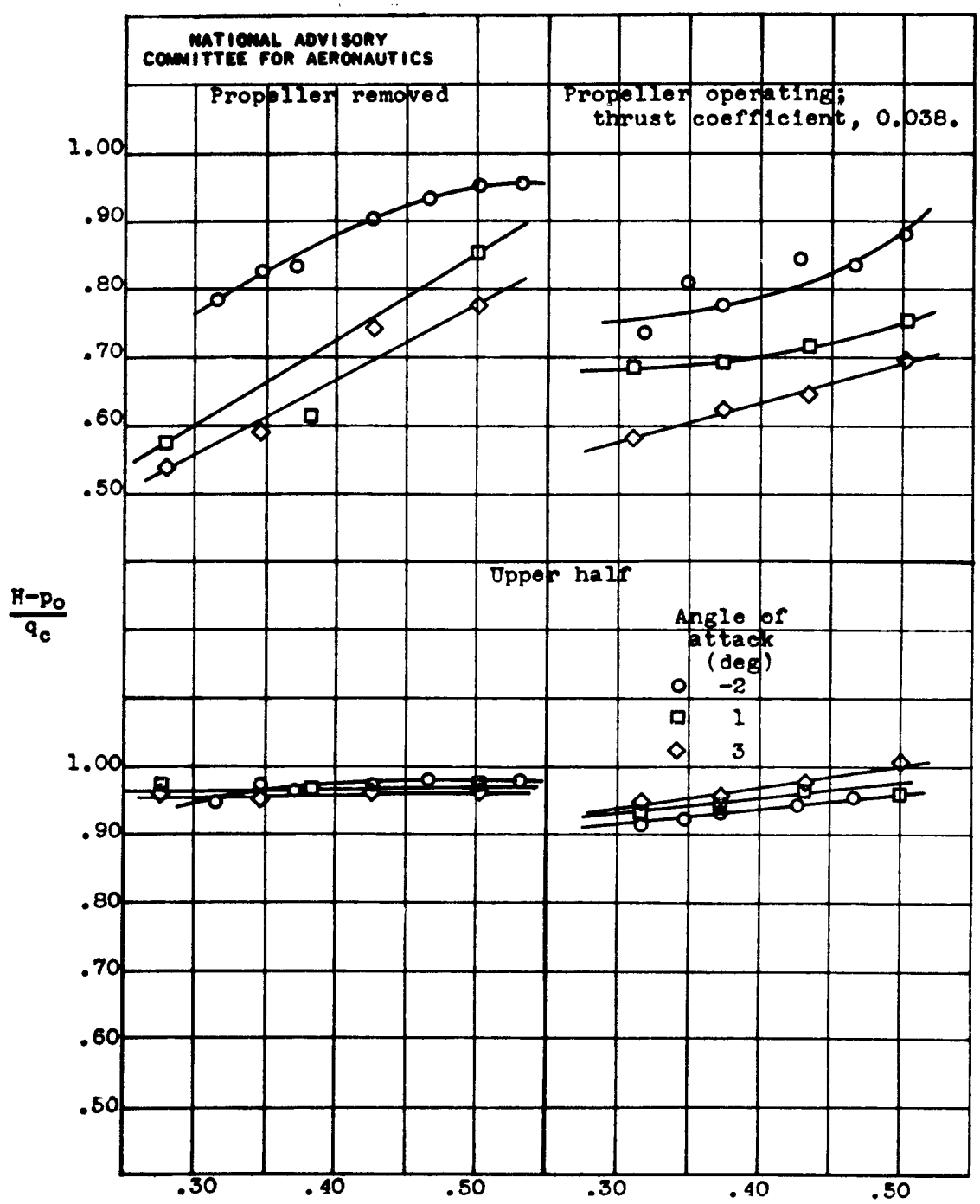

(e) 43-inch-diameter cowl inlet with 32-inch-diameter spinner.

Figure 26. - Concluded. Effect of inlet velocity ratio on average weighted total pressures at upper and lower halves of cowl inlets.

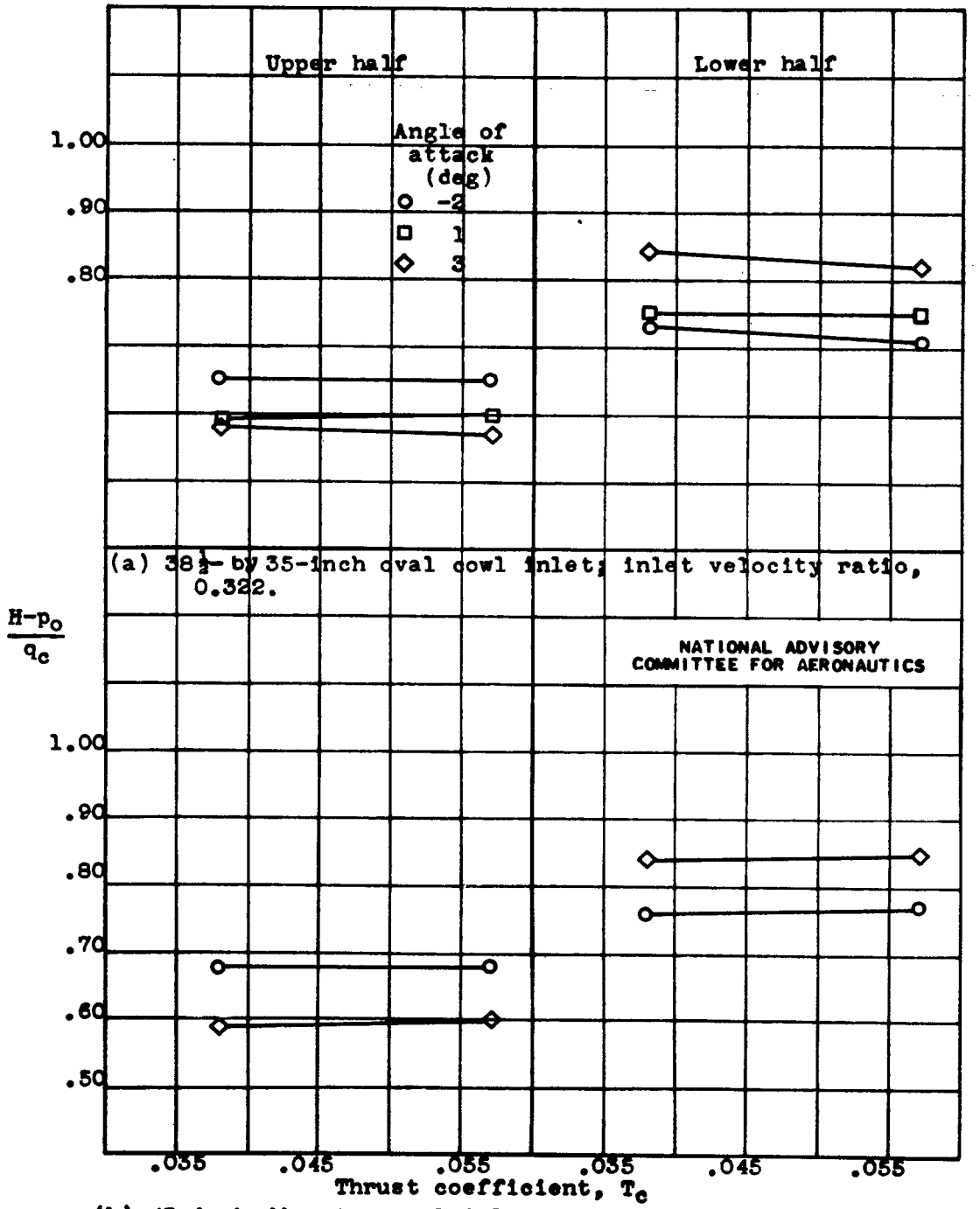

(b) 43-inch-diameter cowl inlet; inlet velocity ratio, 0.190.

Figure 27.- Effect of propeller thrust coefficient on average weighted total pressures at upper and lower halves of cowl inlets.

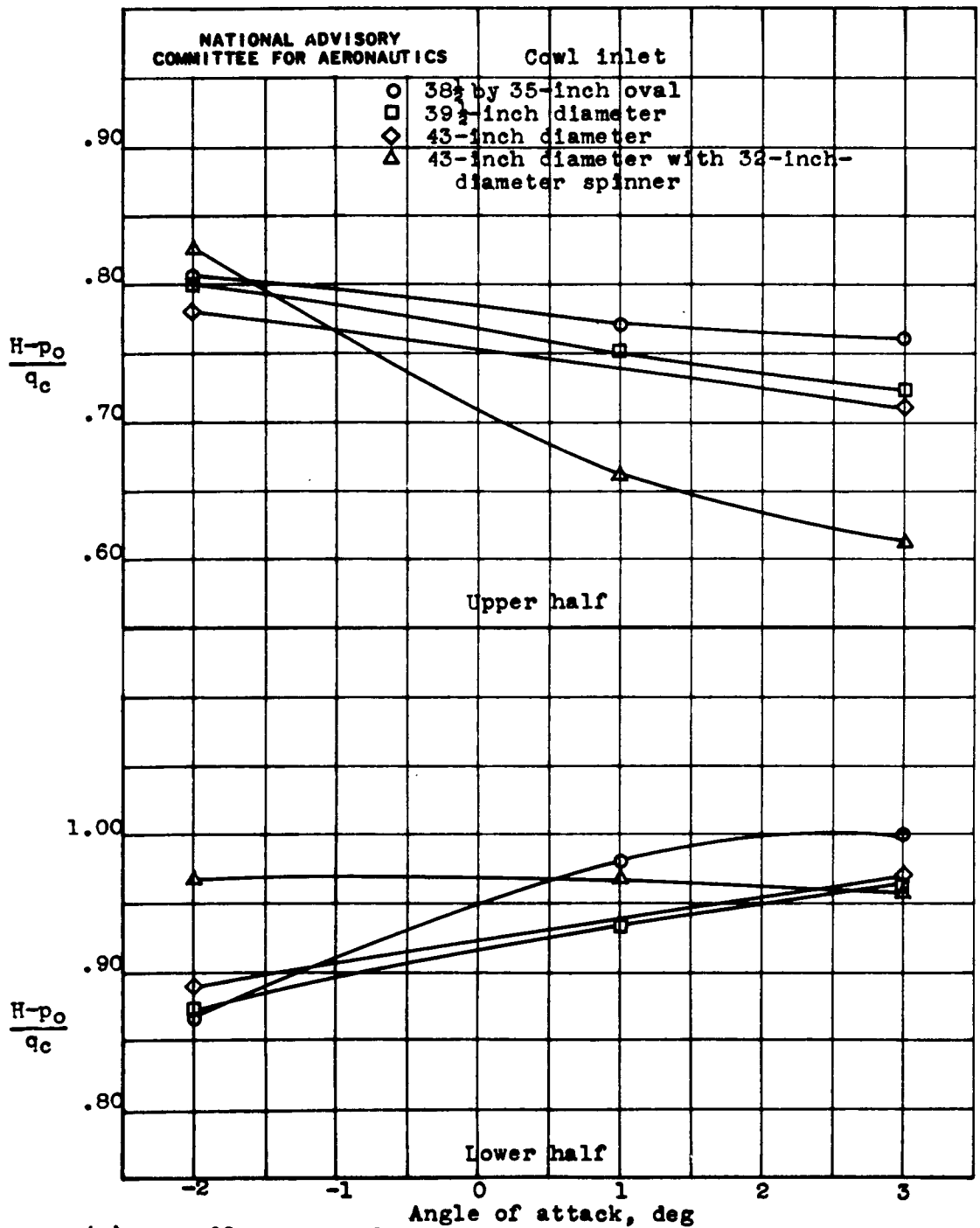

(a) Propeller removed.

Figure 28.- Comparison of average of weighted total-pressure coefficients at cowl inlets of various cowl-inlet configurations. $\Delta p/q_c$, approximately 0.50.

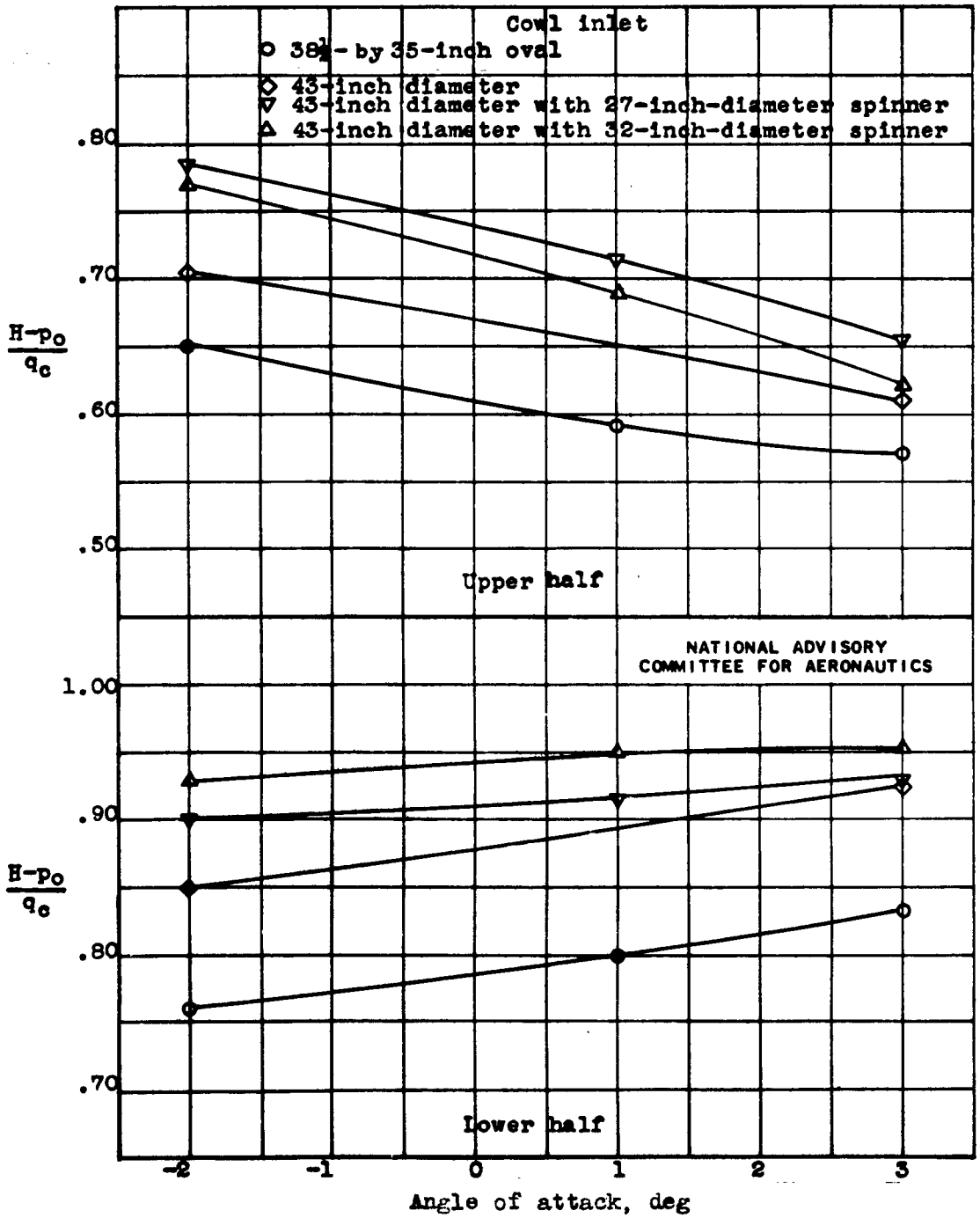

(b) Propeller operating; thrust coefficient, 0.038.

Figure 28. - Concluded. Comparison of average of weighted total-pressure coefficients at cowl inlets of various cowl-inlet configurations. $\Delta p/q_c$, approximately 0.50.

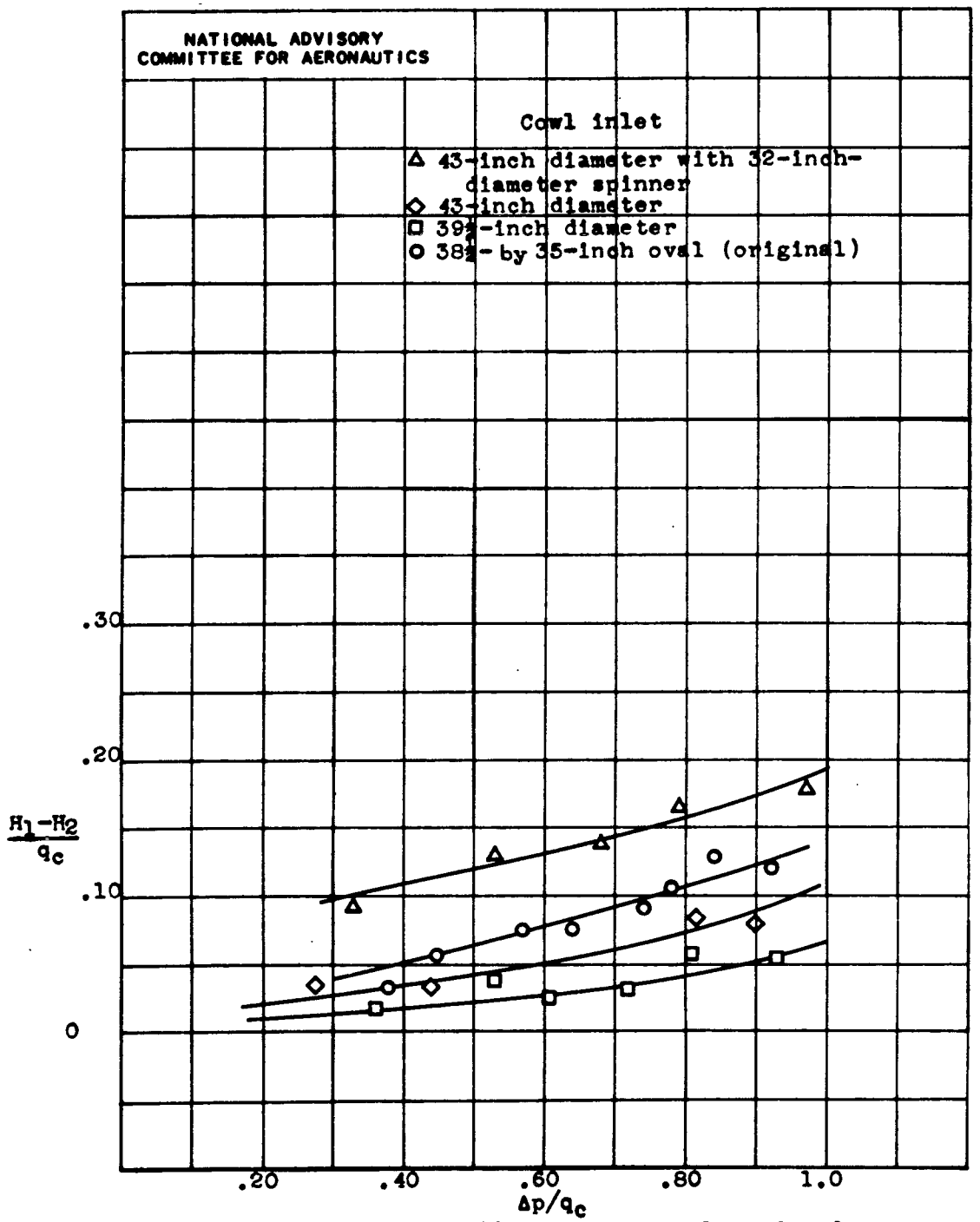

Figure 29.- Comparative diffuser pressure loss for four cowl-inlet configurations with propeller removed. Angle of attack, -2°.

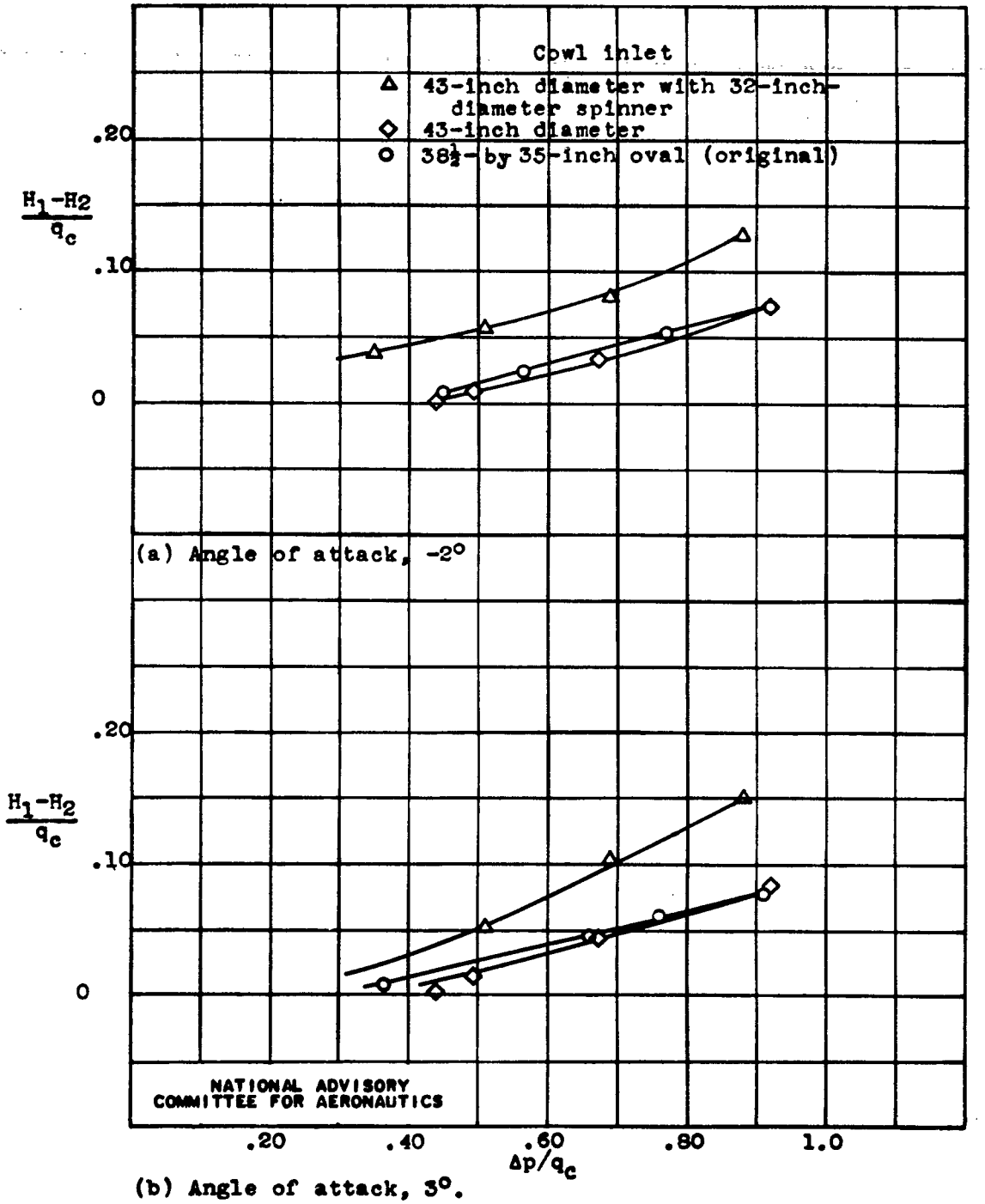

(b) Angle of attack, 3°.

Figure 30.- Comparative diffuser pressure loss for three cowl-inlet configurations with propeller operating. Thrust coefficient, 0.038.

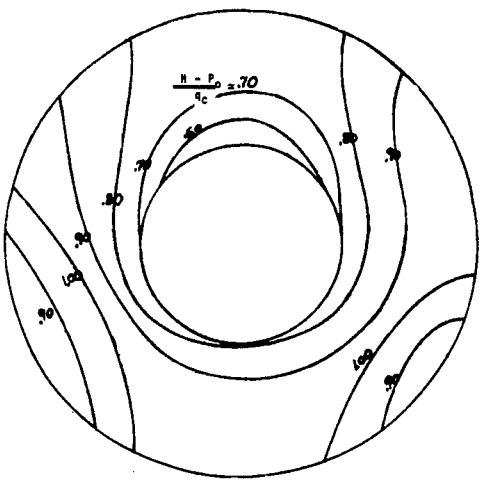

Angle of attack, -2°; inlet velocity ratio, 0.384.

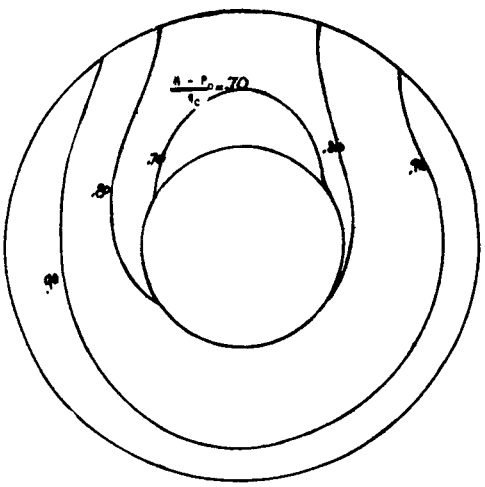

Angle of attack, -2°; inlet velocity ratio, 0.295.

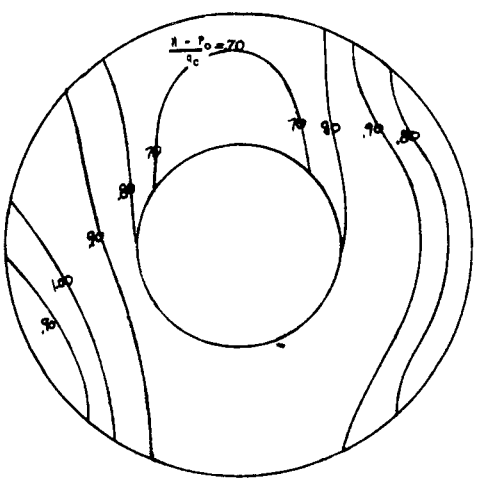

Angle of attack, 3°; inlet velocity ratio, 0.384.

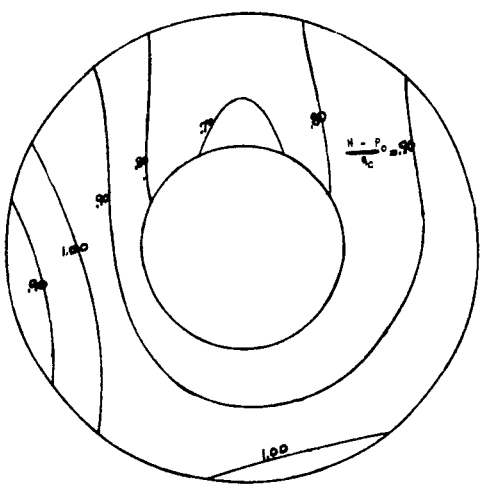

Angle of attack, 3°; inlet velocity. ratio, 0.295.

NATIONAL ADVISORY
COMMITTEE FOR AERONAUTICS

(a) Propeller removed.

Figure 31. - Total-pressure distribution at face of engine with $38\frac{1}{2}$- by 35-inch oval cowl inlet.

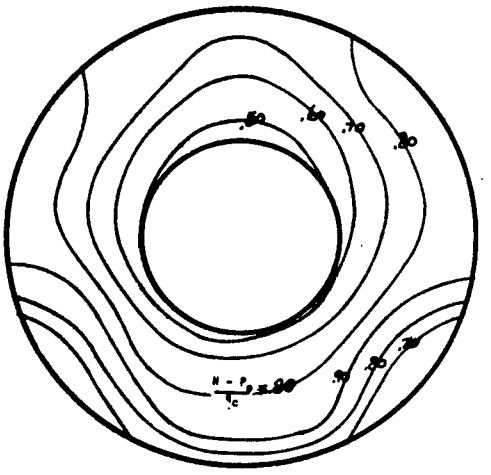

Angle of attack, -2°; inlet velocity ratio, 0.384.

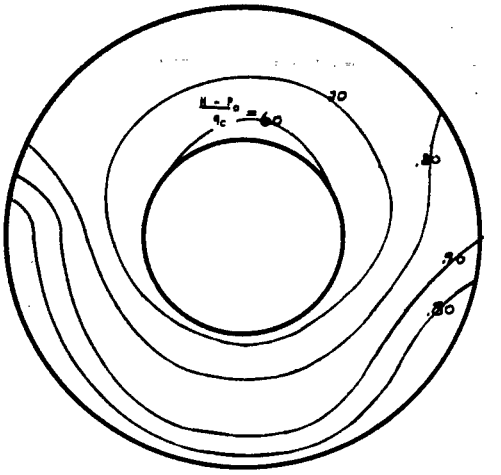

Angle of attack, -2°; inlet velocity ratio, 0.255.

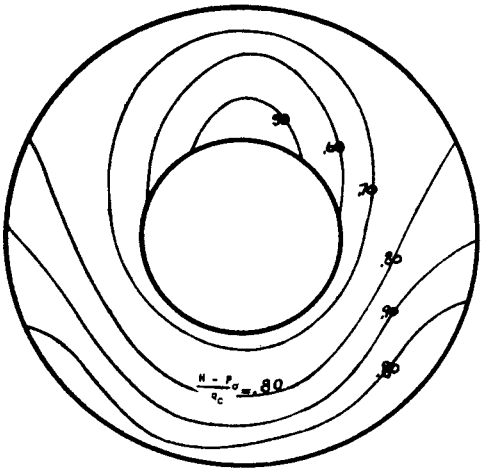

Angle of attack, 3°; inlet velocity ratio, 0.384.

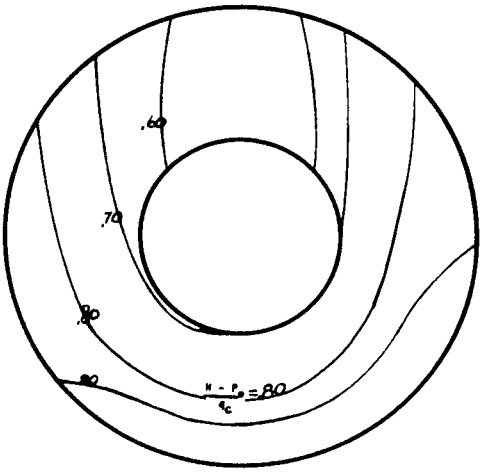

Angle of attack, 3°; inlet velocity ratio, 0.255.

NATIONAL ADVISORY
COMMITTEE FOR AERONAUTICS

(b) Propeller operating; thrust coefficient, 0.038.

Figure 31. - Concluded. Total-pressure distribution at face of engine with $38\frac{1}{2}$- by 35-inch oval cowl inlet.

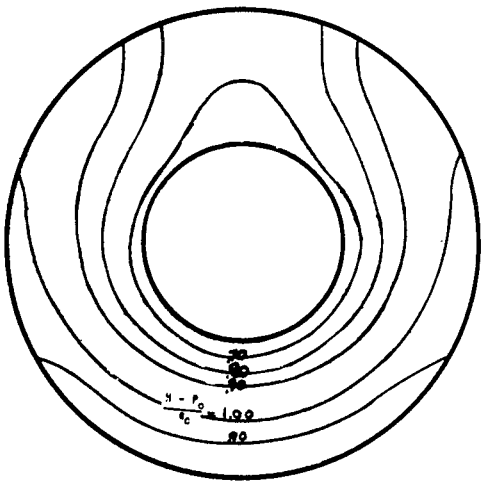

Angle of attack, -2°; inlet velocity ratio, 0.255.

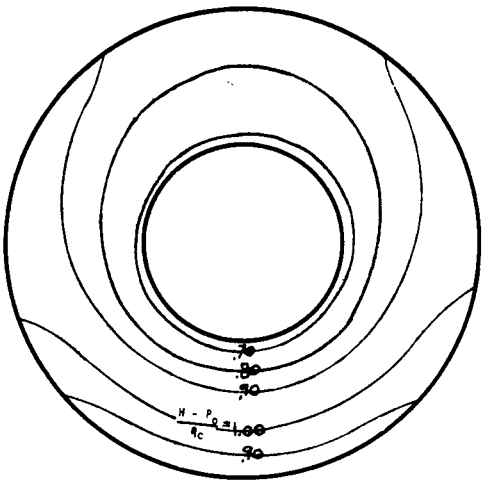

Angle of attack, -2°; inlet velocity ratio, 0.180.

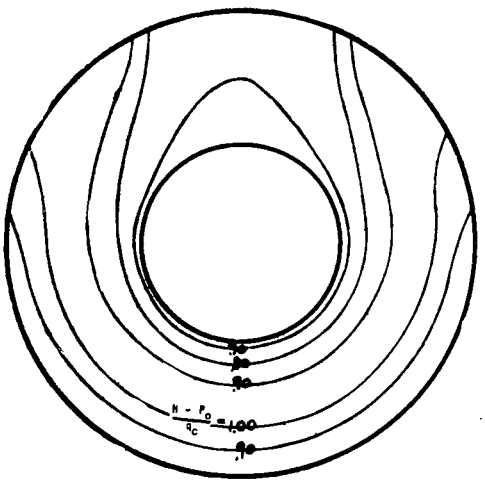

Angle of attack, 3°; inlet velocity ratio, 0.255.

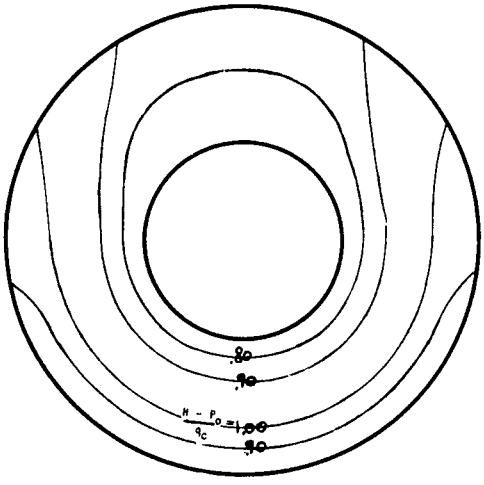

Angle of attack, 3°; inlet velocity ratio, 0.180.

NATIONAL ADVISORY
COMMITTEE FOR AERONAUTICS

(a) Propeller removed.

Figure 32. - Total-pressure distribution at face of engine with 43-inch-diameter cowl inlet.

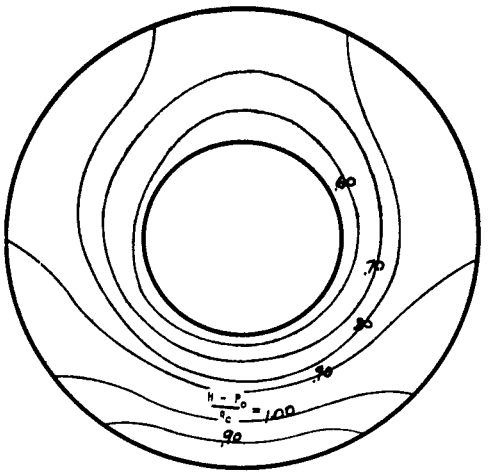

Angle of attack, -2°; inlet velocity ratio, 0.255.

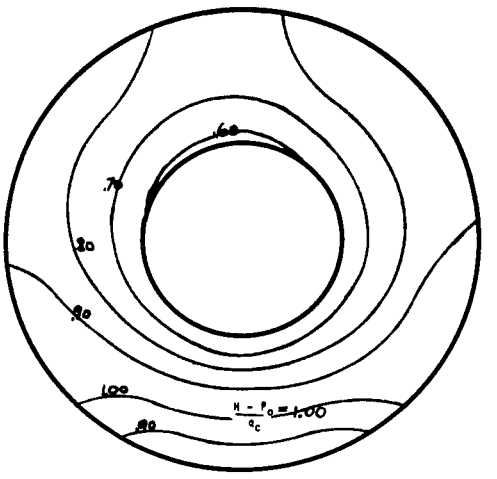

Angle of attack, -2°; inlet velocity ratio, 0.191.

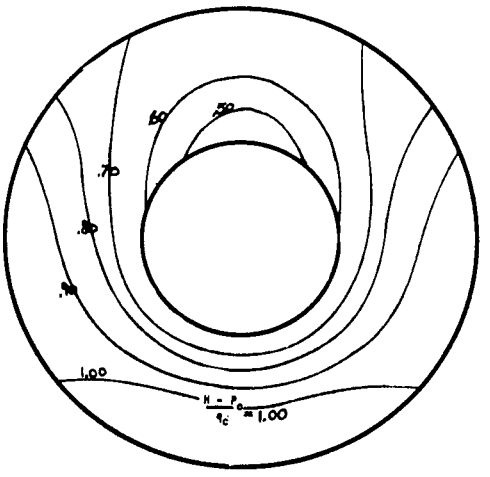

Angle of attack, 3°; inlet velocity ratio, 0.255.

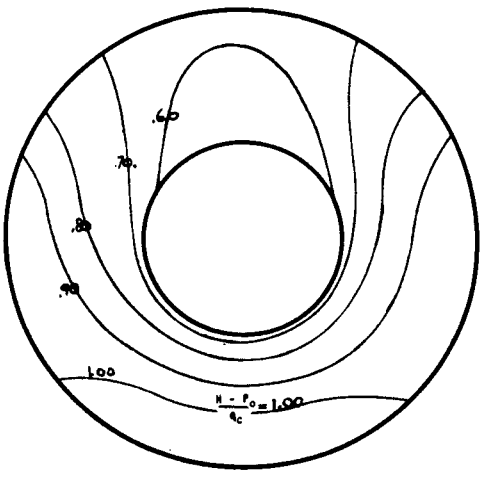

Angle of attack, 3°; inlet velocity ratio, 0.191.

NATIONAL ADVISORY
COMMITTEE FOR AERONAUTICS

(b) Propeller operating; thrust coefficient, 0.038.

Figure 32. - Concluded. Total-pressure distribution at face of engine with 43-inch-diameter cowl inlet.

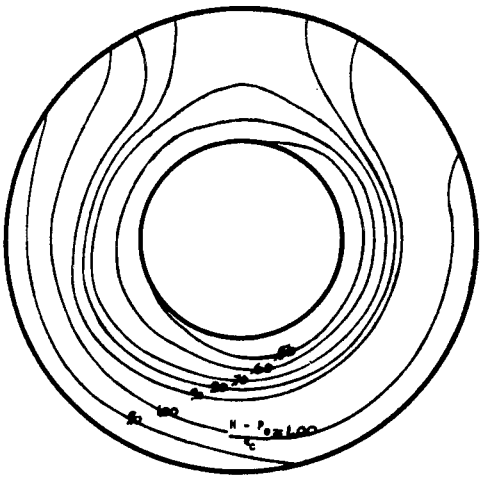

Angle of attack, -2°; inlet velocity ratio, 0.498.

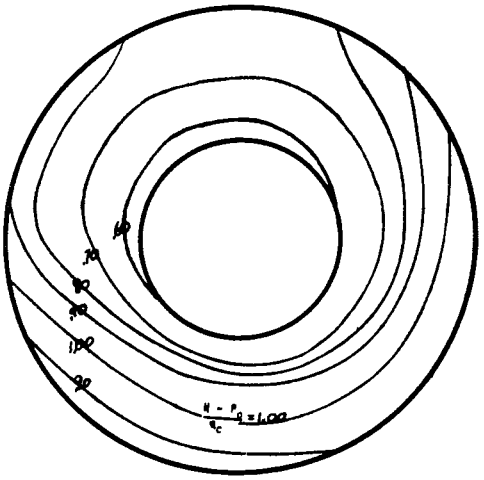

Angle of attack, -2°; inlet velocity ratio, 0.350.

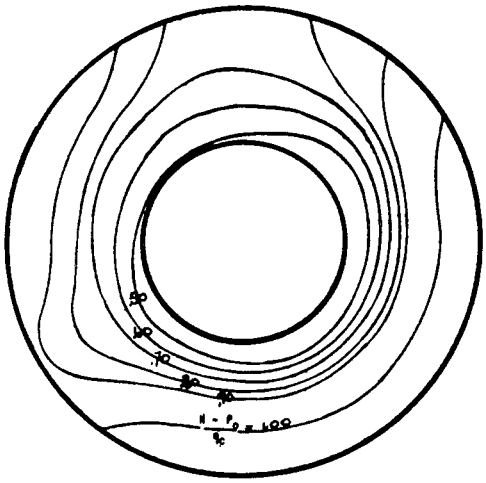

Angle of attack, 3°; inlet velocity ratio, 0.498.

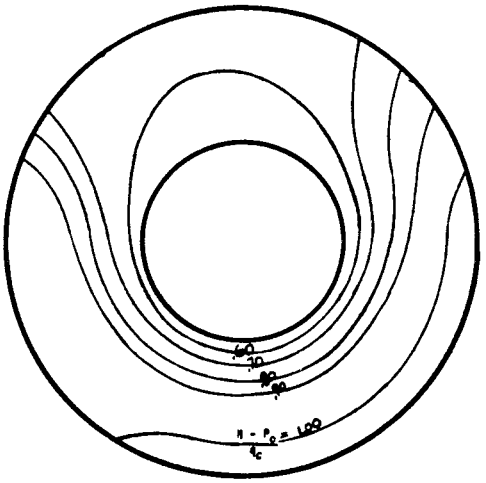

Angle of attack, 3°; inlet velocity ratio, 0.350.

NATIONAL ADVISORY
COMMITTEE FOR AERONAUTICS

(a) Propeller removed.

Figure 33. - Total-pressure distribution at face of engine with 43-inch-diameter cowl inlet with 32-inch-diameter spinner.

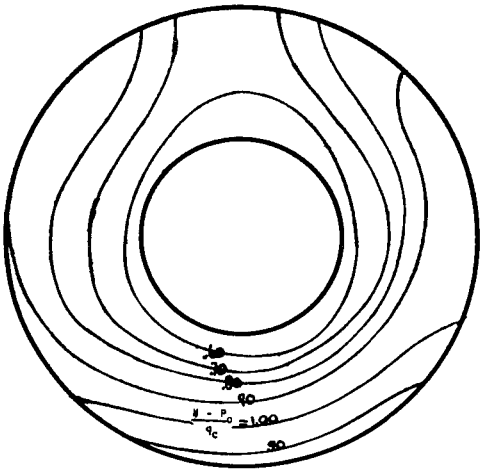

Angle of attack, -2°; inlet velocity ratio, 0.498.

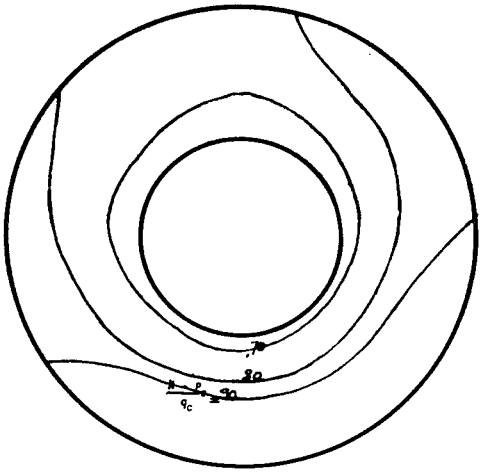

Angle of attack, -2°; inlet velocity ratio, 0.372

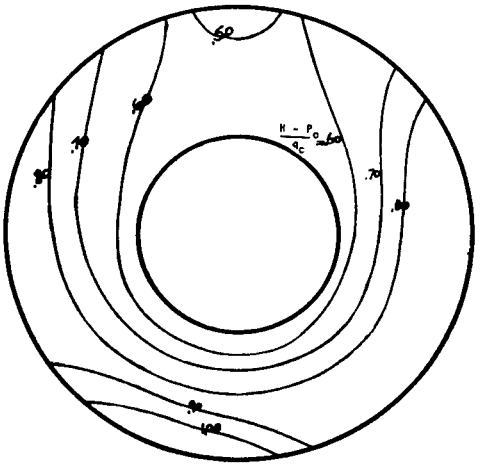

Angle of attack, 3°; inlet velocity ratio, 0.498.

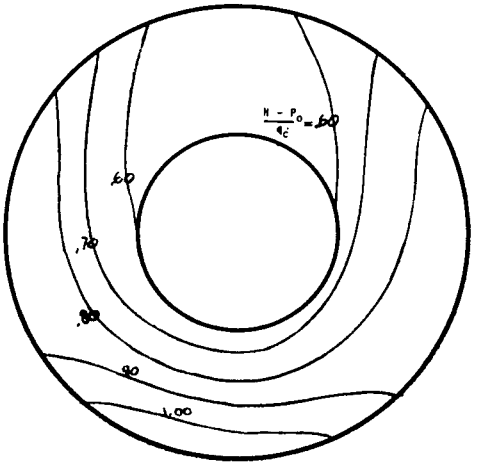

Angle of attack, 3°; inlet velocity ratio, 0.372.

NATIONAL ADVISORY
COMMITTEE FOR AERONAUTICS

(b) Propeller operating; thrust coefficient, 0.038.

Figure 33. - Concluded. Total-pressure distribution at face of engine with 43-inch-diameter cowl inlet with 32-inch-diameter spinner.

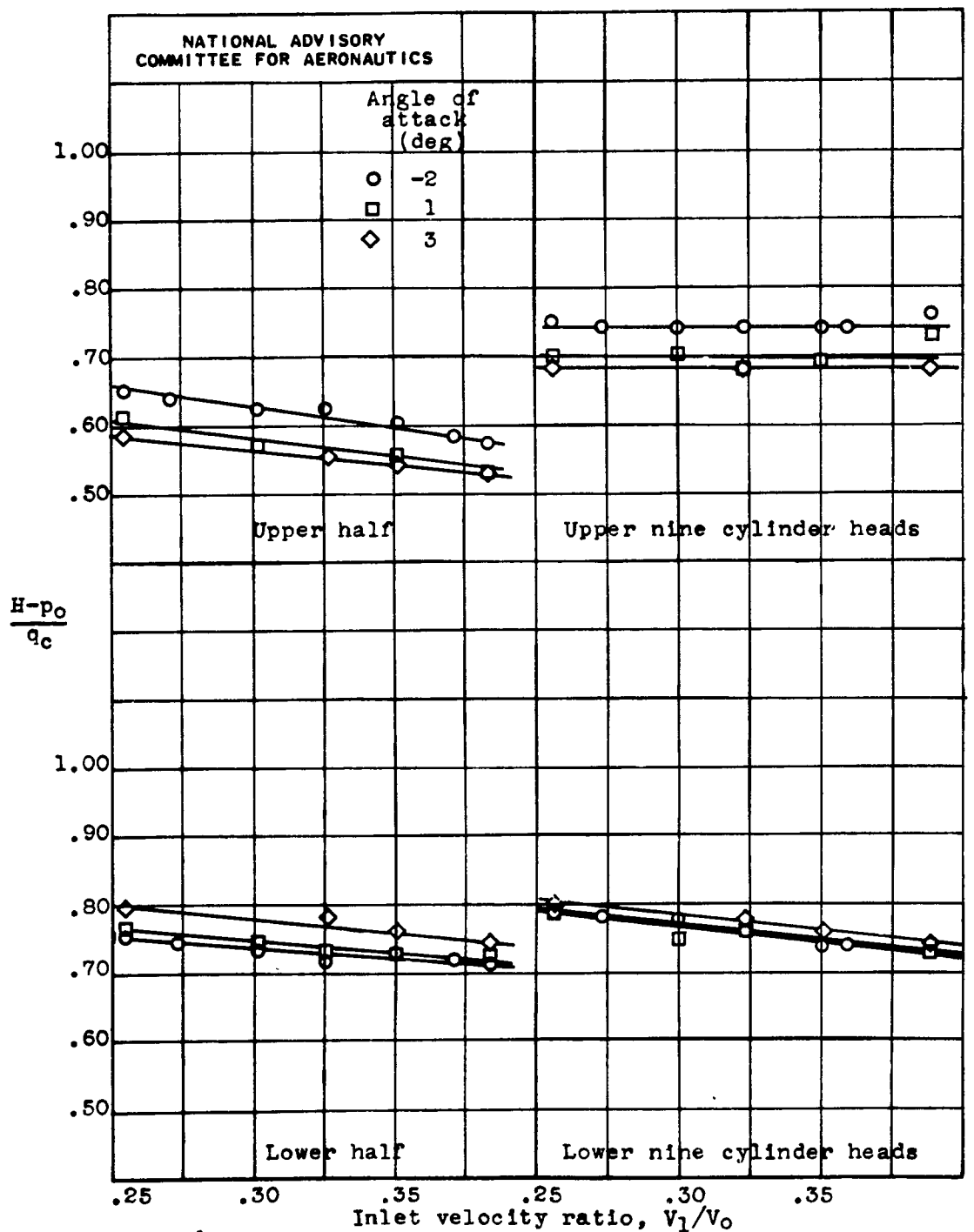

(a) 38½-by 35-inch oval cowl inlet.

Figure 34.- Effect of inlet velocity ratio on average weighted total pressures at face of engine, upper and lower halves, and average total pressures of upper and lower nine cylinder heads. Propeller operating; thrust coefficient, 0.038.

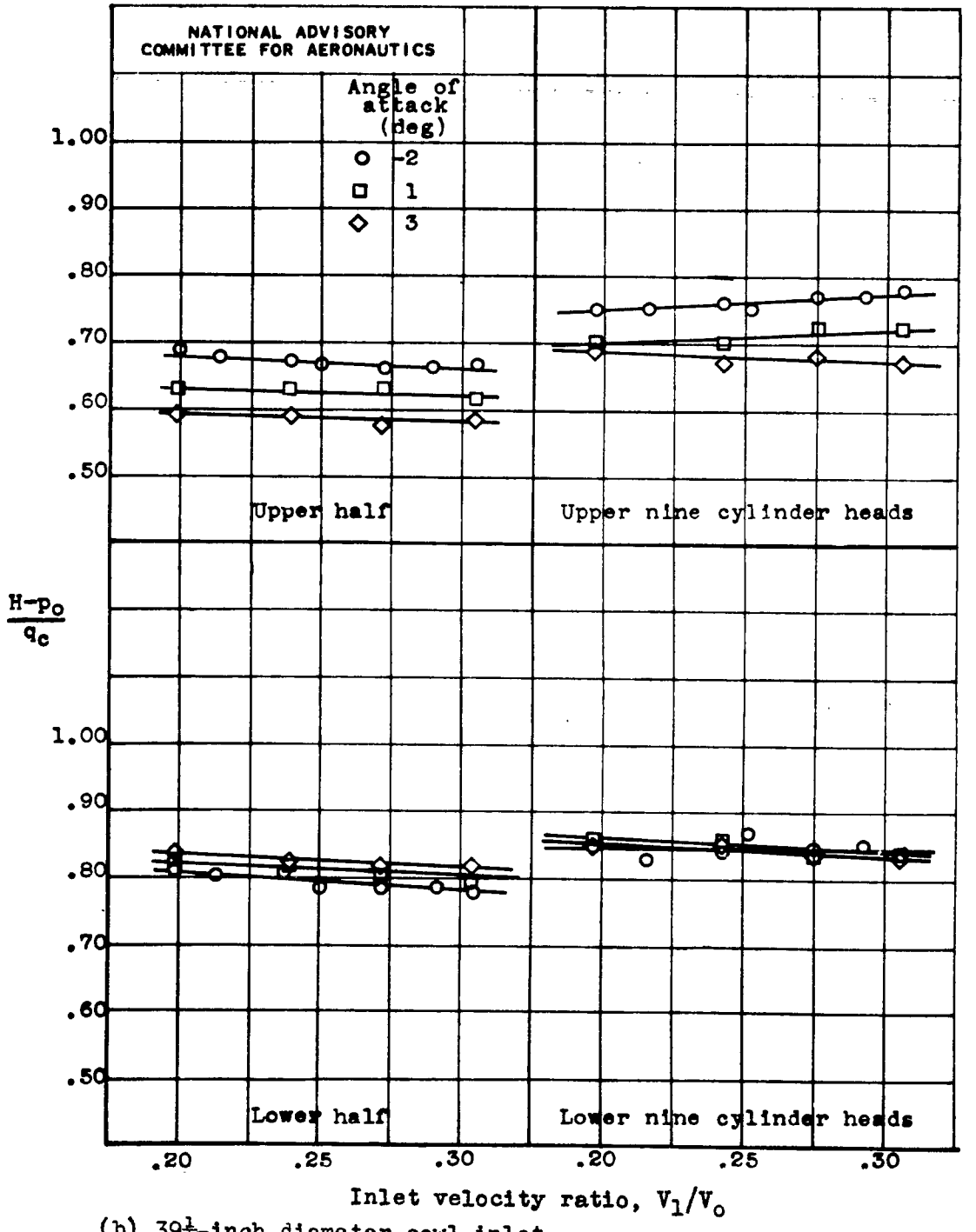

(b) 39½-inch-diameter cowl inlet.

Figure 34. - Continued. Effect of inlet velocity ratio on average weighted total pressures at face of engine, upper and lower halves, and average total pressures of upper and lower nine cylinder heads. Propeller operating; thrust coefficient, 0.038.

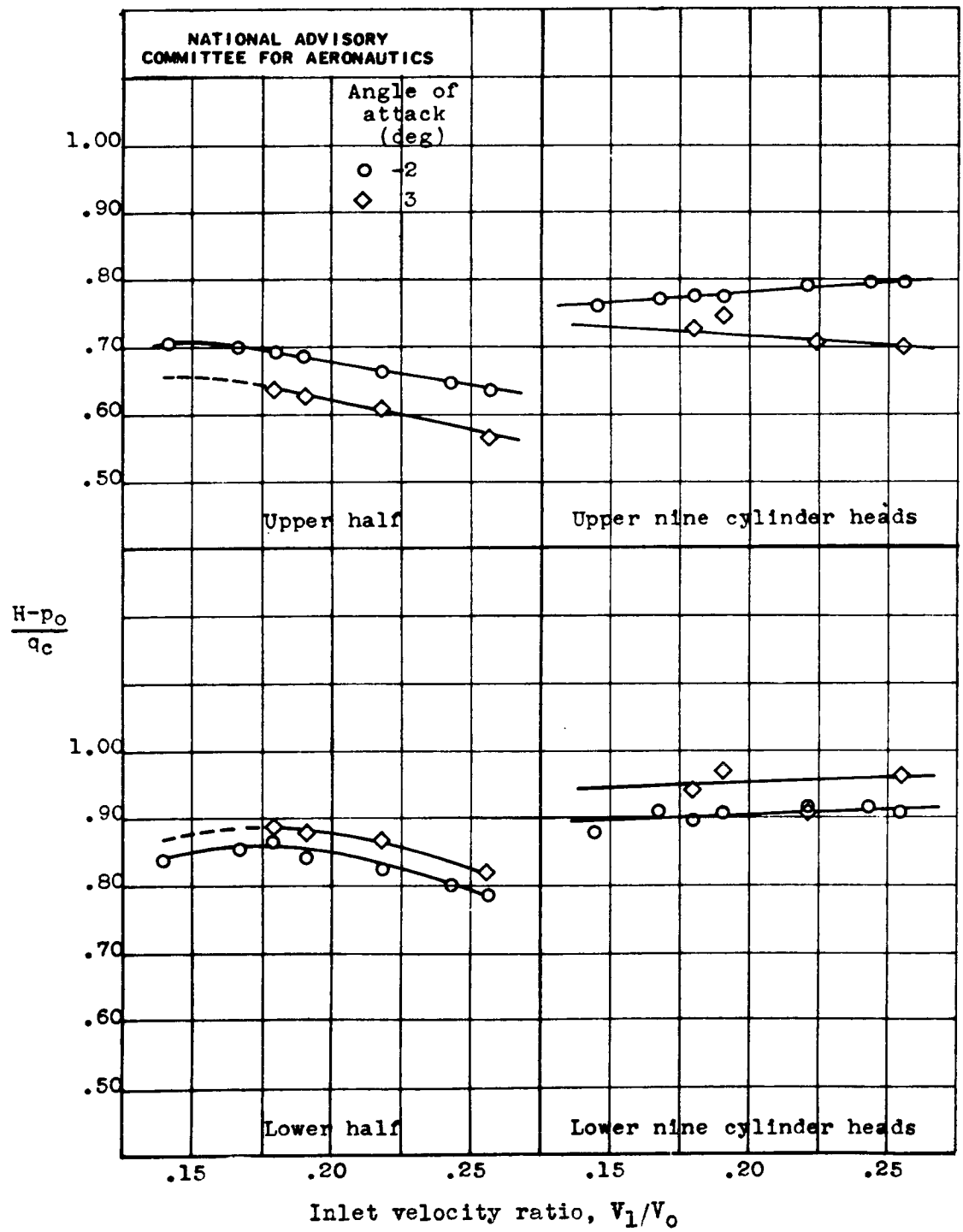

(c) 43-inch-diameter cowl inlet.

Figure 34. - Continued. Effect of inlet velocity ratio on average weighted total pressures at face of engine, upper and lower halves, and average total pressures of upper and lower nine cylinder heads. Propeller operating; thrust coefficient, 0.038.

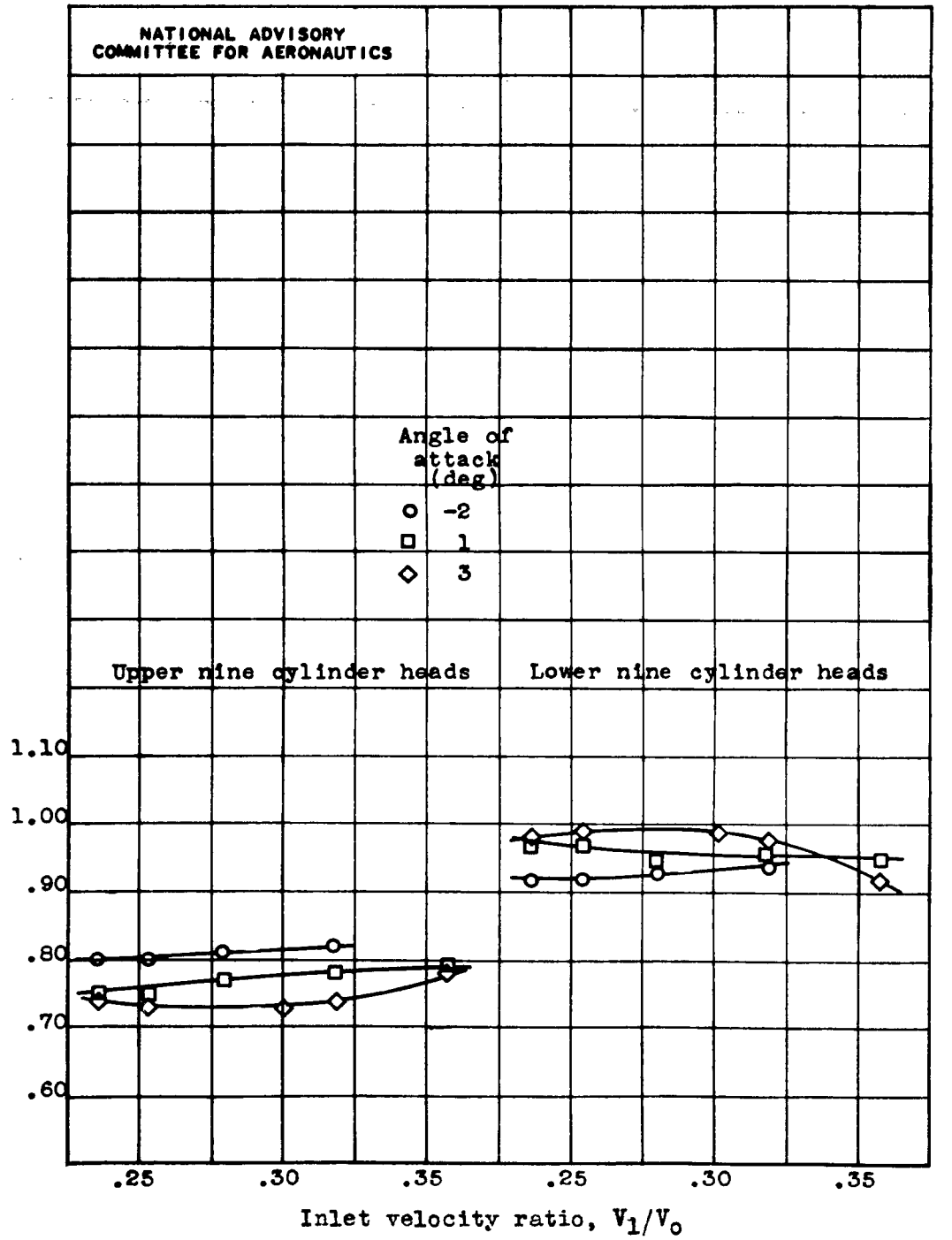

(d) 43-inch-diameter cowl inlet with 27-inch-diameter spinner.

Figure 34. - Continued. Effect of inlet velocity ratio on average weighted total pressures at face of engine, upper and lower halves, and average total pressures of upper and lower nine cylinder heads. Propeller operating; thrust coefficient, 0.038.

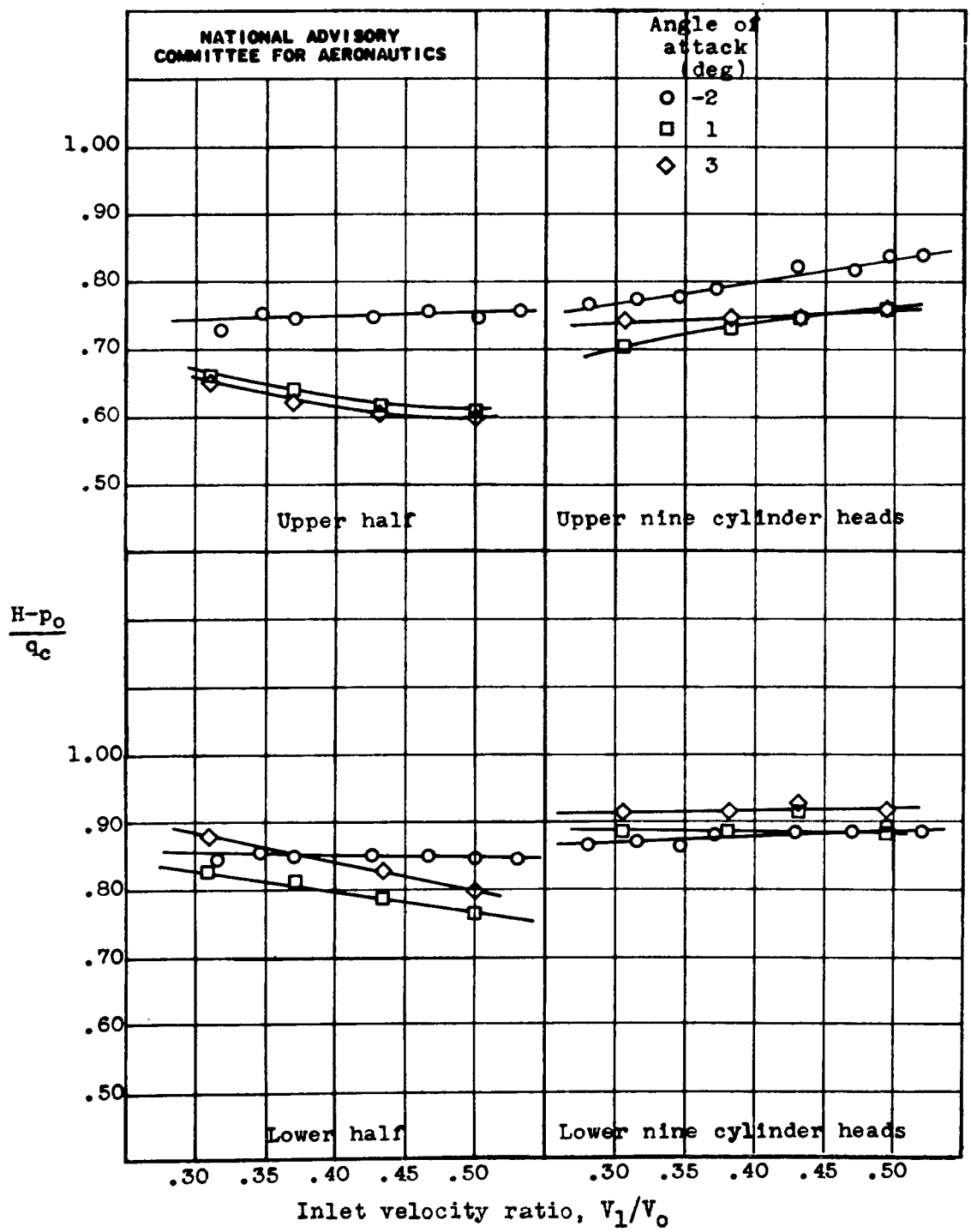

(e) 43-inch-diameter cowl inlet with 32-inch-diameter spinner.

Figure 34. - Concluded. Effect of inlet velocity ratio on average weighted total pressures at face of engine, upper and lower halves, and average total pressures of upper and lower nine cylinder heads. Propeller operating; thrust coefficient, 0.038.

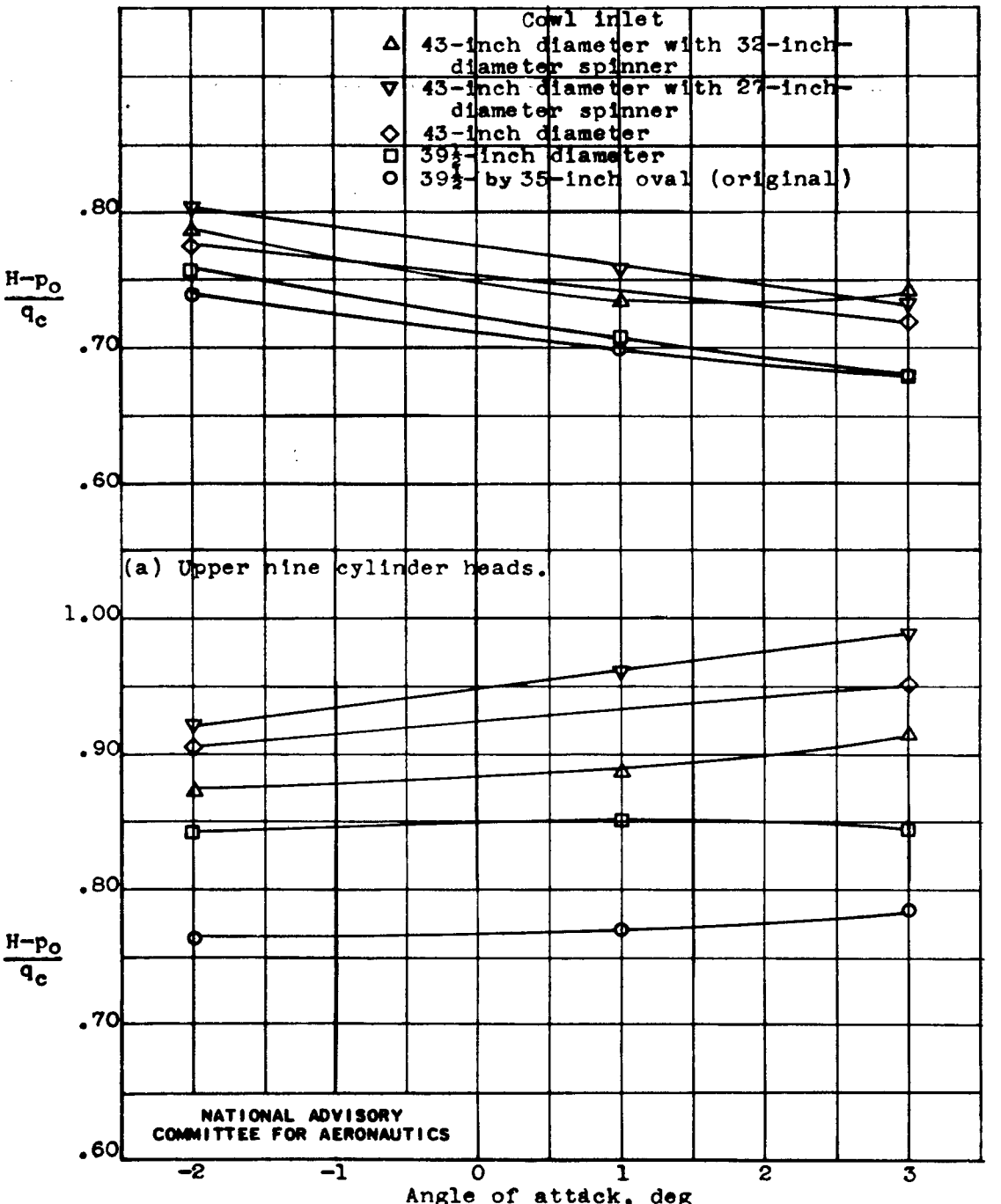

Figure 35.- Comparison of average total pressure at cylinder heads of five cowl-inlet configurations. Propeller operating; thrust coefficient T_c, 0.038; $\Delta p/q_c$, approximately 0.50.

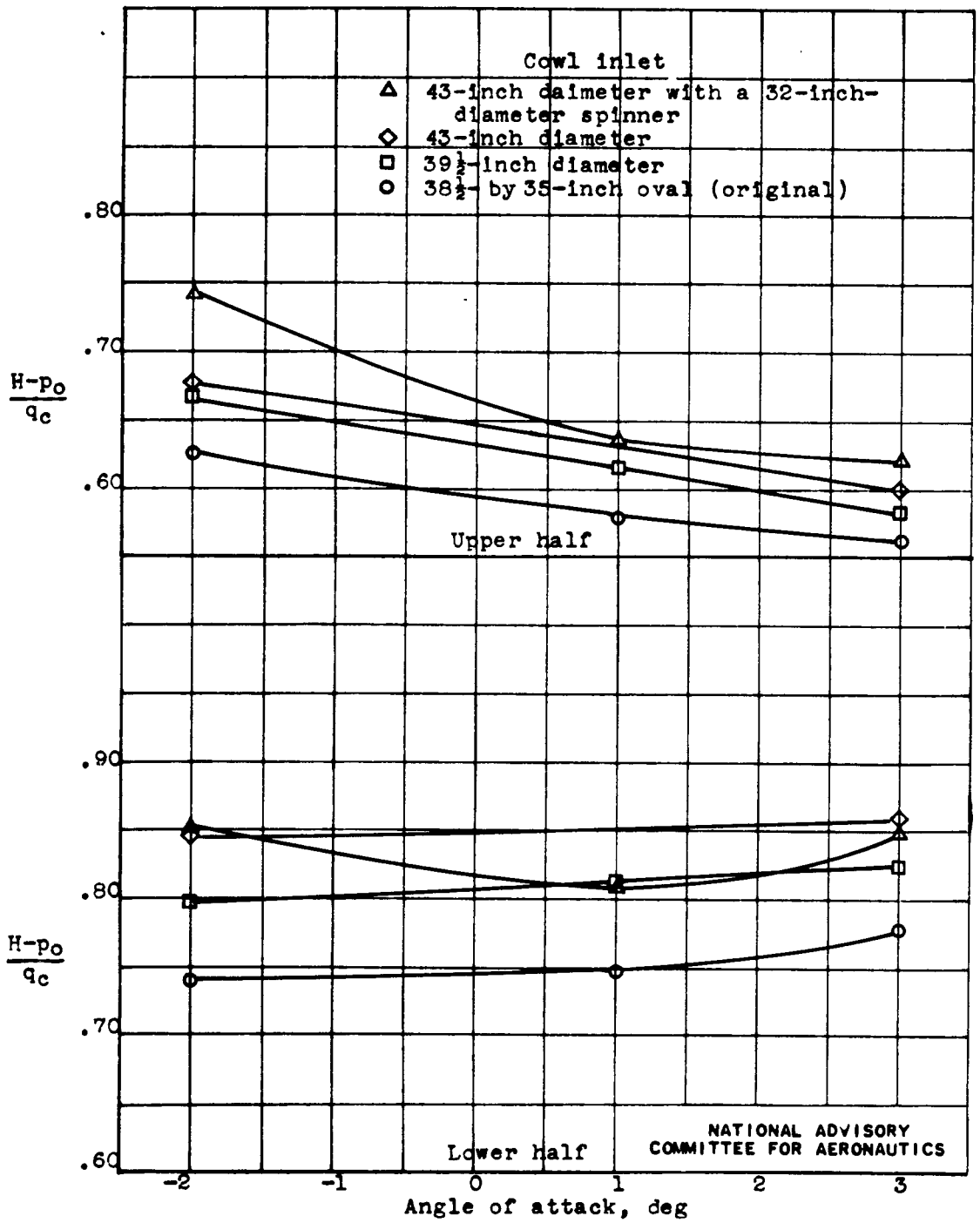

Figure 36.- Comparison of average of weighted total pressures at face of engine of five cowl-inlet configurations. Propeller operating; thrust coefficient T_c, 0.C38; $\Delta p/q_c$, approximately 0.50.

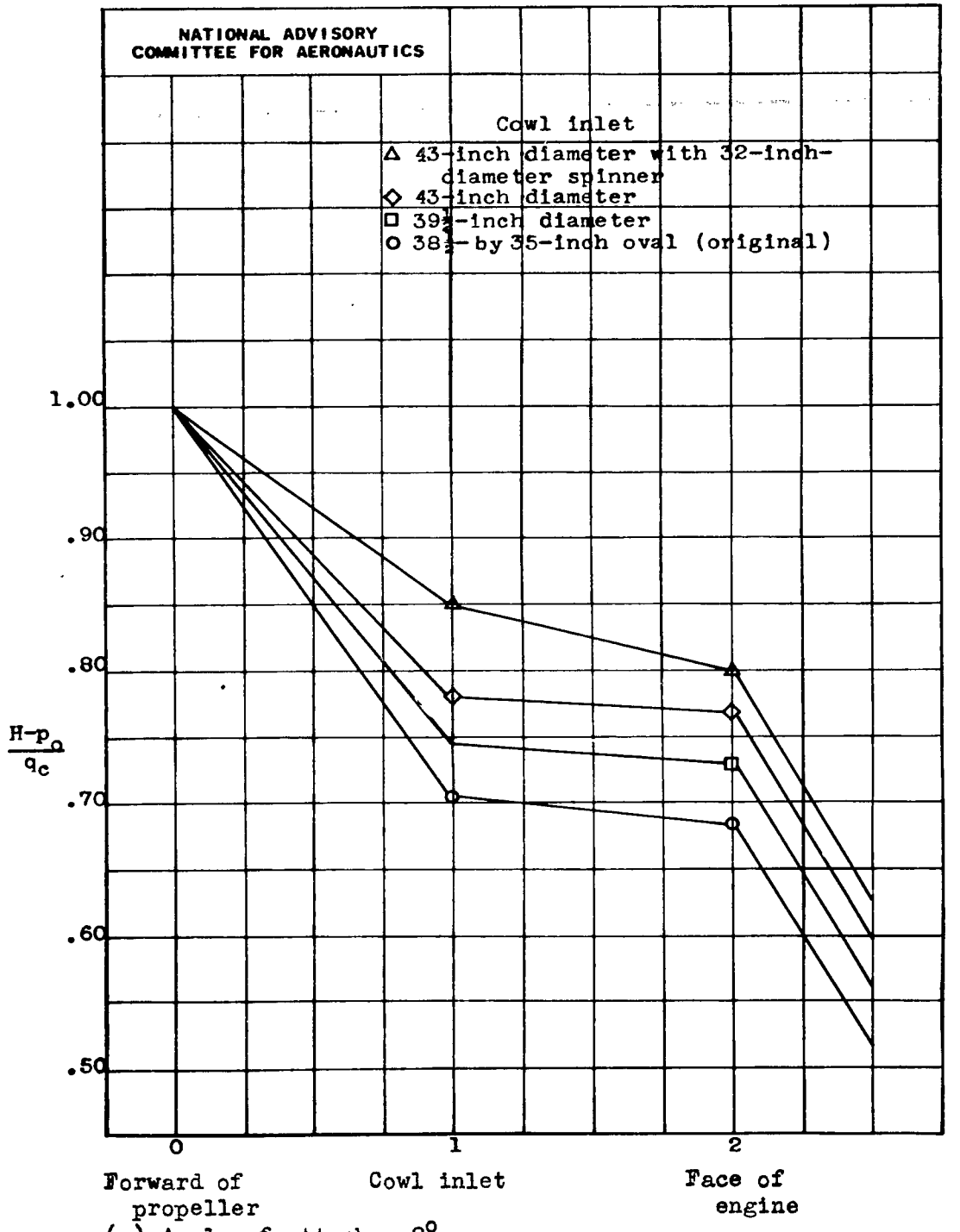

(a) Angle of attack, -2°.

Figure 37. - Total-pressure gradient from free stream to face of engine. Propeller operating; thrust coefficient T_c, 0.038; $\Delta p/q_c$, approximately 0.50.

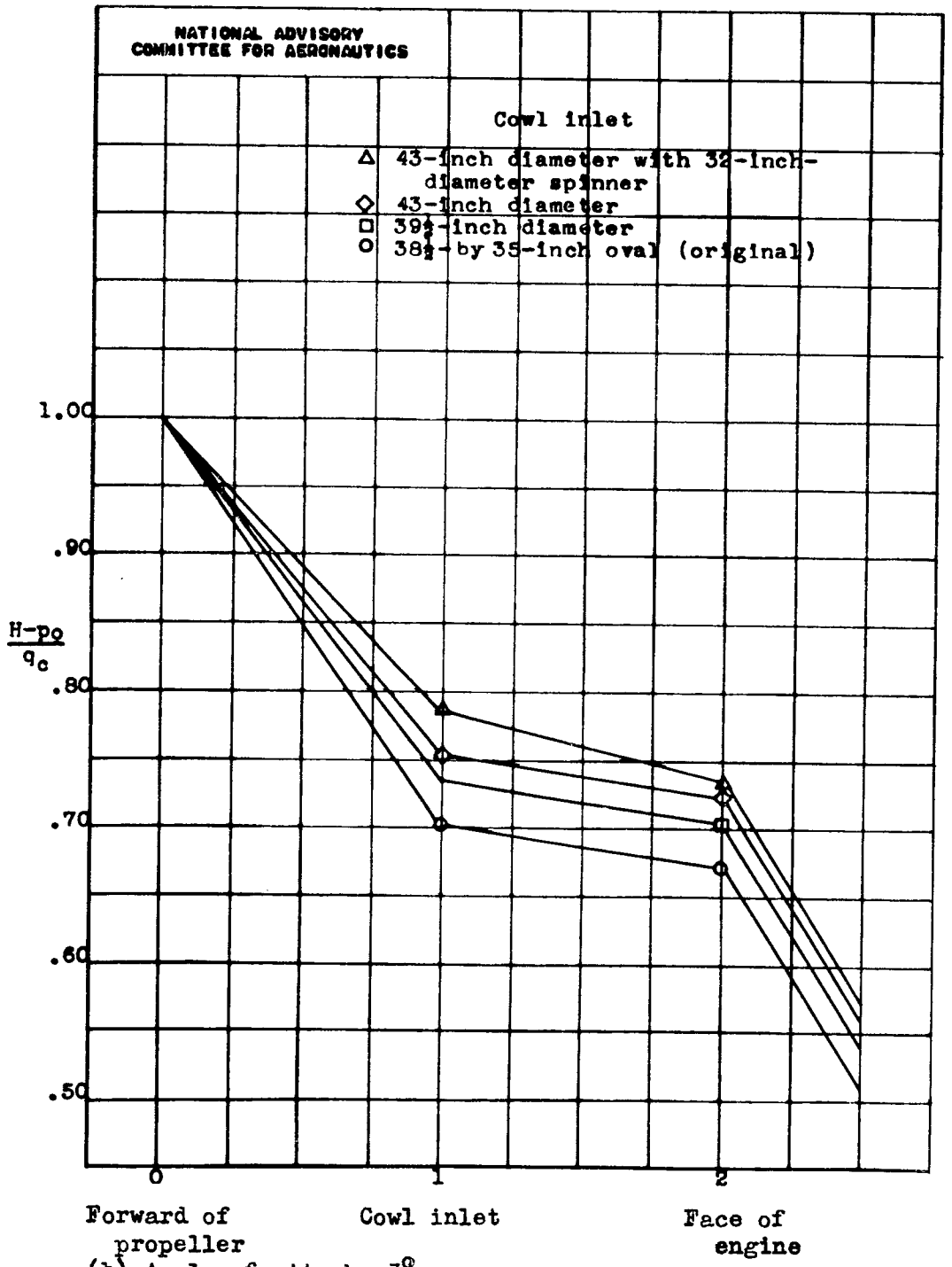

(b) Angle of attack, 3°.

Figure 37. - Concluded. Total-pressure gradient from free stream to face of engine. Propeller operating; thrust coefficient T_c, 0.038; $\Delta p/q_c$, approximately 0.50.

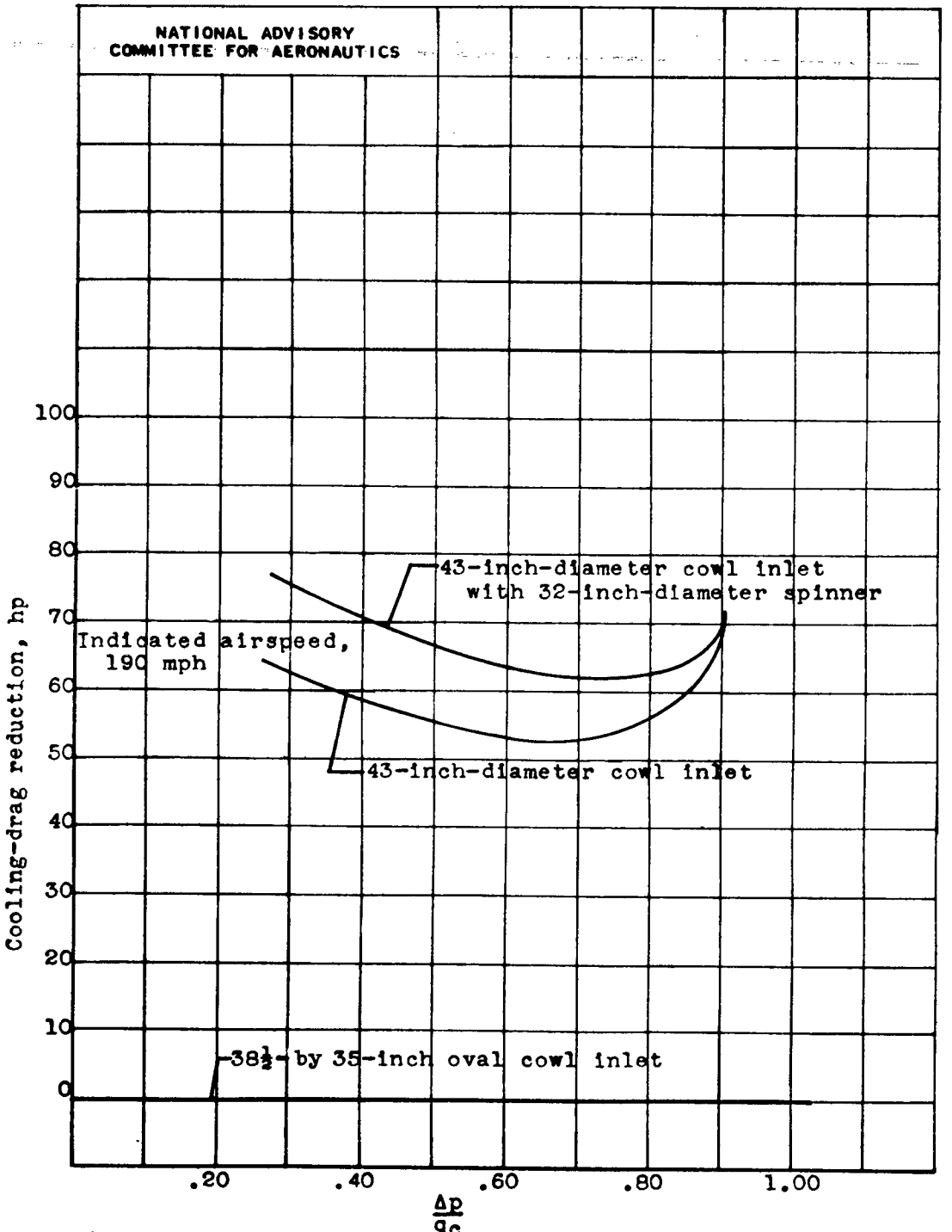

(a) Thrust coefficient, 0.038.

Figure 38.- A comparison of cooling drag reduction of different cowl-inlet configurations. Pressure altitude, 15,000 feet; angle of attack, -2°.

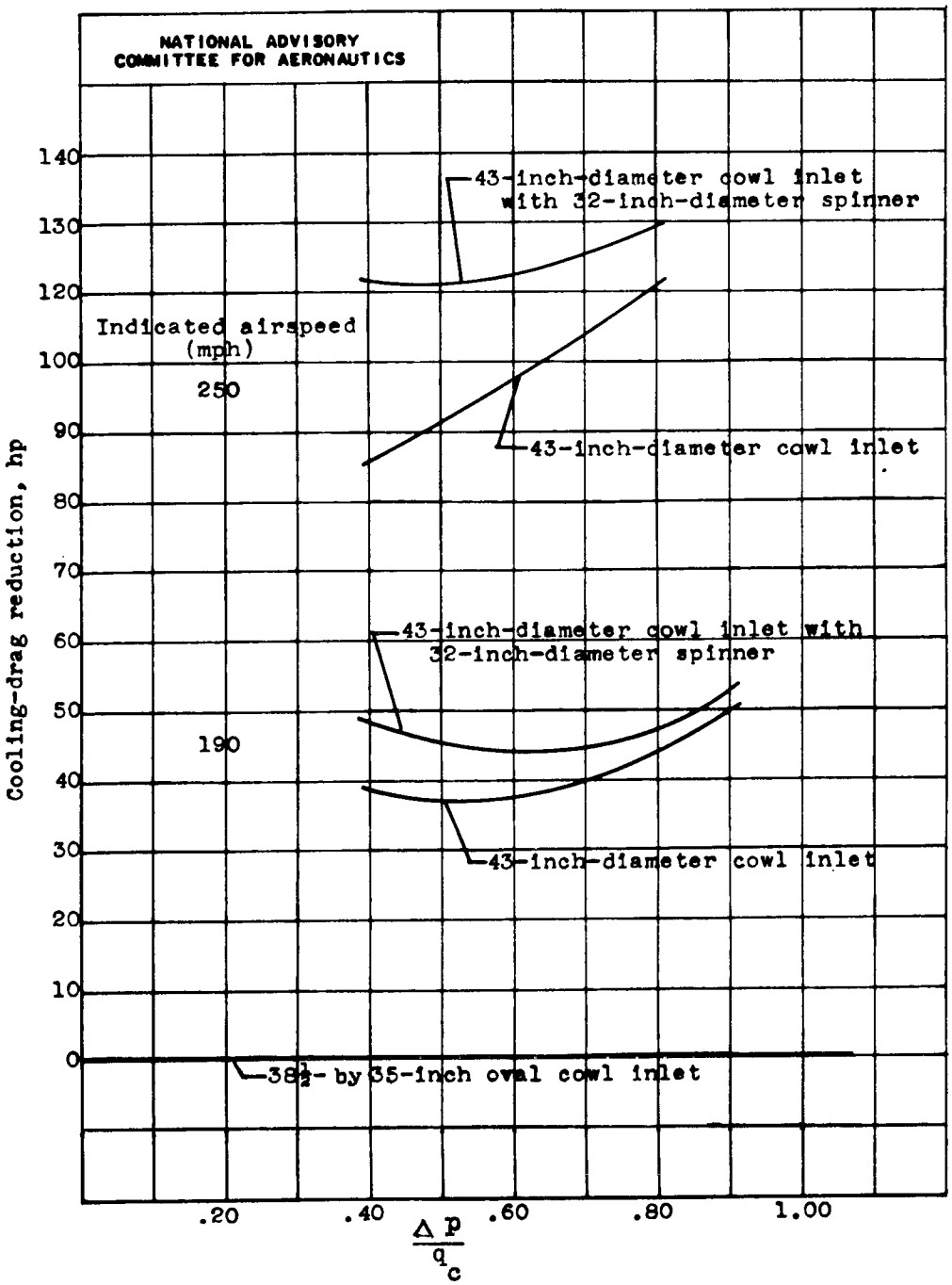

(b) Thrust coefficient, 0.057.

Figure 38. - Concluded. A comparison of cooling drag reduction of different cowl-inlet configurations. Pressure altitude, 15,000 feet; angle of attack, -2°.